TRANSPORTATION RESEARCH RECORD 1032

Evaluation and Control of Expansive Soils

TRB
TRANSPORTATION RESEARCH BOARD
NATIONAL RESEARCH COUNCIL
WASHINGTON, D.C. 1985

Transportation Research Record 1032
Price $10.40
Editor: Edythe Traylor Crump
Compositor: Lucinda Reeder
Layout: Marion L. Ross

modes
1 highway transportation
3 rail transportation
4 air transportation

subject areas
61 soil exploration and classification
62 soil foundations
63 soil and rock mechanics
64 soil science

Transportation Research Board publications are available by ordering directly from TRB. They may also be obtained on a regular basis through organizational or individual affiliation with TRB; affiliates or library subscribers are eligible for substantial discounts. For further information, write to the Transportation Research Board, National Research Council, 2101 Constitution Avenue, N.W., Washington, D.C. 20418.

Printed in the United States of America

Library of Congress Cataloging in Publication Data
National Research Council. Transportation Research Board.

Evaluation and control of expansive soils

(Transportation research record ; 1032)
1. Soil mechanics–Addresses, essays, lectures.
2. Swelling soils–Addresses, essays, lectures.
I. National Research Council (U.S.). Transportation Research Board. II. Series.
TE7.H5 no. 1032 380.5 s 86-682
[TA710] [624.1'5136]
ISBN 0-309-03923-1 ISSN 0361-1981

Sponsorship of Transportation Research Record 1032

GROUP 2–DESIGN AND CONSTRUCTION OF TRANSPORTATION FACILITIES
Robert C. Deen, University of Kentucky, chairman

Geology and Properties of Earth Materials Section
Wilbur M. Haas, Michigan Technological University, chairman

Committee on Engineering Geology
David L. Royster, Tennessee Department of Transportation, chairman
Robert K. Barrett, William D. Bingham, Robert C. Deen, Jerome V. Degraff, Martin C. Everitt, Jeffrey R. Keaton, C. William Lovell, Stephen F. Obermeier, Peter V. Patterson, Rodney W. Prellwitz, Dwight A. Sangrey, Berke L. Thompson, J. Allan Tice, A. Keith Turner, Duncan C. Wyllie

Committee on Environmental Factors Except Frost
Malcolm L. Steinberg, Texas State Department of Highways and Public Transportation, chairman
S. S. Bandyopadhyay, Samuel H. Carpenter, Barry J. Dempsey, Donald G. Fohs, K. P. George, George R. Glenn, Richard L. Guthrie, Wilbur M. Haas, Donald J. Janssen, Badru M. Kiggundu, C. William Lovell, Robert L. Lytton, R. Gordon McKeen, C. Robert McQuary, Gene R. Morris, James B. Nevels, Jr., Zvi Ofer, Albert C. Ruckman, Joe P. Sheffield, Shiraz D. Tayabji, T. Paul Teng, John L. Walkinshaw, William G. Weber, Jr., Gdalyah Wiseman

Neil F. Hawks, Transportation Research Board staff

Sponsorship is indicated by a footnote at the end of each paper. The organizational units, officers, and members are as of December 31, 1984.

1032

Contents

Addresses of Authors

Bauer, Gunther E., Department of Civil Engineering, Carleton University, Ottawa, Canada K1S 5B6
Blight, G. E., Department of Civil Engineering, University of the Witwatersrand, Johannesburg, South Africa
Chen Lin, Yunnan Design Institute, Dongfeng Road, West Section, Kunming, Yunnan, China
El Sohby, Mohamed A., Civil Engineering Department, University of Al-Azhar, Madinet Nasr, Cairo, Egypt
Georghiou, Costa, Bernard Johnson, Inc., Houston, Tex. 77056
Ghazzaly, Osman I., Department of Civil Engineering, University of Houston, Houston, Tex. 77004
Greenstein, J., Louis Berger International, Inc., East Orange, N.J. 07019
Johnson, Lawrence D., U.S. Army Engineer Waterways Experiment Station, Vicksburg, Miss. 39180
Komornik, A., Civil Engineering Department, Israel Institute of Technology, Haifa, Israel
Mazen, Ossama, General Organization for Housing, Building and Planning Research, El Tahreer Street, Dokki, P.O. Box 1770, Cairo, Egypt
Mowafy, Yousry M., Department of Civil Engineering, Carleton University, Ottawa, Canada K1S 5B6
Murthy, B. R. Srinivasa, Indian Institute of Science, Bangalore, India
Nagaraj, T. S., Indian Institute of Science, Bangalore, India
Ofer, Z., Department of Civil Engineering, University of the Witwatersrand, Johannesburg, South Africa
O'Neill, Michael W., Department of Civil Engineering, University of Houston, Houston, Tex. 77004
Rabba, Sayyed A., Civil Engineering Department, University of Al-Azhar, Madinet Nasr, Cairo, Egypt
Sakeb, Fahim H., Civil Engineering Department, University of Al-Azhar, Madinet Nasr, Cairo, Egypt
Singh, Virendra, URS Company, Inc., 625 Delaware Avenue, Buffalo, N.Y. 14202; formerly with ACRES American, Inc., Buffalo, N.Y. 14202-3592
Steinberg, Malcolm L., Texas State Department of Highways and Public Transportation, District 15, P.O. Box 29928, San Antonio, Tex. 78284
Stroman, William R., U.S. Army Engineer Waterways Station, Vicksburg, Miss. 39180
Tian Kaiming, Yunnan Design Institute, Dongfeng Road, West Section, Kunming, Yunnan, China
Wiseman, G., Civil Engineering Department, Israel Institute of Technology, Haifa, Israel

Rational Approach to Predict Swelling Soil Behavior

T. S. NAGARAJ and B. R. SRINIVASA MURTHY

ABSTRACT

The development of swelling pressure, heave, or collapse on wetting due to the changes in the state of soil moisture are some of the most important engineering problems normally encountered with partly saturated soils. A phenomenological model has been formulated with truncated diffuse double layer theory as the scientific base to predict swelling pressure. It defines fully the swelling behavior of soil in terms of four parameters: (a) swollen void ratio, e_s; (b) swelling pressure, p_s; (c) preconsolidation pressure, p_c; and (d) the slope of the line joining the present state to preconsolidation pressure, ρ. It involves four equations in terms of initial void ratio, e_o, void ratio at liquid limit water content, e_L, and effective overburden pressure, p. For a range of values of e/e_L and p, the swelling pressure values have been computed by iteration, and the results are presented in graphic form. A good agreement between predicted and experimental published data emphasizes the applicability of this approach.

Most of natural soil systems above groundwater table, and invariably all the compacted soils in their initial conditions, are in a state of partial saturation. Further, the mechanics of partly saturated soils is of considerable interest in all the areas of the world where there is an annual excess of potential evaporation over precipitation. Even in areas where this condition does not apply, seasonal moisture deficits may occur. It is apparent that far more than one-half of the earth's surface is a moisture-deficit area. The majority of problems encountered in partly saturated soils are a result of the changes in the state of soil moisture and its associated changes in soil state, compatible with external stress conditions.

The mobilization of swelling pressure and heave or collapse of the soil due to the changes in the state of soil moisture is an important engineering problem. According to a general worldwide assessment, it has been estimated that damages due to expansive soils exceed those due to combined damages from floods, hurricanes, earthquakes, and tornados. The need for prevention or at least minimization of the vast damages caused by swelling soils in geotechnical engineering practice has prompted intensive research to understand, interpret, and predict the behavior of swelling soils. Two approaches are pursued: (a) empirical methods in which thorough statistical analysis of experimental data-simple working models are developed, and (b) rigorous scientific approaches based on the fundamentals of soil behavior to unravel the complexity for meaningful interpretation and generalization.

The intent of this investigation is to examine the possibility of providing simple links, both behavioral and parametric, between the preceding approaches for direct practical application by using only normally measured and observed parameters.

BACKGROUND INFORMATION

Attempts have been made to either link swelling behavior of soils directly with the Gouy-Chapman diffuse double layer theory (1-4) or to evolve statistical empirical relationships between involved and/or inferred soil state parameters (5-10).

There are several reports on the swelling properties of clays that are significant studies in soil engineering. Seed et al. and Saito presented experimental studies on the relationship between the swelling properties and consistency or activity of compacted clays (6,8).

Komornik and David, on the basis of the Gouy-Chapman diffuse double layer theory, logically involved the liquid limit of the soil as the needed parameter to define swelling behavior (7). On the basis of extensive test data they generated an empirical interrelationship in the form

$$\log p_s = \bar{2}.132 + 0.0208\,(w_L) + 0.000665\,(\gamma_d) - 0.0269\,w \quad (1)$$

where

p_s = swelling pressure in Kg/cm^2,
w_L = liquid limit in percentage,
γ_d = natural dry density in Kg/m^3, and
w = natural water content in percentage.

The foregoing interrelationship has a poor coefficient of multiple correlation of less than 0.6. Komornik and David have also indicated a relationship between percent swell and plasticity index.

Vijayavergiya and Ghazzaly, on the basis of 270 test results of undisturbed natural soils at shallow depths, proposed two correlations by which the swell pressure and percent swell under 0.1 ton/ft^2 can be predicted (9). The interrelationships have been indicated in the form

$$\log p_s = 1/12\,(0.4\,w_L - w - 0.4) \quad (2)$$

$$\log p_s = 1/19.5\,(\gamma_d + 0.65\,w_L - 139.5) \quad (3)$$

$$\log S = 1/12\,(0.4\,w_L - w + 5.5) \quad (4)$$

$$\log S = 1/19.5\,(\gamma_d + 0.65\,w_L - 130.5) \quad (5)$$

where S is the percent swell at 0.1 ton/ft^2 and γ_d is the dry density of the soil in lb/ft^3. These interrelationships have a correlation coefficient of about 0.7.

Chen, after conducting an extensive study on expansive soils (11), concluded that the swelling pressure of a clay is independent of the surcharge pressure, initial moisture content, degree of saturation, and the thickness of the stratum. The swelling pressure increases with the increase in initial dry density of the soil. Snethan et al. conducted an investigation of the natural microscale mechanisms that cause volume change in expansive clays (10). They stated that "although some interesting trends may be inferred using this approach, it is still not successful to infer the microscale mechanisms from observed macroscopic volume change behaviour." It has been concluded that clay particle attraction and cation hydration microscale mechanisms play the greatest role in causing volume change. At higher moisture contents and higher cation concentration environments, the osmotic repulsion mechanism provides a secondary influence on volume change behavior.

Bolt and Warkentin et al., using the diffuse double layer model, confirmed experimentally the theory of particle repulsion for pure clays (1,2). The swelling pressure is attributed to the osmotic repulsive pressure mobilized due to the imbibition of water. This hypothesis differs from the mechanistic approach, which attributes the imbibition of water to a hydrostatic gradient including flow from the high-pressure zone of the solution to the low-pressure capillary zone between the particles. Komornik and David have indicated that both the mechanisms operate simultaneously in the soil system (7). They have also indicated that the specific surface of the soil being reflected by its liquid limit water content accounts for the osmotic repulsion component and the dry density or void ratio accounts for the capillary suction.

Lambe explained the swelling phenomena of compacted clays from a physicochemical point of view (12). Tsytovich estimated the amount of swelling of clays using a modified consolidation theory (13). Nishida (14) and Nishida et al. (4), on the basis of the Gouy-Chapman diffuse double layer theory, studied the compression index of clay. By extending the diffuse double layer theory, an equation for swelling pressure of clays of low activity has been presented. It has been revealed that the swelling of clays is proportional to the plasticity index and the amount of free swell is proportional to the specific surface of the clay.

Dennisov indicated that the swelling pressure of a soil depends on the overconsolidation and the composition of the soil (15). In an overconsolidated state, all soils are liable to swell after the natural cementation bonds, if any, are broken.

The preceding discussion on the subject, although incomplete, indicates that swelling behavior of soils is yet to be understood. The parameters that affect swelling behavior are quite varied.

Considering the physicochemical interaction forces, the compressibility of the fine-grained saturated soils has been modeled in the stress range of 25 to 800 kPa in the form

$$e/e_L = 1.122 - 0.2343 \log p \quad (6)$$

$$e/e_L = 1.122 - 0.188 \log p_c - 0.0463 \log p \quad (7)$$

for normally and overconsolidated states (16). ["Prediction of Compressibility of Overconsolidated Soils" (authors' communication to Geotechnical Division, ASCE).] The term e/e_L has been referred to as the generalized soil state parameter. The possibility of extending the foregoing considerations to define partly saturated soil behavior merits further consideration. As a first step, the physicochemical state of a partly saturated fine-grained soil is discussed. Further, the possibility of generating a phenomenological model to predict swelling soil behavior is examined.

PHYSICOCHEMICAL STATE OF PARTLY SATURATED SOIL

It is a well-known phenomena that in a clay water electrolyte system, the electronegativity of the surface results in the formation of an electric diffuse double layer. The concentration of ions and co-ions in the diffuse double layer varies from maxima and minima at the particle surface to a value equal to that of bulk solution at a far-off point, roughly in an exponential form. With the progressive removal of moisture from a clay electrolyte suspension, a stage will be reached when the thickness of the water film is less than the diffuse double layer. This may be achieved by moisture removal due to evaporation or by drainage under an applied stress. As the ions are forced to remain in the liquid phase, the extent of the double layer cannot exceed the thickness of the liquid layer in contact with the charged surface. In such an event all the ions present in the suspension are forced into the liquid phase causing a readjustment of the ionic concentration distribution. This condition has been schematically shown in Figure 1. Such a layer is termed by Bolt and Bruggenwert as the truncated diffuse double layer (17).

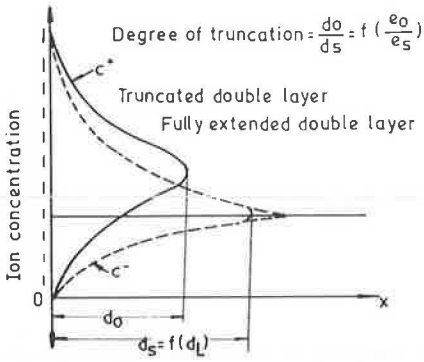

FIGURE 1 Schematic representation of redistribution of ions in a truncated double layer.

The special property of the truncated double layer is to reabsorb moisture forcefully and to develop to an extent commensurate with the concentration of the equilibrium bulk solution. In this process, the double layer reaches a stage at which all the voids are saturated with exertion of swelling pressure for no change in void ratio. If the volume change is permitted, the double layer grows to its full extent. Figure 2 schematically shows the truncated double layer due to partial saturation, the interacting double layer on saturation in equilibrium under swelling pressure, and the fully extended double layer under no load.

PHENOMENOLOGICAL MODELING

From the considerations of the truncated diffuse double layer theory, the compressibility behavior of partly saturated, fine-grained soils has been defined in terms of the external applied stress p and the generalized soil state parameter for the partly

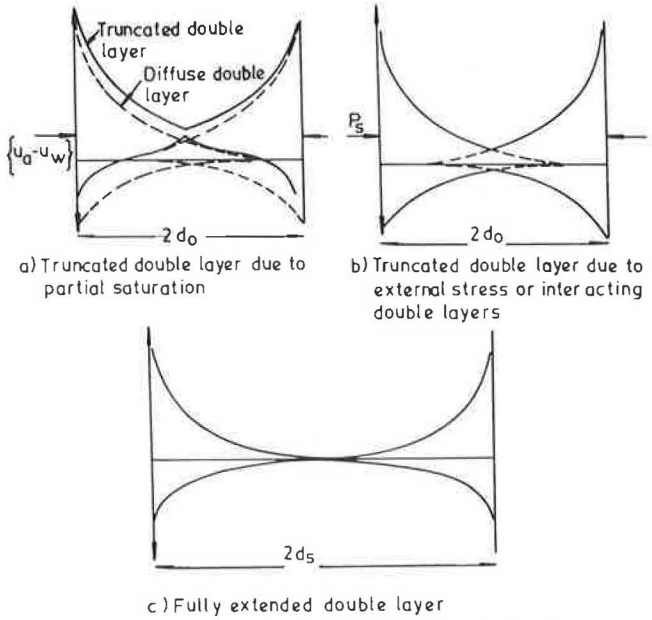

a) Truncated double layer due to partial saturation

b) Truncated double layer due to external stress or interacting double layers

c) Fully extended double layer

FIGURE 2 Schematic representation of ion distribution in truncated and fully extended diffuse double layer.

saturated state $e/e_L\sqrt{S_r}$ (18). ["Generalisation of Compressibility Behavior of Partly Saturated Soil" (authors' communication to Geotechnical Division, ASCE.)] According to Bolt and Bruggenwert, the swelling pressure is always a function of the degree of truncation of the diffuse double layer (17). In the present context, the degree of truncation can be explained as follows. In a constant volume swell pressure test the initial void ratio represents the degree of truncation. The system is in equilibrium under the influence of capillary stresses due to partial saturation and the physicochemical interaction stresses. On imbibition of water, the capillary stresses tend toward zero and the interacting stresses increase, resulting in the development of swelling pressure. At this state, the system can be in equilibrium at the same initial void ratio only under an external applied pressure equal to the swelling pressure. In the process, the truncation due to partial saturation transforms into the one due to saturation and under external pressure. On release of the pressure, the double layer grows to its full extent, compatible with the concentration of the bulk solution. This state at a nominal pressure of 10 kPa is represented as e_s.

Now $e_o = G\gamma_w S d_o \times 10^{-4}$ and $e_s = G\gamma_w S d_s \times 10^{-4}$

$$e_o/e_s = d_o/d_s$$

where

S = specific surface of the soil,
d_o = initial half-space distance,
d_s = final half-space distance in swollen state,
G = specific gravity of soil particles, and
γ_w = density of water.

Then $e_o/e_s = d_o/d_s$ represents the degree of truncation. As such, phenomenologically the equation for swelling pressure can be written as

$$p_s = f\,(d_o/d_s) = f\,(e_o/e_s) \qquad (8)$$

When the soil system is in equilibrium in a partly saturated state under an external load, the volume change behavior of the soil system on saturation depends on the relative magnitudes of the existing pressure and the developed swelling pressure. If the swelling pressure is less than the existing external pressure, the system undergoes consolidation or collapse to reach a compatible state with the external pressure. If the swelling pressure is greater than the existing pressure, the soil swells to reach another equilibrium state (15).

Figure 3 schematically shows the initial partly saturated state in equilibrium under the external pressure p by point A, and on inundation, the swelling pressure p_s required to keep the system in equilibrium at the same initial void ratio by point B. Also shown in Figure 3 are the overconsolidated saturated line BC, the normally consolidated saturated line CE, and the swollen void ratio e_s along the rebound path CBD. It is evident geometrically from Figure 3 that $p_s = f\,(e_o/e_s)$.

Effect of Preconsolidation Pressure

The rebound of a saturated soil on unloading is proportional to the interacting repulsive pressure mobilized at the time of unloading, which is otherwise balanced by the external pressure in its equilibrium state. The repulsive pressure mobilization is a function of the interacting specific surface at any equilibrium state. The effective inter-

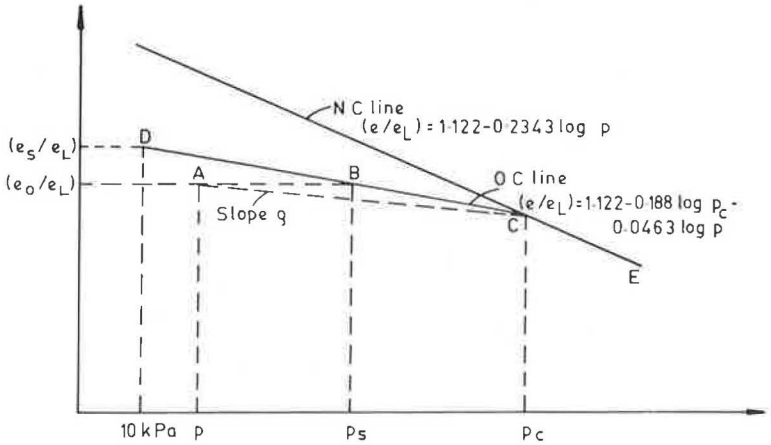

FIGURE 3 Schematic representation of states before and after saturation.

acting specific surface reduces with an increase in stress due to the formation of clusters, packets, and domains (16). Hence, the mobilized repulsive pressure at any equilibrium state depends on the stress level of rebound, that is, preconsolidation pressure p_c. It has been shown (authors' communication to Geotechnical Division, ASCE) that the saturated average rebound recompression lines of all fine-grained soils bear a unique slope value of $\rho = 0.0463$ in the (e/e_L) - log p plot (Equation 7). It can logically be expected that the swollen void ratios of all the soils bear a unique relationship with e_L and the preconsolidation pressure p_c.

Now in Figure 3, the point B represents the saturated equilibrium state under the external pressure equal to the swelling pressure along the average rebound recompression line. Thus the swollen void ratio at a pressure of 10 kPa can be obtained by substituting p = 10 kPa in Equation 7.

$$(e_s/e_L) \text{ @ } 10 \text{ kPa} = 1.08 - 0.188 \log p_c \quad (9)$$

or

$$(e_s/e_L) \text{ @ kPa} = f (\log p_c) \quad (10)$$

Now a combination of Equations 6 and 10 results in

$$p_s = f (e_o/e_L, \log p_c) \quad (11)$$

This is further substantiated by putting $p = p_s$ in Equation 7 at the same (e_o/e_L). It is apparent because at p_s, (e_o/e_L) is the same before and after saturation.

$$\text{That is, } (e_o/e_L) = 1.122 = 0.188 \log p_c - 0.0463 \log p_s \quad (12)$$

This implies that, for known values of p_c and (e_o/e_L), the swelling pressure of the soil can be predicted.

In any of the earlier approaches, either empirical or rational, the involvement of p_c, accounting for the change in the effective specific surface, is not indicated. The other two factors e_o and e_L represent similar terms d and w_L, used for prediction by various investigators.

Dennisov has indicated the need for the parameter p_c in the prediction of the swelling behavior of soils (15). He has stated that only overconsolidated soils can exhibit swelling. For a partly saturated soil at field conditions, existence of preconsolidation pressure is not apparent. It may be termed as an equivalent preconsolidation pressure. The present state of the soil is due to several cycles of alternate wetting and drying and the corresponding alterations in the capillary stresses. Parry and Bjerrum have stated that such a type of overconsolidation is identical to conventionally known stress-release type of overconsolidation (19-21).

Determination of Preconsolidation Pressure for a Partly Saturated Soil

For a given partly saturated soil, the preconsolidation pressure cannot be determined with any of the known methods. The following method is tentatively proposed. It is shown schematically in Figure 3 that the slopes of the line joining the present state to the preconsolidation pressure can define the preconsolidation pressure. The equation of this line can be written in the form

$$(e/e_L) = 1.122 - (0.2343-\rho) \log p_c - \rho \log p' \quad (13)$$

where (e/e_L) is the generalized soil state parameter at stress p' the value p' is between p and p_c or p' = p, corresponding to (e_o/e_L), the initial state,

$$(e_o/e_L) = 1.122 - (0.2343-\rho) \log p_c - \rho \log p \quad (14)$$

From the schematic diagram shown in Figure 3, it is clear that the slope ρ can be related to (e_o/e_L), p and p_s, which eliminates p_c.

$$\text{Thus, } \rho = f (e_o/e_L, p, p_s) \quad (15)$$

Now, phenomenologically developed equations can be listed as

$$p_s = f (e_o/e_s) \quad (16)$$

as well as Equations 10, 14, and 15

$$(e_s/e_L) = f (\log p_c)$$

$$(e_o/e_L) = 1.122 - (0.2343 - \rho) \log p_c - \rho \log p$$

$$\rho = f (e_o/e_L, p, p_s)$$

In the preceding four interrelationships, for known values of (e_o/e_L) and p, the other four quantities ρ, p_c, e_s, and p_s can be evaluated. Because with the present state of the art these forms of equations cannot be generated from the fundamental principles, recourse to a semiempirical method is taken. On the basis of a set of experimental data, generation of the type of equations cited earlier is attempted.

SEMIEMPIRICAL EQUATIONS

To generate the possible type of equations cited earlier, the extensive experimental data of Snethan et al. (10) are selected. Of the available 20 constant volume swell pressure test data, results of 13 tests, conforming to a high degree of final saturation, are selected. The data in Table 1 indicate the analyzed test data of Snethan et al. (10). The swollen void ratio e_s has been selected at a pressure of 10 kPa. The additional computed terms presented in Table 1 are p_c and ρ.

The term p_c is calculated from the equilibrium condition at p_s, corresponding to the same initial state (e_o/e_L) as per Equation 7. Then the (e/e_L) at p_c is calculated by using Equation 6 for the normally consolidated saturated state and, thus, the slope is computed using the equation

$$\rho = [(e_o/e_L) - (e/e_L \text{ @ } p_c)]/(\log p_c - \log p) \quad (17)$$

The tabulated results are statistically interrelated to obtain the functional relationships of Equations 8, 10, 14, and 15 in the form

$$(e_o/e_s) = 1.00571 - 0.0004036 p_s \quad (18)$$

$$(e_s/e_L) = 1.068 - 0.1934 \log p_c \quad (19)$$

$$\rho = 0.0601 - 0.0297 [(e_o/e_L) + \log (p_s/p)] \quad (20)$$

with correlation coefficients of 0.97, 0.994, and 0.996, respectively. In the preceding equations p_s, p_c, and p are all in kPa.

Equations 18-20 together with Equation 14 will define completely the swelling behavior of soils. It is interesting to note that Equation 19 is similar to Equation 9 for p = 10 kPa.

$$\text{That is, } (e_s/e_L) = 1.076 - 0.188 \log p_c \quad (21)$$

TABLE 1 Collected and Collated Data *(10)*

Sl No/	Sl No in Ref	e_o	e_L	e_o/e_L	e_s	e_o/e_s	e_s/e_L	p_s in kPa	p_c in kPa	ρ	$(e_o/e_L)+\log(p_s/p)$
	1	2	3	4	5	6	7	8	9	10	11
1/1		1.155	2.798	0.413	1.370	0.843	0.490	382	1364	0.0152	1.548
2/2		0.716	1.635	0.438	0.749	0.956	0.458	96	1411	0.0317	0.973
3/3		1.265	2.611	0.485	1.279	0.989	0.490	43	973	0.0407	0.671
4/4		0.686	1.523	0.450	0.690	0.995	0.453	35	1554	0.0437	0.547
5/6		0.421	0.962	0.438	0.424	0.993	0.441	66	1548	0.0364	0.810
6/7		0.544	1.320	0.412	0.553	0.984	0.419	65	2136	0.0373	0.778
7/10		0.727	1.517	0.479	0.755	0.963	0.498	93	861	0.0301	1.000
8/12		0.736	2.063	0.357	0.769	0.957	0.373	95	3825	0.0348	0.887
9/14		0.765	1.568	0.488	0.791	0.967	0.505	80	800	0.0318	0.944
10/15		1.125	1.739	0.647	1.133	0.993	0.652	38	760	0.0275	1.069
12/19		0.589	1.904	0.309	0.597	0.986	0.313	59	7686	0.0402	0.633
13/20		0.99	2.176	0.455	1.069	0.926	0.492	254	902	0.0169	1.413

e_o - Initial void ratio, e_L - void ratio at liquid limit, e_s - swollen void ratio upon saturation at 10 kPa, ρ - slope. The overburden pressure is constant at 28 kPa for all the tests.

The difference in the values of intercept and slope are negligible. The minor difference is due to the backward extrapolation of Equation 7 to a low stress level of 10 kPa. Because the computations of other equations are based on the test results of Snethan et al., Equation 19 is preferred.

For computing the swelling pressure, e_s is eliminated between Equations 18 and 19 resulting in

$$p_s(\text{kPa}) = 2492 - 12811.3\ (e_o/e_L)/(5.522-\log p_c) \quad (22)$$

The other two equations are Equations 20 and 14:

$$\rho = 0.0601 - 0.0297\ [(e_o/e_L) + \log\ (p_s/p)]$$

$$(e_o/e_L) = 1.122 - (0.2343-\rho)\ \log p_c - \rho \log p$$

Equations 14, 20, and 22 have three unknowns in p_s, p_c, and ρ. It is not possible to simplify further to directly solve for p_s. In addition, Equations 14 and 22 are nonlinear. As such, solutions to these equations are obtained by the following iteration process. For known field values of (e_o/e_L) and the overburden effective pressure p, a value of swelling pressure p_s is assumed. For the assumed value of p_s and the known value of p, the slope of the line joining the partly saturated state point to the p_c point (Figure 3) is computed using Equation 20. With the computed value of ρ and known values of (e_o/e_L) and p, the preconsolidation pressure p_c is calculated using Equation 14. Using Equation 22 for a known value of (e_o/e_L) and a computed value of p_c, p_s is calculated. This procedure is repeated assuming a new value of p_s until this assumed value agrees with the finally computed value of p_s. The entire operation has been programmed to the DEC-10 system, and p_s values have been generated for the entire range of (e_o/e_L) and p values. The results are plotted in a semilog plot as (e_o/e_L) versus log p_s for various p values (Figure 4). For known values of (e_o/e_L) and p, the swelling pressure can be directly read from the graph. In Figure 4 a small region is indicated in which the soil is susceptible to collapse under an overburden pressure of 200 kPa. Similarly, for higher p values, zones of collapse may be marked.

VALIDITY OF THE APPROACH

To examine the validity of the approach, published experimental swell pressure data of Komornik and David are probed (7). Of the available data on 125 soils, only those for which all the relevant information, such as initial void ratio, overburden pressure, initial moisture content, final void ratio, and final degree of saturation, are available have been selected. Further, probing is restricted to soils conforming to identical initial and final void ratios, a high degree of final saturation, and a swelling pressure greater than the overburden pressure. For all such soils, the experimental and the predicted swelling pressure values have been indicated in Table 2. The comparison indicates a fair agreement.

There are a few cases in which the predicted value is higher than the experimental value. The reason for this behavior may be due to the presence of natural cementation or desiccated bonds that reflect lower experimentally determined swelling pressure. Similarly, a few cases for which the predicted values are lower than their respective experimental values are also indicated. The reason for such a discrepancy may be the result of deviations in the assessed values of overburden pressure.

In general, it may be stated that the swelling pressure of a soil may be predicted within the limits of accuracy at engineering level. Once the swelling pressure is predicted, all other swelling behaviors, such as percent swell, heave, or collapse, may be predicted.

CONCLUDING REMARKS

On the basis of the truncated double layer theory applicable to a partly saturated soil system, a

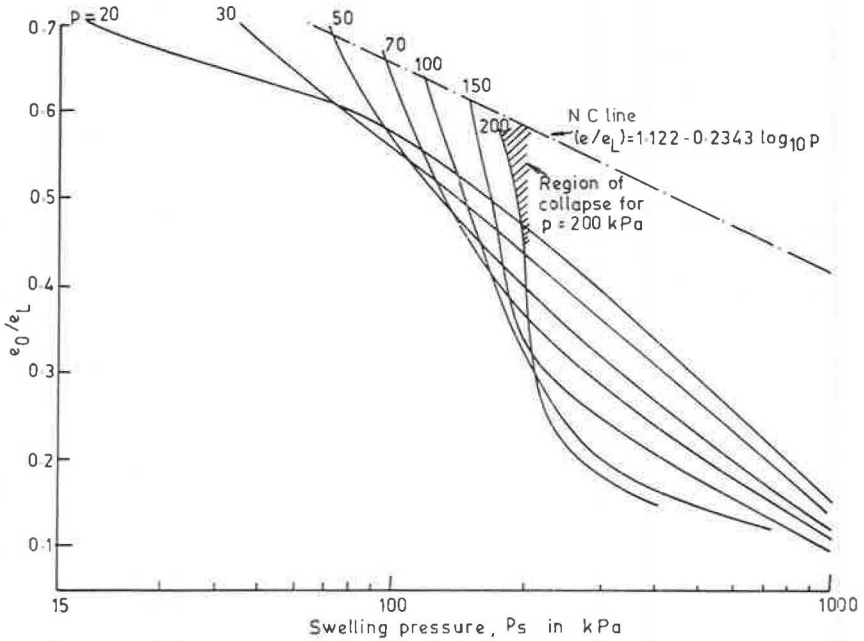

FIGURE 4 Prediction of swelling pressure of soils.

TABLE 2 Analysis of Data for Predicting Swelling Pressure *(7)*

Sl No / Sl No (Ref)	e_o	w_L	e_L	e_o/e_L	p in kPa	p_s (Expt) in kPa	p_s (Computed) in kPa
1	2	3	4	5	6	7	8
1/10	0.442	35	0.928	0.476	62	127	140
2/11	0.510	45	1.224	0.417	47	190	190
3/12	0.876	76	2.098	0.418	61	191	180
4/13	0.680	61	1.665	0.408	63	223	185
5/14	0.651	57	1.562	0.417	50	222	185
6/23	0.868	78	2.114	0.411	75	155	165
7/29	0.785	73	2.029	0.387	66	222	192
8/37	0.900	79	2.244	0.401	48	175	195
9/39	0.618	52	1.440	0.429	25	151	220
10/40	0.548	42	1.147	0.478	30	103	155
11/42	0.911	70	1.981	0.460	38	128	160
12/43	0.568	41	1.111	0.511	32	48	127
13/45	0.535	55	1.485	0.360	42	248	255
14/46	0.468	33	0.884	0.529	61	128	120
15/48	1.236	62	1.693	0.730	17	24	18
16/51	0.760	69	1.898	0.400	59	225	190
17/52	0.854	61	1.696	0.504	92	175	142
18/53	0.702	53	1.463	0.480	138	200	170
19/56	0.766	71	1.945	0.394	58	325	205
20/58	0.657	67	1.882	0.349	137	200	195
21/59	0.687	71	1.938	0.354	176	200	200
22/63	1.320	85	2.295	0.575	25	54	85
23/64	1.180	85	2.295	0.515	25	70	128
24/66	1.250	96	2.717	0.460	21	196	203
25/102	0.570	116	3.190	0.179	133	455	420
26/103	0.500	103	2.936	0.170	146	805	430
27/104	0.520	122	3.477	0.150	145	805	550
28/105	0.61	97	2.668	0.229	141	417	280
29/106	0.53	110	3.08	0.172	143	570	440

e_o - initial void ratio, w_L - liquid limit,
p - effective over burden pressure in kPa,
p_s - swelling pressure in kPa

phenomenological model has been generated to define the swelling behavior of soils. Using experimental test data, a semiempirical model analogous to the phenomenological model has been developed. The semiempirical model involving (e_o/e_L), p, p_s, and p_c, has been solved for the possible range of values of (e_o/e_L) and p. The results have been represented in the form of (e_o/e_L) versus log p_s plot for various values of p. The p_s value can be predicted using the foregoing plot for known values of (e_o/e_L) and p. The validity of the approach has been substantiated in relation to the published data.

REFERENCES

1. G.H. Bolt. Physico-chemical Analysis of the Compressibility of Pure Clays. Geotechnique, No. 2, Vol. 6, 1956, pp. 86-93.
2. B.P. Warkentin, G.H. Bolt, and R.D. Miller. Swelling Pressure of Montmorillonite. Soil Science Society of America Proceedings, Vol. 21, 1957, pp. 495-497.
3. R.N. Yong and B.P. Warkentin. Physico-chemical Analysis of High Swelling Clays. Proc., 1st Pan-American Conference on Soil Mechanics and Foundation Engineering, Mexico, Vol. 2, 1960, pp. 865-888.
4. Y. Nishida. A Brief Note on Compression Index of Soil. Journal of Soil Mechanics and Foundations Division, ASCE, Vol. 82, No. SM3, 1956, pp. 1027-1 to 14.
5. J.H. Gibbs and W.G. Holtz. Engineering Properties of Expansive Clays. Transactions, ASCE, Vol. 121, Paper 2814, 1956, pp. 641-663.
6. H.B. Seed, R.J. Woodward, and R. Lundgren. Prediction of Swelling Potential for Compacted Clays. Soil Mechanics and Foundation Engineering, ASCE, Vol. 88, No. SM3, New York, 1962, pp. 53-87.
7. A. Komornik and D. David. Prediction of Swelling Pressure of Clays. Soil Mechanics and Foundation Engineering, ASCE, Vol. 95, No. SM1, 1969, pp. 209-225.
8. T. Saito and K. Yanai. Some Swelling Characteristics of Compacted Soils. Transactions, Japan Society of Civil Engineering, No. 172, 1969, pp. 11-18.
9. V.N. Vijayavergiya and O.I. Ghazzaly. Prediction of Swelling Potential for Natural Clays. Proc., 3rd International Conference on Expansive Soils, Haifa, Israel, Vol. 1, 1973, pp. 227-236.
10. D.R. Snethan, L.D. Johnson, and D.M. Patrick. An Investigation of the Natural Microscale Mechanisms that Cause Volume Change in Expansive Clays. Interim Report FHWA-RD-77-75, FHWA, U.S. Department of Transportation, 1977.
11. F.H. Chen. Foundations on Expansive Soils. Elsevier Scientific Publishing Co., Amsterdam, The Netherlands, 1975.
12. T.W. Lambe. The Structure of Compacted Clay and The Engineering Behavior of Compacted Clay. Soil Mechanics and Foundation Engineering, ASCE, Vol. 84, No. 5, New York, 1958.
13. N.A. Tsytovich, N.K. Zaretsky, and Z.G. Ter-Martirosyan. Problems of Soil Swelling on Wetting. Proc., 3rd Asian Regional Conference on Soil Mechanics and Foundation Engineering, Haifa, Israel, Vol. 1, 1967, pp. 120-123.
14. Y. Nishida, S. Nakagawa, and H. Koike. On Swelling Pressure of Clays. Proc., 4th Asian Regional Conference on Soil Mechanics and Foundation Engineering, Bangkok, Thailand, 1971, pp. 391-395.
15. N.Ja. Dennisov. Discussion on the Heaving of Buildings and the Associated Economic Consequences with Particular Reference to the Orange Free State Goldfields by J.E. Jennings and J.W. Kerrich. The Civil Engineer in South Africa, 1963.
16. T.S. Nagaraj and B.R. Srinivasa Murthy. Rationalisation of Skemptons Compressibility Equation. Geotechnique. Vol. 33, No. 4, 1983, pp. 433-443.
17. G.H. Bolt and M.G.M. Bruggenwert. Soil Chemistry--A, Basic Elements. Elsevier Science Publishing Co., New York, 1976.
18. T.S. Nagaraj and B.R. Srinivasa Murthy. Prediction of Compressibility of Partly Saturated Soil. Indian Geotechnical Conference, Madras, India, Vol. 1, Dec. 1983, pp. I-27-32.
19. R.H.G. Parry. Field and Laboratory Behavior of Lightly Overconsolidated Clay. Geotechnique, Vol. 18, No. 2, 1968, pp. 151-171.
20. R.H.G. Parry. Some Properties of Heavily Overconsolidated Oxford Clay at a Site near Bedford. Geotechnique, Vol. 22, No. 3, 1972, pp. 485-507.
21. L. Bjerrum. Problem of Soil Mechanics and Construction of Soft Clay and Structurally Unstable Soils. General Report, Session 4, Proc., 8th International Conference Soil Mechanics and Foundation Engineering, Moscow, USSR, Vol. 3, 1973, pp. 111-159.

Publication of this paper sponsored by Committee on Engineering Geology.

Spatial Characterization of Expansive Clays

COSTAS GEORGHIOU, MICHAEL W. O'NEILL, and OSMAN I. GHAZZALY

ABSTRACT

A site on which a building was to be constructed was studied by conducting a large number of pH and Atterberg limit tests on grab samples of soil and in situ resistivity tests on a grid pattern. Contour plots were then made of these indicator properties to attempt to identify zones of high and low potential expansion and horizontal expansion potential gradients. Characteristic surface waveforms were also studied at the site by time-delayed differential surveys of two lines of 128 surface markers, the Fourier transforms of which provided signatures of ground surface movements. Surveys of the soil-supported first floor slab made after construction suggest that the strongest correlation of floor movement was with plasticity index gradient.

Expansive clay problems are well known throughout the world. They are of particular importance to transportation engineers who deal with large-scale projects such as highways and airfields, which are vulnerable to differential soil movements that are the result of water movements through expansive clays. As the use of shallow abutment and pier foundations increases, bridge engineers are also becoming concerned with expansive clays.

Several general procedures exist for the identification of potentially expansive soils (1). For purposes of this paper these procedures can be classified into two groups: (a) traditional methods, and (b) spatial methods.

Traditional methods rely on tests on samples from a limited number of undisturbed sample borings; for example, the widely spaced borings used in the development of bearing capacity parameters for a building, bridge, or culvert. Traditional methods use a variety of indicators to establish the expansive potential. These indicators include liquid limit, plasticity index, a combination of liquid limit and natural water content, soil suction, and one-dimensional swell or zero swell pressure.

A typical example is the procedure by Vijayvergiya and Ghazzaly (2). This method correlates a swell index (ratio of natural water content to the liquid limit) with one-dimensional swell test results and zero swell pressure data. From these correlations a tabulation was developed between the swell index and ranges of probable swell. A similar traditional method, widely used by transportation engineers, is McDowell's method (3), which provides a technique for computing the potential vertical rise (PVR) from classification tests and a family of curves of stress versus volumetric swell. The method applies only to natural soils. A comparable method for compacted soils was proposed by Seed et al. (4).

Some traditional methods rely on direct measurements for the determination of swell potential. Jennings and Knight (5) proposed a method for the determination of potential soil heave from a double oedometer test. Snethen and Johnson (6) proposed a methodology for characterization of expansive soils using measured or estimated changes in soil suction.

Traditional methods suffer from the problem that, because so few sampling points exist, only a general qualitative picture (e.g., "moderate" swell potential) or at best a single quantitative parameter (e.g., 4-in. swell potential) is developed for a site. However, swell potential gradients, particularly in the horizontal direction, are more important than average magnitudes in forecasting distress in pavements and structures. Mound-depression (gilgai) structure and other swell anomalies are not usually identified by traditional methods.

Spatial methods, on the other hand, allow for the assessment of the variation of swell indicators in three dimensions and thereby permit the construction of indicator gradients. Spatial methods (involving gradients) are more relevant for assessing possible structural distress because they may lead to correlations with differential movements. Pioneering work has been done in spatial characterization by Lytton (7) and McKeen Nielson (8), among others.

McKeen and Nielson (8) proposed a spatial methodology whereby soil suction is measured on a large number of soil clods (directly or indirectly), recovered at shallow depths over a large area (e.g., an airfield site), permitting swell potential contour maps to be drawn and swell potential gradients to be established. They also describe a method to evaluate differential swell potential across a site by making accurate level readings on lines of equally spaced markers (stakes) at different times. Variations between readings at each stake at different times are converted into Fourier transforms to obtain wavelength and amplitude characteristics of the site.

APPLICATION OF THE SPATIAL METHOD

A variation of McKeen's spatial method was applied to a specific site in Houston, Texas, on which a building ("new engineering building," Figure 1), whose structural frame was supported on shallow drilled footings and whose first floor slab was supported on soil, was to be constructed. The site, which was essentially flat, had no vegetation but grasses except along the eastern and northeastern portions of the building line, where several small groves of oak, pine, and mimosa trees with trunk diameters of up to 14 in. existed, as shown in Figure 1. The site is situated on the Beaumont clay formation, which is a stratified deltaic deposit composed of preconsolidated clays and occasional fine sands and silts (9). A general profile of the site is shown in Figure 2.

Undeveloped areas of the Beaumont formation present gilgai features on aerial photographs, according to Dawson (9). Because the soils were deposited

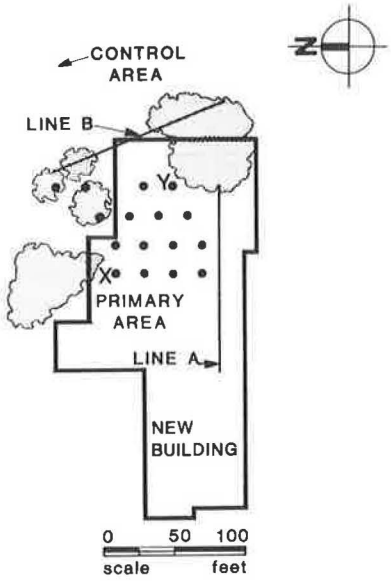

FIGURE 1 Area map.

intermittently over a long period of geological time, the possibility exists that immature gilgai have been buried beneath the surface. According to O'Neill and Ghazzaly (10), buried gilgai fields may result in movements of footings if buried gilgai are exposed during construction.

The structure is a four-story steel frame building with no basement. The frame is supported on drilled piers that extend approximately 10 ft below natural grade. The upper 4 ft of the soils at the site directly under the building were removed and replaced with a controlled fill having a plasticity index of less than 20 as a way of minimizing the effect of the expansive clay on the building. The fill was extended 3 ft above grade to accommodate placement of the first floor slab, which was constructed about 1 year after the surface soils were removed. The slab was supported directly on the fill without any dowels to grade beams or columns.

Construction took place from the summer of 1981 through the summer of 1983. Climatic conditions at the site, which is in a relatively humid area, during 1980-1984 are shown in terms of the monthly Thornthwaite moisture ratio (11) in Figure 3, which also indicates the timing of major events relative to this paper. The monthly moisture ratio is defined in Equation 1:

$$\text{Monthly moisture ratio} = (p - e)/e \quad (1)$$

where p is monthly precipitation and e is evapotranspiration for the month computed in terms of average temperature for the month. Published 20-year rainfall and temperature averages, rather than specific measured values, were used for November and December of 1984. Relatively dry conditions (for the area) existed during construction of the fill and foundation.

The spatial characterization process consisted of three simple steps. First, two lines of 128 (2^7) wooden stakes located 1 ft apart were driven 6 in. into the soil. The locations of these two lines are shown in Figure 1. The purpose of locating the stakes along those specific lines was to study the difference in surface movement patterns between an area free from substantial vegetation and an area where trees were prevalent. The level readings were taken on the stakes from September to December 1980, which was during a period of increasing moisture ratio. The second step involved establishment of a grid on the site as shown by the heavy dots in Figure 1. X and Y are reference markers used to relate grid locations and orientations in Figure 1 with those in later figures. Grab samples were taken at depths of 0 to 1, 3 to 4, and 6 to 7 ft at the grid points, and Atterberg limits and pore water extract pH tests were conducted on the samples. Wenner bridge resistivity tests were also conducted at the grid points with electrodes spaced so as to provide soil resistivity values at the average depth intervals described earlier. [The use of Atterberg limits, pH, and resistivity as indicators of expan-

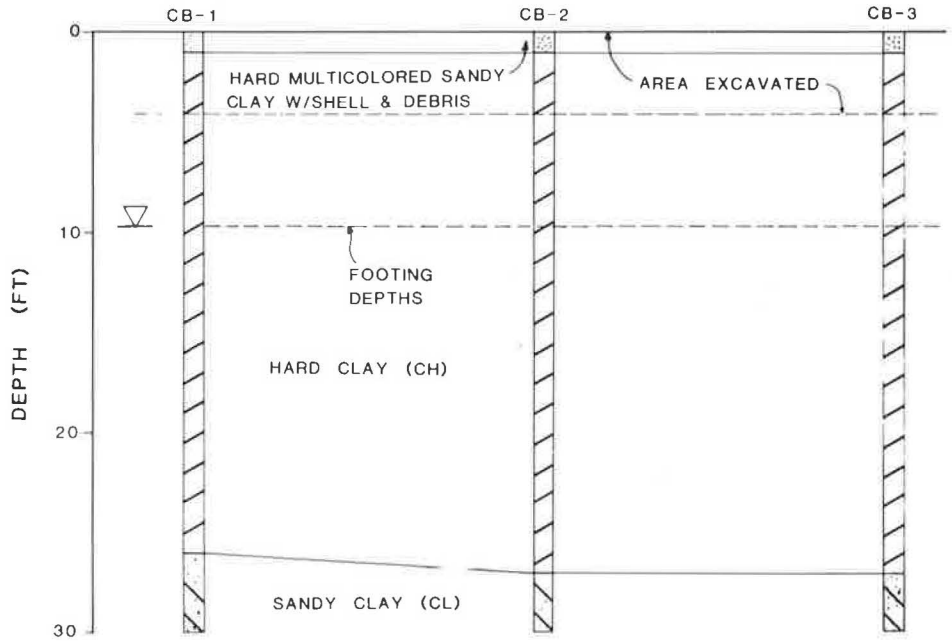

FIGURE 2 Soil profile.

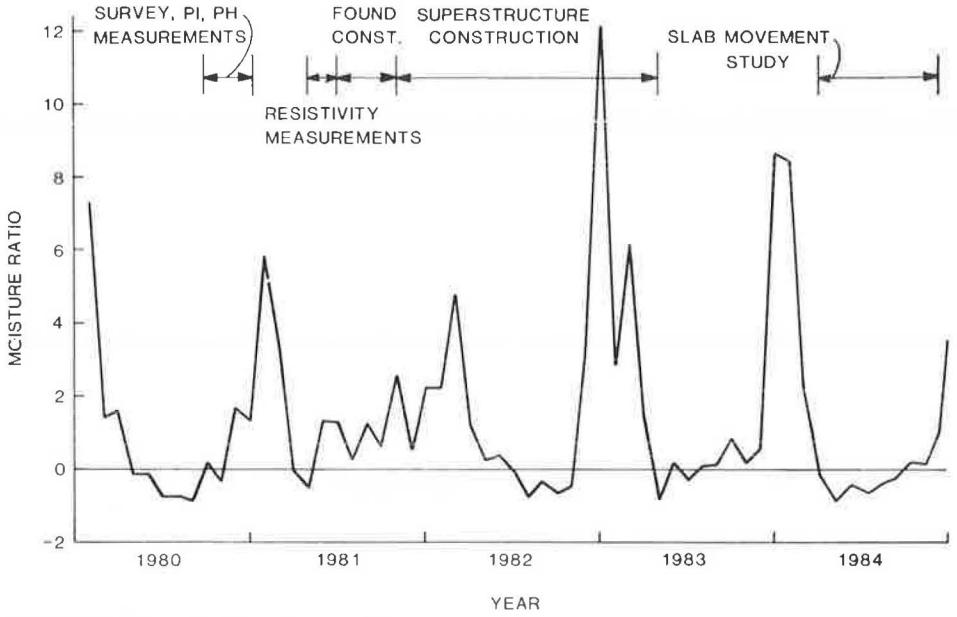

FIGURE 3 Thornthwaite moisture ratio versus time.

sion (or shrinkage) was considered appropriate because the value of each factor reflects, to some degree, pore fluid electrolyte concentration. In turn, electrolyte concentration is related to osmotic suction, which is a relatively important component of total soil suction in a "wet" climate, such as exists in Houston. In addition, resistivity is affected by pore air content and thus is hypothetically an indirect indicator of matrix suction.] Twenty of the grid points were located beneath the eastern half of the building (near the trees) and nine were located in a separate control area outside of the building (primary) area away from any trees. The second step operations (except for the resistivity tests) occurred during a period of increasing moisture ratio, shown in Figure 3.

The third step consisted of the instrumentation of three footings with electronic resistance strain gauges (mounted as full bridges at several levels on the longitudinal reinforcing steel in the plinths) as a means of directly measuring the effects of expansive soil movements. During the ensuing 3 years the measured strains were very small, so that it was not possible to separate strains produced by vertical soil straining from those due to electrical drift and other factors. This suggests that shear stresses on the plinths were small, probably owing to the existence of the 7 ft of controlled fill. No further observations concerning this step are given.

An additional post-construction phase of the study was added in 1984 after a crack was observed in the interior of the building. This phase involved taking measurements of the grade-supported first floor slab to determine if differential soil movement was taking place. Three sets of measurements were taken, one in March 1984, one in May 1984, and one in November 1984. The area of the slab that was accessible for this phase is shown in Figure 1.

RESULTS

Contour plots of plasticity index (PI), pH, and resistivity are presented in Figures 4-6 for the primary area. It is assumed that the contour patterns are later reflected in the pattern of movements in the completed structure; thus, high gradients in these indicators suggest potentially high rates of rotation in structures supported in the soil. Close examination of the PI contours shows no correlation of the contours at 0 to 1 ft depth with deeper contours. The maximum mean values of PI were observed at the 3 to 4-ft level, although general magnitudes appear to remain about constant with depth. At depths of 3 to 4 ft (shallowest depth

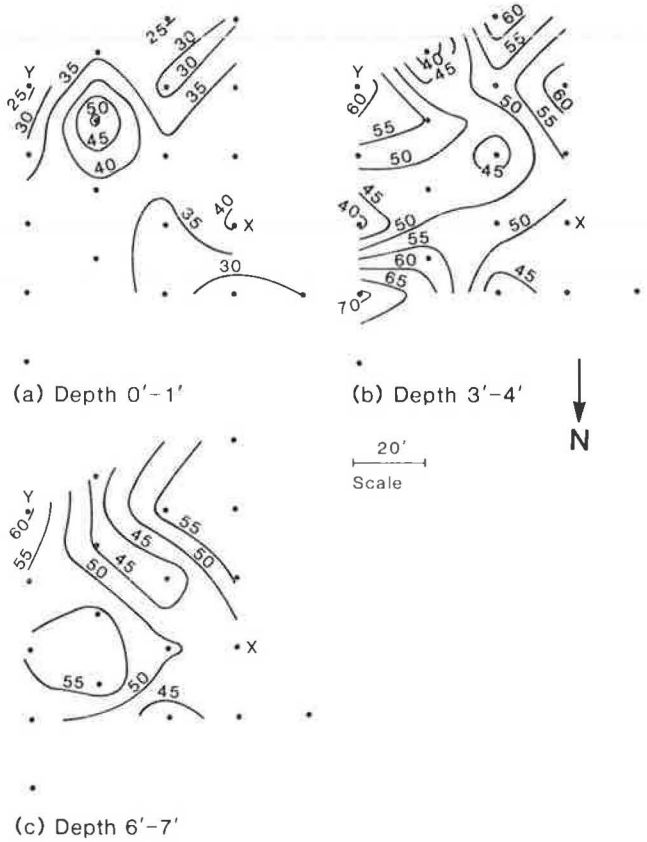

FIGURE 4 Primary area plasticity index contours.

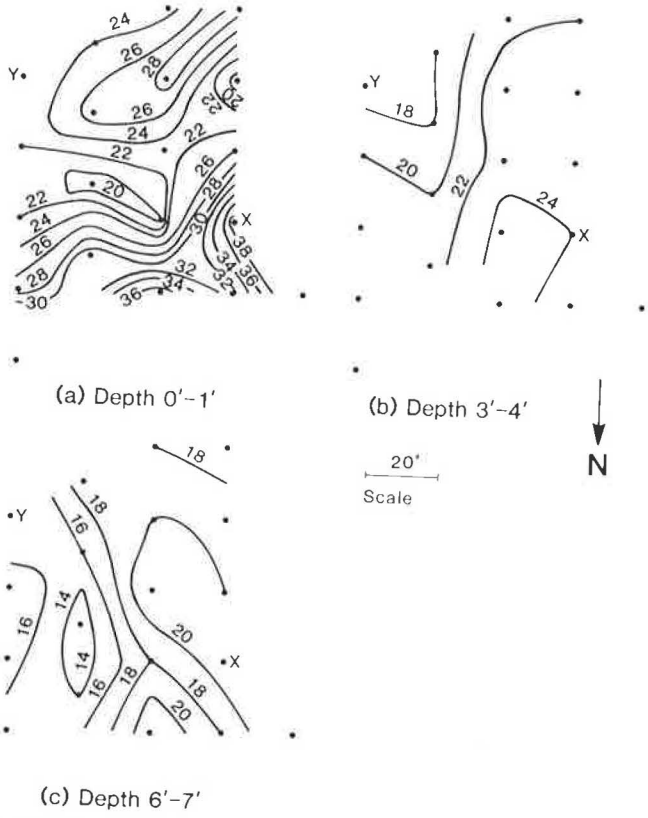

FIGURE 5 Primary area resistivity contours.

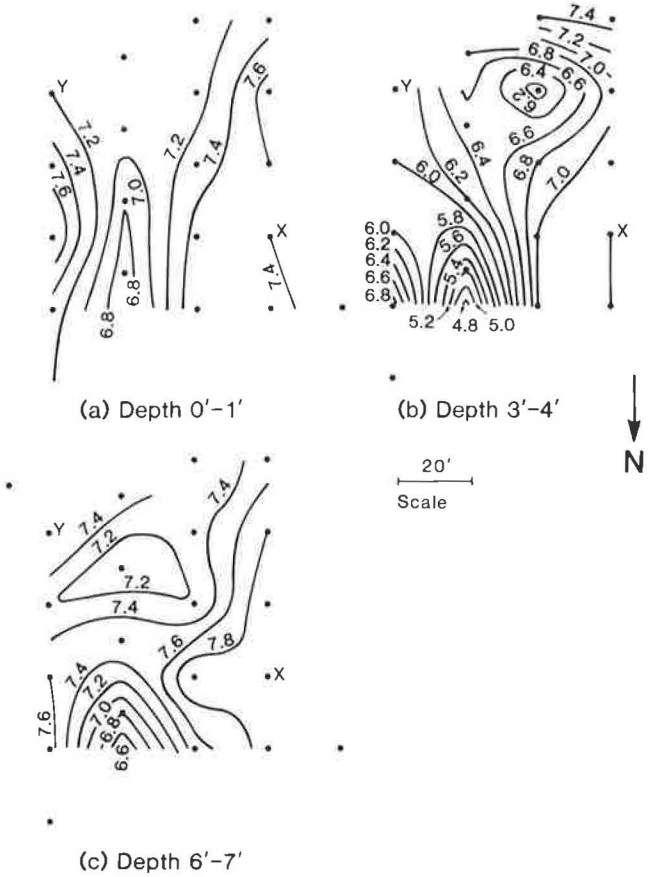

FIGURE 6 Primary area pH contours.

representing soil that was not excavated) and below, there appears to be a pattern of higher horizontal gradients than at the shallower depth (excavated soil). The gradients are highest in the north-east sector of the grid at a depth of 3 to 4 ft, near several trees.

The pattern of PI contours appears to be a complex one of ridges, troughs, mounds, and pits. PI maxima (peaks) are in the range of 60 to 70 at the lower two depths and minima (valleys) are in the range of 40 to 45. At the 6 to 7-ft depth there is a peak near marker point Y and one near the north arrow that correlate between the two depths. The shortest spans (wavelengths) between maxima at the 3 to 4 and 6 to 7 ft levels are 50 to 60 ft. This observation suggests that maximum differential movements in the structure due to free field expansion and contraction in the soil would develop (a) over a distance of 25 to 30 ft (one-half the wavelength) and (b) in areas where correlations in maxima and minima exist between depths of 3 to 4 and 6 to 7 ft. Condition (b) appears east-to-west over the top (south) part of the grid.

The resistivity contours in Figure 5 show a clear trend of lower general magnitude with increasing depth. A comparison of contours at the three different levels shows no clear correlation of results at different depths and no identifiable peak-to-valley distances at any depth. Another observation is the reduction of horizontal gradient of resistivity below 0 to 1 ft. This may be because resistivity was measured in situ with electrodes at spacings that increased with depth of resistivity value, which may have had an averaging effect over increasingly larger areas. It therefore appears that resistivity measured in the manner described was not a sensitive indicator of soil expansion potential variability at the depths at which soil was not excavated.

Figure 6 shows the pH contours. A comparison of the results at the three levels indicates a fairly close correlation depthwise of contours of high acidity and alkalinity. The extreme values of pH were 4.8 and 7.8. The pH contours are rather strongly influenced by the results at a single grid point near a tree, where the pH was very low at all depths. If the results of that point were to be ignored, a weaker correlation would be present among the three levels.

The soil is generally more acid at 3 to 4 ft than at 0 to 1 or 6 ft. Acid soils tend not to produce diffuse double layers that are as large as those in basic soils, which suggests that the soils at 6 to 7 ft may have more involvement in the development of expansion potential than those at 3 to 4 ft. The extreme acidity (pH < 6) at the 3 to 4-ft level, however, is physically associated with the presence of tree roots, which, when removed, could conceivably have resulted in the lowering of matrix suction in the soil, with resultant swelling. (No evidence of heave in the portion of the completed floor slab situated above the soil with pH < 6 was observed, which suggests that significant suction reduction either has not yet occurred or that it occurred rapidly, before the floor slab was placed.)

The pH contours have a topographic form similar to those for PI, although the extreme value-to-extreme value spacing below 0 to 1 ft is not well-defined within the grid that was used. The spacing (wavelength) appears to be slightly higher than that observed in the PI contours.

By comparing the three indicator contours at all levels, no evident correlation exists among the three indicators. The few depthwise correlations of the PI contours found in the primary area were absent in the control area (Figure 7), possibly because the control area was too small. At the 6 to 7-ft level

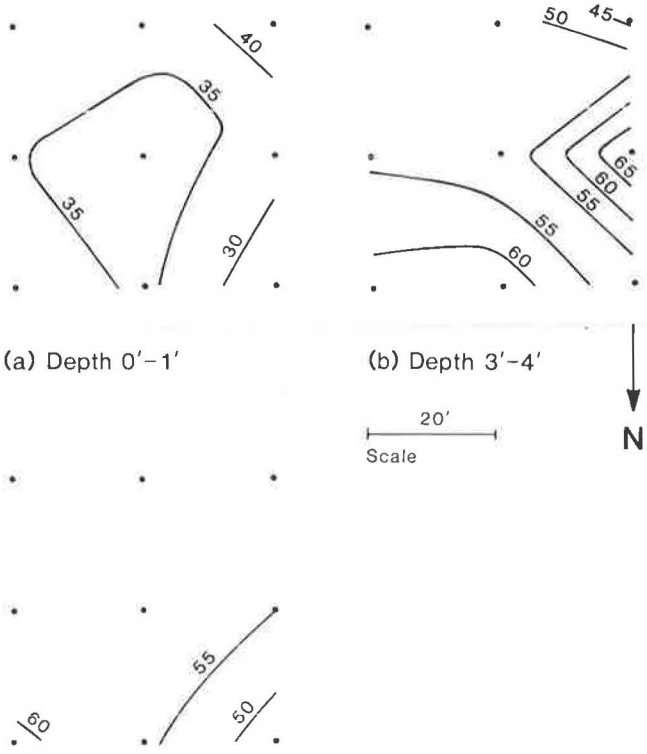

(a) Depth 0'-1' (b) Depth 3'-4'

(c) Depth 6'-7'

FIGURE 7 Control area plasticity index contours.

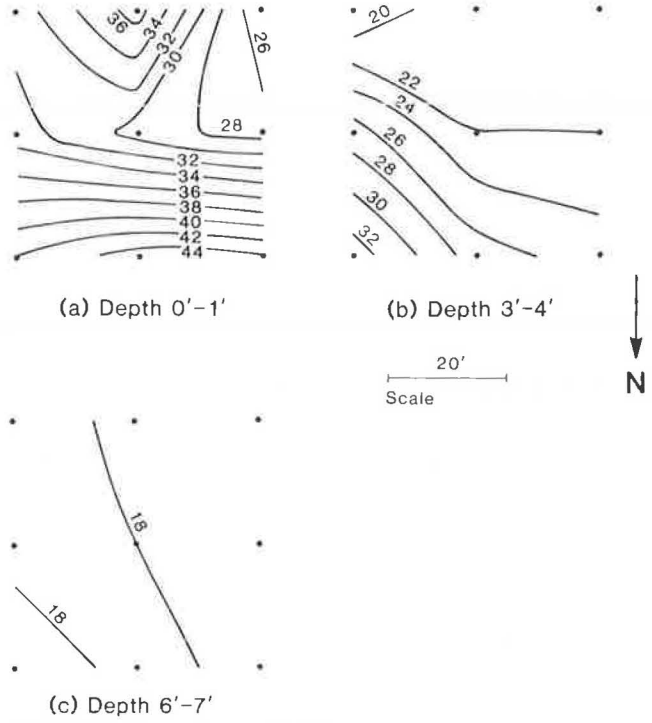

(a) Depth 0'-1' (b) Depth 3'-4'

(c) Depth 6'-7'

FIGURE 8 Control area resistivity contours.

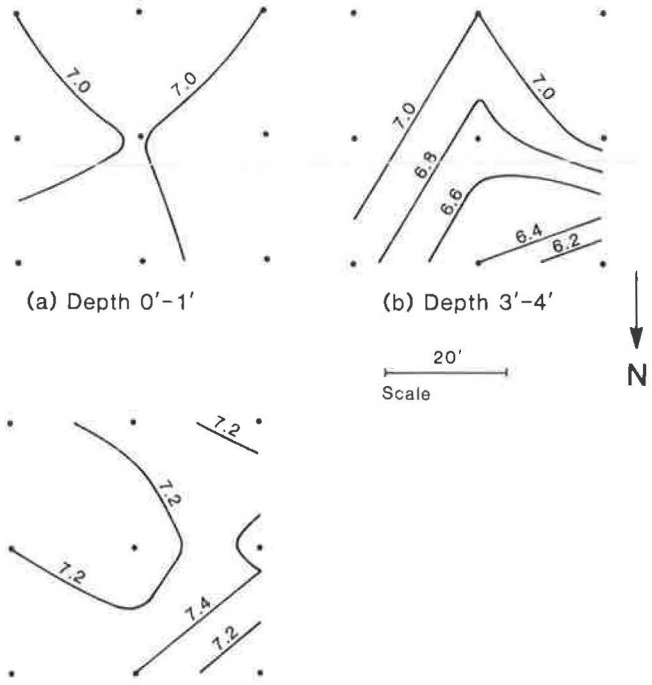

(a) Depth 0'-1' (b) Depth 3'-4'

(c) Depth 6'-7'

FIGURE 9 Control area pH contours.

there is very little variation in PI in the control area. The gradient variations between the control and primary areas may be due to the differences in vegetation in the two areas.

The observations made for the resistivity contours in the primary area apply to the control area. As shown in Figure 8, the horizontal resistivity gradients and the general magnitudes decreased with depth. At the 6 to 7-ft level, the resistivity was essentially uniform horizontally.

The pH contours in the control area, shown in Figure 9, indicate smaller horizontal gradients than in the primary area. The pH at 0 to 1 ft and 6 to 7 ft is essentially uniform over the area, with values near neutral. Only the layer from 3 to 4 ft showed pH variation.

Discrete Fourier transforms (12) of surface elevation changes along the lines of stakes also provided information on potential differential soil movements. Transforms of differences in elevation at each of a number of vertical movement markers over a fixed period of time provide descriptions of prominent wavelengths of surface deflection in the free-field (without structure) soil and their relative magnitudes. The appropriate transform equation is

$$X_k(f) = \Delta h \sum_{n=1}^{N} x_n e^{-2\pi j(kn/N)} \quad (2)$$

where

Δh = stake spacing (1 ft);
n = stake number (1, 2, . . . , 128);
N = total number of stakes (128);
x_n = difference in elevations at stake n over the time period;
$j = (-1)^{0.5}$; and
X_k = Fourier amplitude.

The parameter k is defined by the wavelength λ_k for which X_k is computed by Equation 3, in which Δf is a numerical constant.

$$\lambda_k = (k\Delta f)^{-1} \quad (3)$$

The Fourier transforms of the surface elevation studies are shown in Figures 10 and 11. Both figures are plots of Fourier amplitude versus n. The wavelength (λ_k) is 128 ft/n.

Only the first n/2 frequency components are unique in the transform and therefore have any physical significance. The second half is a mirror image of the first half.

The surface elevation studies were performed in the fall of 1980 during a period of increasing moisture ratio (Figure 3). The solid lines in Figures 10 and 11 are transforms of elevation differences taken during an initial 45-day interval; the dashed lines represent differences during a 45-day interval immediately following the first interval.

No discernible periodicity appears along Line A and no particular trend toward increasing amplitude with time is evident, except for one major peak at n = 3 (λ_n = 42.7 ft), which is interpreted as the potential fundamental wavelength for the portion of the site without trees. This is contrasted with 50 to 60 ft observed in the PI contours (Figure 4). The amplitudes and periodicity are much stronger along Line B (through the area with trees) than along Line A, especially for low values of n. Prominent peaks are observed at n = 6, 9, 15, 21 and 33 (λ_n = 21.3, 14.2, 8.5, 6.1, and 3.9 ft). They probably represent movements due to differential suction that is influenced by the presence of the three root systems. There is no clear trend of increasing or decreasing Fourier amplitude with time along Line B. Behavior of the type found along Line B suggests that differential free-field soil movements occur over short enough distances to cause potential harm to a light structure even if the trees are removed, since stabilization at reduced suction may require many years following tree removal.

Finally, the slab movement study results are shown in Figure 12 in which plus (+) values indicate heave and minus (-) values indicate settlement. These measurements were initiated after a crack developed in a corridor wall on the western edge of the study area. The period between the two sets of measurements in Figure 12a (March 1984 to May 1984) was very dry. Zones of heave and settlement correlate very generally at areas of high and low PI, respectively, although no complete wave pattern appeared in the slab. The general mode of movement of the slab during that period was settlement, with an average value of about 0.02 ft measured. Settlement reached as much as 0.05 ft, 20 ft south of Marker X (and 20 ft north of the crack), the reason for which is unknown. Heave up to 0.03 ft was detected just east of Marker Y, which was near a peak in the PI contours for the level of 6 to 7 ft and also in the former grove of trees, through which elevation Line B had been installed 3 1/2 years earlier. No distress was discernible in the building in the zone of heave at that time.

Figure 12b shows slab movement contours over a longer period of time (March-November) in which the short-term differential movements (Figure 12a) appear to continue but with a tendency toward further settlement. One additional wall crack 25 ft southeast of Marker X developed during May-November.

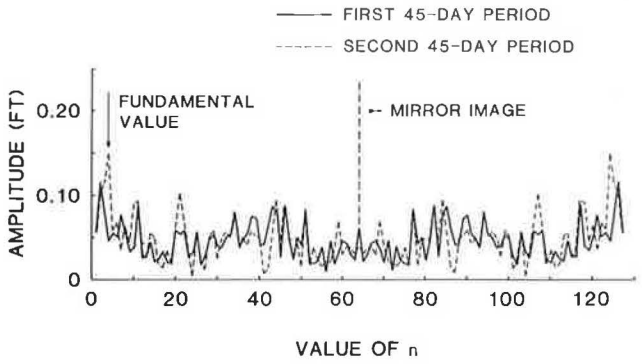

FIGURE 10 Line A Fourier transform.

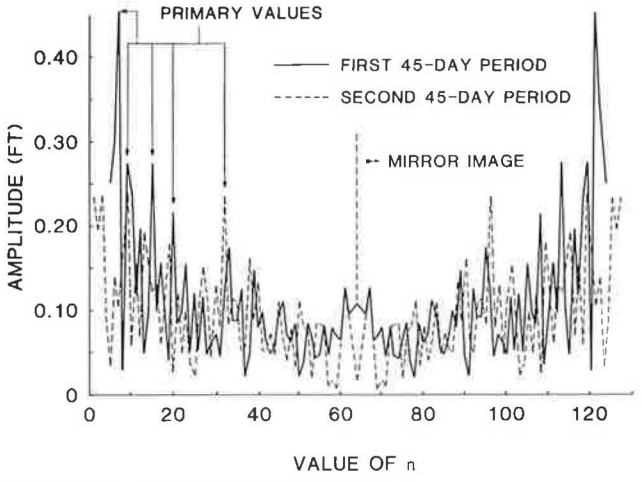

FIGURE 11 Line B Fourier transform.

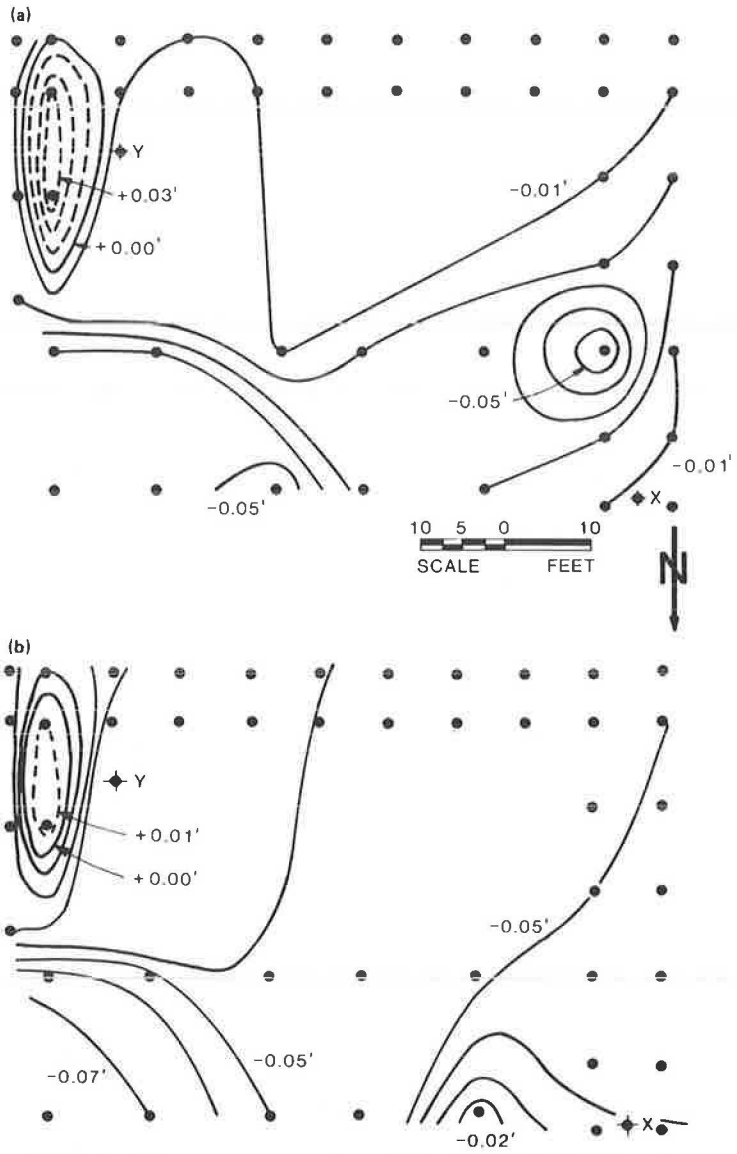

FIGURE 12 Slab movement contours: (a) March-May 1984; (b) March-November 1984.

CONCLUSIONS

The following conclusions are drawn from the study:

1. No obvious correlation could be found between PI, resistivity, and pH.
2. Resistivity was not a suitable indicator at the study site.
3. There appears to be a vague correlation between the slab movement contours and the PI contours at 6 to 7 ft.
4. The Fourier transforms appear to provide good indications of the relative expansive potential of the soil.
5. The spatial techniques described are relatively quick and inexpensive to perform. More studies of the type reported here are needed to establish their general reliability.

ACKNOWLEDGMENTS

The study reported in this paper represents the combined efforts of McBride Ratcliff and Associates, Inc., McClelland Engineers, Inc., F.E. Willcox, David Broussard, and the Office of Facilities Planning and Construction of the University of Houston. The authors are indebted to these organizations and individuals for their assistance and support. Appreciation is also extended to Le T. Pham for her help in preparing the figures.

REFERENCES

1. D.R. Snethen, L.D. Johnson, and D.M. Patrick. An Evaluation of Expedient Methodology for Identification of Expansive Soils. Report FHWA-RD-77-94. FHWA, U.S. Department of Transportation, Washington, D.C., 1977.
2. V.N. Vijayvergiya and O.I. Ghazzaly. Prediction of Swelling Potential for Natural Clays. Proc., 3rd International Research and Engineering Conference on Expansive Clay Soils, Haifa, Israel, Vol. 1, 1973, pp. 227-234.
3. C. McDowell. The Relation of Laboratory Testing to Design for Pavements and Structures on Ex-

pansive Soils. Colorado School of Mines Quarterly, Vol. 54, No. 4., 1959.
4. H.B. Seed, J.K. Mitchell, and K.C. Chan. Studies on Swell and Swell Pressure Characteristics of Compacted Clays. Bull. 313, HRB, National Research Council, Washington, D.C., 1961, pp. 12-39.
5. J.E. Jennings and K. Knight. The Prediction of Total Heave from the Double Oedometer Test. Symposium on Expansive Clays, Transactions, South African Institute of Civil Engineers, 1957.
6. D.R. Snethen and L.D. Johnson. Characterization of Expansive Soil Subgrades Using Soil Suction Data. Presented to Transportation Research Board Committee on Environmental Factors Except Frost, Washington, D.C., Jan. 1977.
7. R.L. Lytton, R.L. Boggess, and J.W. Spotts. Characteristics of Expansive Clay Roughness of Pavements. Transportation Research Record 568, TRB, National Research Council, Washington, D.C., 1976, pp. 9-23.
8. R.G. McKeen and J.P. Nielson. Characterizing Expansive Soils for Airport Pavement Design. Report FAA-RD-78-59. FAA, U.S. Department of Transportation, 1978.
9. R.F. Dawson. Land Subsidence Problems. Transactions, ASCE, Vol. 130, 1965, pp. 206-207.
10. M.W. O'Neill and O.I. Ghazzaly. Swell Potential Related to Building Performance. Journal of the Geotechnical Engineering Division, ASCE, Vol. 103, No. GT12, Dec. 1977, pp. 1363-1379.
11. C.W. Thornthwaite. An Approach Towards a Rational Classification of Climate, Geographical Review, Vol. 38, 1948, pp. 55-94.
12. J.W. Cooley and J.W. Tukey. An Algorithm for the Machine Calculation of Complex Fourier Series. Mathematics of Computation, Vol. 19, No. 90, April, 1965, pp. 297-301.

Publication of this paper sponsored by Committee on Environmental Factors Except Frost.

Measurement of Swelling Pressure in the Laboratory and In Situ

Z. OFER and G. E. BLIGHT

ABSTRACT

During the past 30 years more than 25 methods for the determination of the engineering characteristics of expansive soils and the prediction of heave have been proposed in the western world. Many of the proposed methods relate to laboratory or index tests whereas in situ tests, being more complex, have received less attention. Some commonly used laboratory and in situ testing methods for the determination of heave and swelling pressure are reviewed. Two instruments developed in South Africa are described, and test results are presented and compared with field loading test results. It is concluded that if sampling disturbance, size effects, selectivity in soil sampling, and simulation of actual site conditions are accounted for, laboratory and in situ test results are in good agreement.

Expansive clays are soils that exhibit unusually large volume changes as a result of moisture variations and environmental changes. The behavior of expansive soils affects the performance of structures buried in and founded on these soils; therefore, the understanding of their properties and their engineering characterization is of great importance. Engineers are well aware of the distress that lightly loaded structures, roads, runways, and utilities buried at a shallow depth in a swelling soil can suffer. The damage caused to such structures may be considerable, and rehabilitation at an early stage of a structure's life may be required, which imposes a heavy economic burden on the owner or user.

During the past 30 years more than 25 methods for the determination of the characteristics of expansive soils and the prediction of heave have been proposed in the Western world (1). However, a universally accepted method has yet to be developed. Many of the proposed methods relate to laboratory or index tests whereas in situ tests, being more complex, have received less attention. The purpose of this paper is to review some commonly used laboratory and in situ methods for the measurement of swelling pressure and heave. Two instruments developed in South Africa are described, and test results are presented and compared with some field loading test results. The relationship between laboratory

and in situ test results and field observations is discussed.

REVIEW OF SOME LABORATORY METHODS

Swelling clays exert pressure against confining stresses when water and electrolytes are available for volume increase. The swelling pressure may exceed the external stress, which will then decrease but will not prevent volume change. The relationship between applied external load and the volume change resulting from swelling of the soil is commonly used for the characterization of expansive soils. In the direct model method (2) an undisturbed sample, or alternatively a remolded sample, is placed in an oedometer and subjected to the in situ overburden pressure or the vertical stress that will exist at the end of construction. Water is then introduced to the sample and the subsequent vertical deflection is observed.

A series of swelling tests with varying initial density, moisture content, and vertical stress yields the swelling characteristic of the soil, and the following two quantitative parameters are evaluated:

1. The percentage swelling (which is the vertical swelling strain under a token load), and
2. The swelling pressure (which is the maximum vertical stress required to keep the soil sample at the initial volume when the sample is inundated with water and full swell occurs).

Many other methods for the determination of swelling characteristics using standard and modified oedometer type equipment have been developed (3-7). It has been observed that the prediction of heave using a direct model method generally underestimates the actual field heave primarily as a result of sampling disturbance.

Results of constant volume oedometer tests on an undisturbed soil are also used for heave prediction (8). An undisturbed specimen is placed in an oedometer and subjected to overburden stress. It is then flooded with water and the load is adjusted so that the specimen retains its initial volume. Once the full swelling pressure has developed, the sample is allowed to swell under reduced stress. The heave is calculated from the vertical strain occurring on the rebound curve between the constant volume condition and the post-construction pressure. Sampling disturbance is not compensated and this method also underestimates heave.

The double oedometer method (9) uses consolidation tests conducted on two nominally identical undisturbed clay samples. The samples are placed and sealed in oedometer rings under an initial token load of 1 kPa. One of the specimens is then inundated with water and allowed to swell under the token load. Both samples are then subjected to consolidation under increasing load. The stress-strain relationship for the soil at natural water content is adjusted vertically to coincide with the curve for the soaked specimen at the highest stress, and heave is then calculated from the void ratio difference between the two curves for the expected in situ effective stress change. Comparison of predicted values and field observation indicates satisfactory agreement when the method is applied under South African conditions.

The simplicity of the conventional consolidometer test has attracted the attention of many researchers and practicing engineers who use the test for the design of footings in and on expansive clay (10,11). The test data used in the design process are the coefficient of swell (and sometimes the coefficient of consolidation), incorporated with an estimate of the in situ change in the effective stress. The coefficient of swell; that is, the slope of the swell versus log vertical stress line in the oedometer, is a useful parameter for heave prediction, as it is relatively insensitive to sampling disturbance (12).

Test data, however, do not refer directly to soil suction but to changes in effective stress in the soil from an inferred initial condition to a predicted final state. The soil suction or soil water potential is defined as the amount of work that must be done per unit quantity of pure water to transport isothermally and reversibly an infinitesimal quantity of water from a reservoir of pure water at a specified elevation and atmospheric pressure to that point in the soil under consideration. The total suction of the soil is a combination of the matrix or capillary suction, the osmotic or solute suction, and the gravitational potential. The gravitational potential is often negligible compared with the other components of the total suction. The process of swelling in situ reduces the matrix and osmotic suctions, but does not affect the gravitational potential.

Swelling tests that incorporate directly controlled suction were first performed by using a specially designed oedometer-type test cell connected to a suction pump (13). The apparatus provided only limited control of the matrix suction, however, and tests under large suction values were not attempted.

Laboratory swelling tests under indirectly controlled suction conditions may now be performed by using controlled water flow, controlled air pressure supply, reference osmotic solution, or total suction determination. In the controlled water flow method (14), a clay specimen is allowed to absorb small measurable quantities of water.

The volume change, or alternatively the resultant swelling pressure, is then related to the increase in the water content of the clay. However, the suction control is very rough and the moisture distribution throughout the clay specimen is not uniform.

In the axis translation technique (15), air pressure, applied to a soil sample, isotropically compresses both the soil particles and the water and because both are relatively incompressible, the value of the matrix suction does not change. Continuity of air spaces in the specimen is necessary to validate this assumption, which cannot be achieved when the degree of saturation is high and occluded air is contained in the soil volume.

An accurate control of suction in a clay specimen may be achieved by placing an osmotic solution in contact with the soil through a semipermeable membrane (16,17). Depending on the suction of the osmotic solution, water will flow through the membrane from the solution to the soil or vice versa. The volume change or swelling pressure that develops during this process is recorded, and, hence, the swelling characteristics of the soil are determined.

A variation of the foregoing technique is used in the membrane oedometer (18). This is a modified oedometer that places a clay sample in contact with a semipermeable membrane inside a pressure cell. The clay is subjected to controlled external loading, and matrix and solute suction. Each of these components can be varied independently to simulate in situ changes and record the corresponding strain response.

An Australian method for the prediction of surface heave is based on the membrane oedometer test (18). This method and the design method that relates to it incorporate the concepts of the direct method, axis translation, and osmotic suction control and

hence provides considerable possibilities for simulating environmental and applied stress changes.

Another way of quantitative characterization of swelling soil in the laboratory is by means of total suction determination using psychrometers (18,19) or the filter paper method (20). Psychrometers, either of the thermistor or thermocouple type, cover a wide range of total suction and are relatively inexpensive and simple to use. The relative humidity in a cavity in the soil is determined by means of the psychrometer, and total suction of the soil specimen is related to the relative humidity.

A series of psychrometer tests yields a total suction-water content relationship for a particular soil, which, in turn, can be used to calculate swell volume change. Total suction may also be determined by using the filter paper method. A disc of uniform filter paper of known dry mass is enclosed with a soil sample in a sealed container. After equilibrium has been reached, the filter paper is reweighed and its water content determined. The suction is then assessed from a suction-water content calibration of the paper.

Many empirical methods have been devised for the prediction of heave and swelling pressure from index properties of the expansive soil. A method based on a correlation of plasticity index and clay fraction with the total surface heave of a soil profile has been proposed by van der Merwe (21). Another relationship between void ratio, water content, and plasticity index--the external load and the potential percent swell and swelling pressure--has been suggested by Brackley (22). In Israel a relationship between the liquid limit, dry density, water content, and potential swelling pressure has been used successfully (23,24). A comparative study of various empirical methods concluded that empirical relationships may yield unreliable predictions of swelling, and additional geological and experimental information is necessary to validate any empirical relationship when it is used in an unfamiliar situation.

All the methods reviewed so far refer to heave and swelling pressure in an unaxial system. However, during swelling, clay exhibits anisotropic behavior, and the lateral swelling pressure may exceed the vertical pressure in many cases. The relationship between the horizontal and vertical components of stress at a point within a soil mass depends to a great extent on the stress history of the soil mass (26). Any process that involves compaction and excavation results in a change in the overconsolidation ratio (OCR) of the soil, and consequently the horizontal-to-vertical stress ratio will vary (27,28).

The lateral and swelling pressure of clay can be measured in a modified oedometer ring, and Ofer concludes that using a modified oedometer for lateral swelling pressure tests is convenient (29). A number of instruments have been developed for this purpose (29-31). An instrument of this type developed by the first author (29) is shown in Figure 1. The center section of an oedometer ring wall is trimmed to a wall thickness of 0.75 mm, and two 70 mm long strain gauges are cemented to the thin wall section at its mid-height. A casing is placed onto the ring and an airtight chamber containing a temperature compensator is formed. Swelling pressure can be measured either by measuring strain in the oedometer ring or by maintaining a null-strain condition.

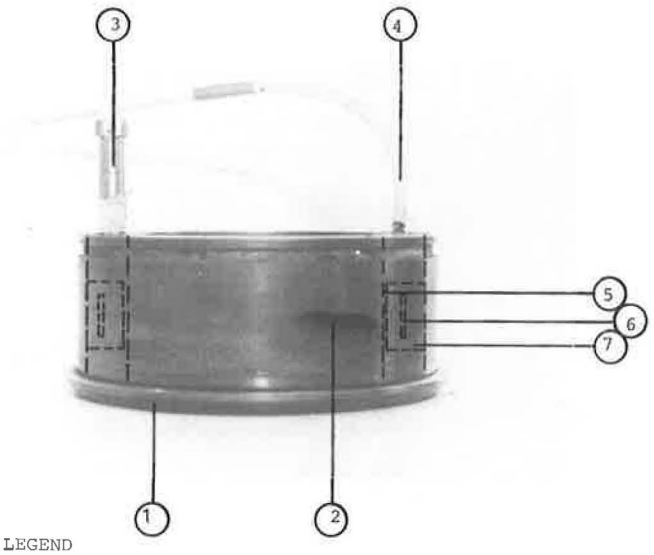

LEGEND
1. Modified oedometer ring
2. Casing
3. Air pressure inlet
4. Electrical leads
5. Thin wall section
6. Temperature compensator
7. Annular chamber

FIGURE 1 The lateral soil pressure ring.

IN SITU DETERMINATION OF SWELLING CHARACTERISTICS

In situ swelling tests are complex and difficult to perform, and relatively few attempts have been made to determine the swelling pressure developed in situ in clay fills or expansive soil profiles. The various approaches that have been tried include the determination of suction and suction changes, strain measurements on buried instrumented pipe or pile sections, and the use of pressure transducers or probe. In situ soil suction and suction changes may be measured by using tensiometers and psychrometers, which measure the low and high range of suction, respectively (20,32). These instruments are buried in the fill or soil profile at various depths, and suction readings are taken periodically in conjunction with surface heave readings. These tests, which correlate suction and surface heave, are time consuming and expensive and are valuable mainly for theoretical studies. Instrumented pipe sections (33) and instrumented piles (11,34-36) have been installed in clay, and the swelling forces that result from environmental variations have been recorded. These tests, however, are also time consuming and costly. Pressure cells buried in heaving clay with the sensitive faces vertical and horizontal have also been used to determine pressures in soil during construction and subsequent swelling (32,33,38). This method is suitable for measuring swelling pressure in fills and could conceivably also be used for measurements in undisturbed profiles.

Probe-like devices, for example, pressure meters, flat dilatometers, and the Iowa Stepped blade, have also been used to determine the in situ horizontal-to-vertical stress ratio in clay soils, either before or after swelling. These instruments, however, have not yet been developed so as to follow the swelling process and to record in situ swelling pressure as it develops.

A probe and testing technique that potentially will allow the in situ determination of lateral swelling pressure in expansive soils has been developed by Ofer (39,40). The cylindrical in situ soil pressure probe is shown in Figure 2. It has an outside diameter of 70 mm, a length of 225 mm, and consists of five modules:

1. Pressure transducer,
2. Two wetting rings,
3. Cutting edge,

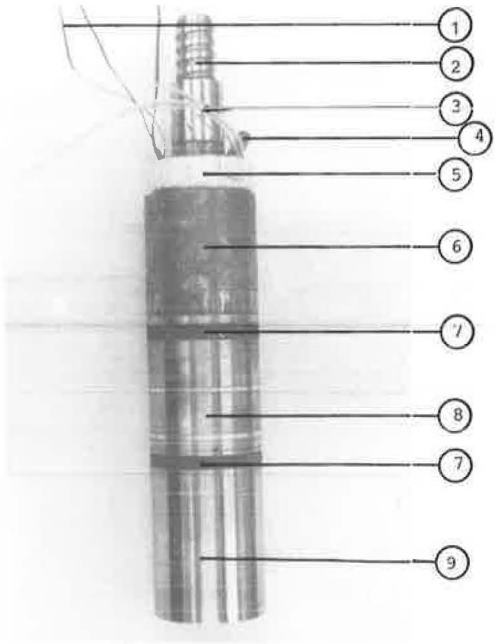

LEGEND
1. Electric leads
2. Drilling rod connector
3. Water supply tubes
4. Air pressure inlet
5. Temperature compensator
6. Guard sleeve and connection head
7. Porous ring
8. Pressure transducer
9. Cutting edge

FIGURE 2 The in situ soil pressure probe.

4. Temperature compensator, and
5. Connection head and guard sleeve.

The pressure transducer has a thin-walled section to which two 70 mm long strain gauges are cemented. The strain gauges are enclosed in an air-tight chamber allowing either strain or null type pressure measurements. The wetting rings are located at either end of the transducer module. Each ring has a porous section connected to a water reservoir located at the surface. The cutting edge is located below the lower wetting ring and the connecting head, guard sleeve, and temperature compensator are bolted to the top wetting ring.

In an in situ test the probe is attached to a frame anchored to the ground, shown in Figure 3. The probe is pushed into a predrilled hole with a minimum of disturbance. Water is then introduced into the soil, and the subsequent swelling pressure developed against the probe is recorded. The instrument has been used at various levels in a clay profile, and the test results have been compared with the results of laboratory swelling tests performed on undisturbed clay specimens from the same site, using a modified oedometer ring (27). The remainder of this paper will concentrate on reporting further measurements made with these two instruments, which have been fully described in earlier papers.

SWELLING TESTS AT ONDERSTEPOORT

The soil profile in Onderstepoort (39) consists of a 3 m-deep residual clay of norite gabbro origin underlain by parent rock. The dominant mineral of the clay is smectite with some traces of kaolinite.

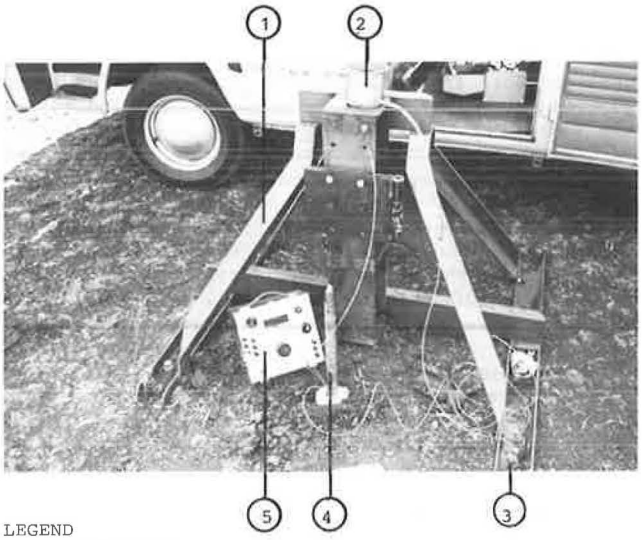

LEGEND
1. Ground frame
2. Water reservoir
3. Ground anchor
4. Drilling rod
5. Strain indicator

FIGURE 3 Field test using the in situ soil pressure probe.

Calcite and calcrete nodules are found in the profile. The clay has a liquid limit ranging from 79 to 99 percent, a plasticity index from 39 to 49 percent, and a clay fraction from 40 to 45 percent. Its linear shrinkage is about 20 percent. In profile the soil is stiff, fissured to shattered, and slickensided.

A series of laboratory and in situ swelling tests using the laboratory ring and the in situ probe was performed on the Onderstepoort clay. Remolded clay was tested in the laboratory in an attempt to simulate known site conditions and to compare the in situ swelling characteristic of an undisturbed clay and a controlled fill using the same material. Also, because the swelling characteristic is sensitive to sampling and test disturbance (39), laboratory swelling tests performed on remolded clay provide a wider range of possible results that can then be correlated to various field conditions.

Time-lateral pressure relationships for a series of in situ and laboratory tests are shown in Figure 4. In an in situ test, the introduction of water to the soil results in a decrease in lateral pressure, which occurs 30 to 60 min after water is introduced. The increase in the lateral pressure is associated with a decrease in the rate of flow of water into the soil, due to the low permeability of the saturated swelling clay around the probe.

The shape of the in situ time-lateral pressure relationship curve has a characteristic that is similar to the pressure-deformation relationship obtained in a cavity expansion test, for example, a pressuremeter test. The similarity can be explained by the fact that only the soil near the probe saturates, softens, and swells; the soil farther away from the probe does not suffer any significant change in its water content during the test and it acts as a stiff confining media (39). The in situ shear strength of the wet material determined after a test is in the range of 25 to 50 kPa, which provides further support to the statement explaining the lateral pressure determined in situ. The shallow test (Test 1 in Figure 4) was performed in a heavily desiccated section of the soil profile, and the introduction of water to the clay reduced the suction to zero and, consequently, a high lateral pres-

Test No.	Location	Depth, m.	Dry unit Weight, kN/m³	Initial moisture content %
1	In situ	0,62	14,9	23
2	In situ	1,70	14,6	28
3	Laboratory	0,60	14,5	20
4	Laboratory	1,50	14,5	25
5	Laboratory	1,50	14,5	25

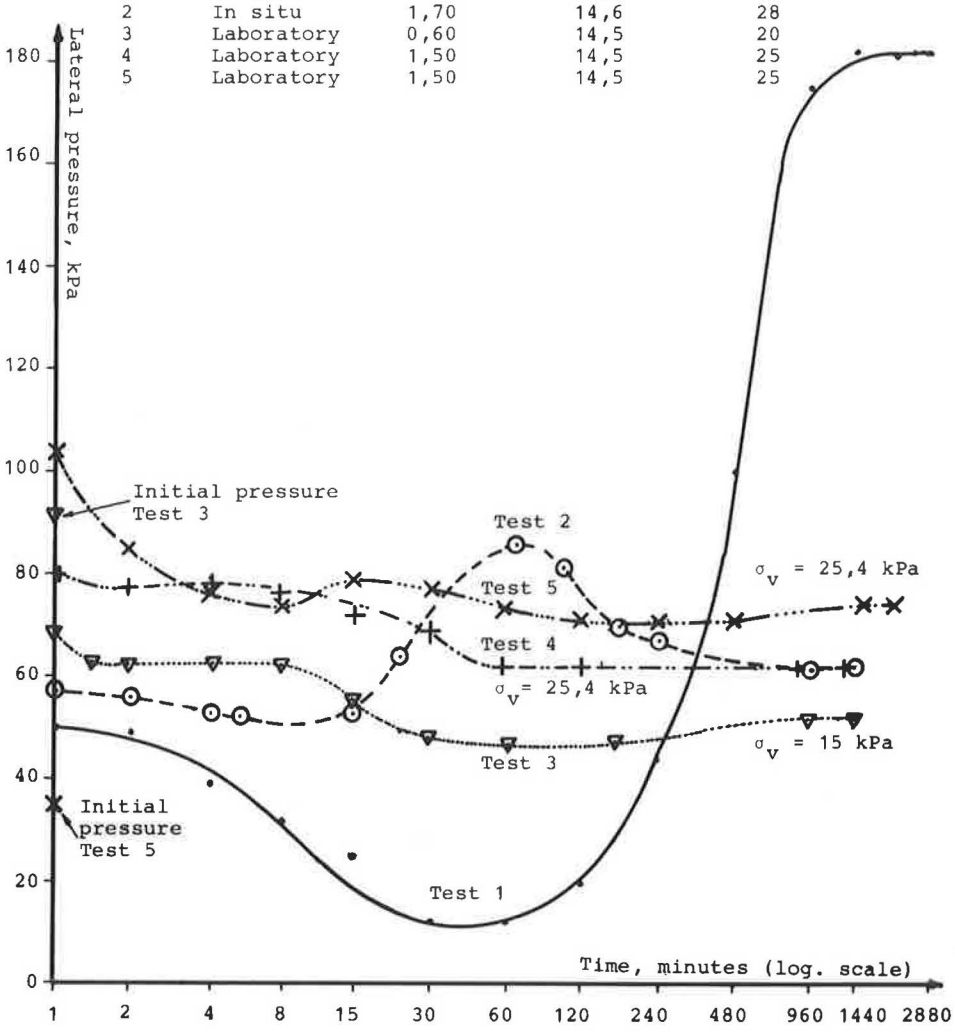

FIGURE 4 Time-lateral pressure relationship for swelling tests at Onderstepoort.

sure developed. The test was carried out at the end of the dry season when the clay is desiccated and the suction values are very high (pF 4,8). The lateral pressure recorded in this test represents the swelling pressure developed in the clay layer, near the probe, where it is confined by stiff clay that did not absorb the water supplied from the instrument. In the deeper in situ test (Test 2), the soil had both a lower density and a lower suction (pF 3,8), which explains the lower lateral pressure developed during the swelling test.

The laboratory tests were performed on statically compacted clay specimens. Subsequent to flooding, a decrease in the lateral pressure was observed in Tests 3 and 4; however, in Test 5, an immediate sharp increase in the lateral pressure was observed, followed by a subsequent decrease. The explanation for this anomaly in Test 5 is that at placement moisture content, the clay is in a granulated form and air voids exist between the specimen and the ring. Subsequently, some evaporation, drying, and shrinkage occurred, and the lateral pressure recorded initially in Test 5 before water was introduced to the sample was considerably lower than the initial lateral pressure recorded in Tests 3 and 4.

In all the tests an irregularity in the time-lateral pressure relationship was noted when water was introduced to the top of the sample and 15 min after it was introduced to the bottom of the sample. One hour after the specimen was flooded, the lateral pressure readings stabilized. However, the clay was still absorbing water and further volume increases were observed.

Good agreement was found between the deeper in situ test (Test 2) and the corresponding laboratory tests (Tests 4 and 5) in which the final lateral swelling pressure was similar. The lateral pressure determined in situ 24 hr after water was introduced was 61 kPa, and the lateral swelling pressures determined in the laboratory in Tests 4 and 5 were 62 kPa and 74, respectively. It is concluded that the remolded clay tested in the laboratory performed similarly to the in situ clay. However, the in situ conditions of very shallow layers were not reproduced adequately in the laboratory.

An analysis of the in situ test results using plane strain constitutive equations for soils (28) relating the lateral-to-vertical effective stress ratio and the overconsolidation ratio provided unreasonable results. The overconsolidation ratio of the in situ clay is approximately 20 at a depth of 0.6 m and decreases to approximately 18 at a depth of 1.7 m. Using Hardin's equations, the corresponding effective angle of friction $\phi' = 90°$, or al-

ternatively, if $\phi' = 20°$ (reasonable value) the overconsolidation ratio, OCR = 30,500. The reason for this is that the in situ swelling test is in fact a cavity expansion test in which a layer of clay next to the probe expands and compresses the soil around it and the pressure monitored by the probe indicates the resistance of the partly saturated clay to compression.

TESTS AT LETHABO

The Lethabo site is underlain by horizontally bedded sedimentary rock of the Ecca subgroup, which is a part of the Karoo supergroup, overlain by layers of transported and residual soils. Residual soils are mainly weathered siltstones and occur as stiff to very stiff, fissured and shattered clayey silts. The residual siltstone grades with depth to very soft rock. Mineralogical analysis of the residual soil and siltstone indicated that about 30 percent of the silt-sized particles are quartz and the remainder is fine-grained micaceous clay. X-ray diffraction of the clay fraction shows that the dominant clay minerals are smectite and kaolinite with a small amount of illite.

In situ swelling tests on large-diameter, instrumented, bored cast in situ piles were performed during an investigation of piled foundations for a power station (11-35). The piles were 1050 mm in diameter, 33 m long, and were instrumented by means of vibrating wire gauges and electrical resistance strain gauges mounted in a central steel shaft. Three of a group of seven piles were instrumented. A month after the piles were constructed, water was introduced to the soil through a grid of watering holes, and subsequent soil heave and strain in the piles were recorded. In addition, a series of plugs 1050 mm in diameter and 2 m long was constructed at various depths in the clay. After wetting the soil in the manner described earlier, the pullout force-displacement relationship was recorded and hence the in situ shear strength of the soil determined.

Results of the in situ tests on instrumented piles and pullout plugs at the Lethabo site (11,35) and results of laboratory tests conducted on undisturbed siltstone specimens cut out from block samples from the same site are shown in Figures 5 and 6. Two types of laboratory swelling tests were carried out, for example, constant volume swelling pressure tests and heave under constant load tests. In both series of tests the siltstone specimens were initially placed in the oedometer ring for a period of 24 hr under a vertical pressure equal to the total in situ overburden pressure. The samples were then inundated and the swelling pressures or heave developed subsequent to flooding were recorded.

Lateral swelling pressures inferred from the plug pullout tests are considerably lower than the corresponding lateral swelling pressures determined in the laboratory. The reasons for this discrepancy are related to scale effects and selectivity in soil sampling. Intact specimens were tested in the laboratory, hence the swelling characteristic so determined yields conservative values, and it should be anticipated that in situ test results will be lower. In addition, the residual siltstone in the soil profile was fissured and shattered at the top of the soil profile and roots were observed down to 15 m, which allows a high apparent lateral compressibility. Hence the lateral swelling pressure developed in situ should be lower than the lateral swelling pressure recorded in a laboratory test on an unfissured specimen.

The relationship between the horizontal and vertical stress and the depth for the in situ tests and the laboratory tests is shown in Figure 5. It can be seen that from a depth of 4 to 10 m the lateral pressure inferred from the plug pullout tests is almost equal to the total vertical pressure in the profile. However, it can be seen in Figure 6 that the in situ lateral-to-vertical stress ratio K increases with increasing depth. In the laboratory tests, very high lateral swelling pressure was recorded in samples taken from a depth of 6 and 9 m, and the stress ratio K determined in these tests was

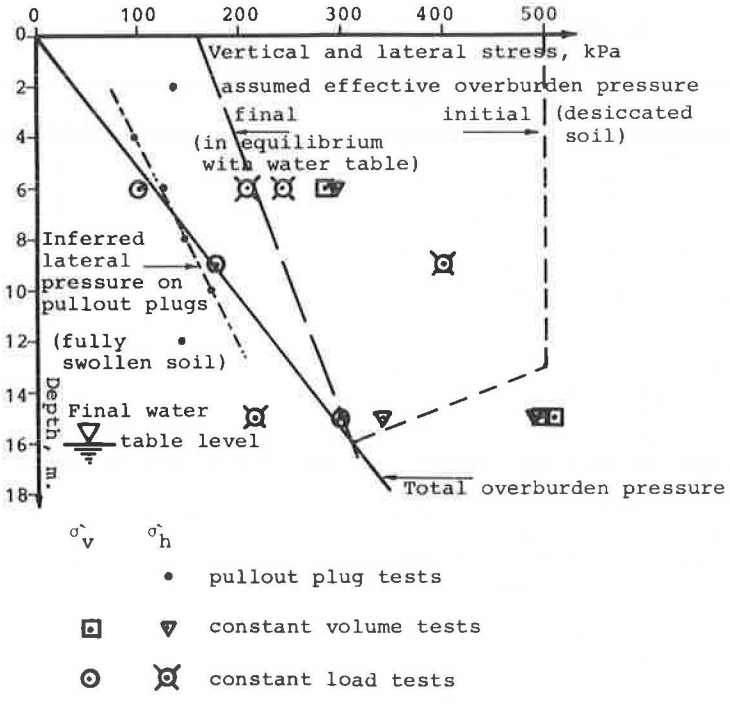

FIGURE 5 Vertical and lateral stress-depth relationship for tests at Lethabo.

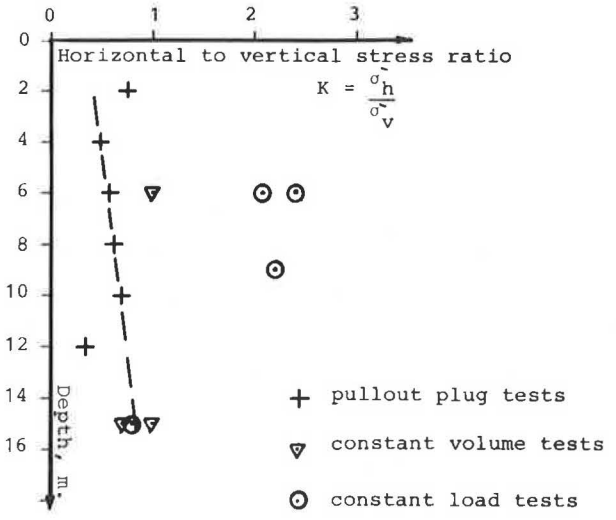

FIGURE 6 Stress ratio-depth relationship for tests at Lethabo.

considerably higher than 1. In samples taken at a depth of 15 m, the stress ratio K was approximately 1.

The scatter of the laboratory test results was high as a result of the sensitivity of the laboratory instrument to varying lack of fit of the specimen, the selectivity in soil sampling from the block samples, and possible drying of the samples between sampling and testing. However, it can be observed that both constant volume tests and constant load tests under a high overburden pressure gave stress ratio values that were in fair agreement with the values determined in the field tests. The initial total vertical stress was approximately the assumed initial in situ effective overburden pressure (shown in Figure 5); hence, the results show no effect of sampling disturbance and the simulation of true field conditions in the laboratory was good.

CONCLUSIONS

Some commonly used laboratory and in situ methods for the determination and prediction of swelling pressure and heave have been reviewed. Two instruments developed in South Africa have been described, and results of tests using these instruments have been presented and compared with field swelling and shear test results.

The effect of sampling and reproducing true in situ conditions in a laboratory swelling test on the laboratory test results is demonstrated. The selectivity in soil sampling and the small size of the laboratory specimens result in an overprediction of swelling pressure.

The laboratory instrument and the testing technique are very sensitive to specimen variability; therefore, an extensive laboratory testing program is necessary to obtain an improved relationship between laboratory and in situ test results. It is important to note that once true field conditions are well simulated in the laboratory and the effects of sampling disturbance and sample size are eliminated, the laboratory and in situ test results are in reasonably good agreement.

Results of laboratory tests on clay from Onderstepoort and the in situ test were in fair agreement; hence, it is concluded that it is possible to perform swelling tests on remolded clay in the laboratory and obtain valid and useful results correlating well to in situ swelling tests on soil at similar water contents. The swelling pressures recorded in an in situ test represent the swelling pressure developed in a limited annulus of clay around the probe, confined by a mass of stiff drier clay. It will be necessary to conduct a swelling test over a long time period that will allow saturation of the clay farther away from the probe before this effect can be eliminated.

REFERENCES

1. R.G. McKeen. Design and Construction of Airport Pavements on Expansive Soils. Report FAA/RD-76/66. FAA, U.S. Department of Transportation, 1976.
2. W.G. Holtz and H.J. Gibbs. Engineering Properties of Expansive Clays. Transactions, ASCE, Vol. 121, 1956, pp. 641-663.
3. R.M. Palit. Determination of Swelling Pressure of Black Cotton Soil. Proc., 3rd International Conference on Soil Mechanics and Foundation Engineering, Zurich, Switzerland, Vol. 1, 1952, pp. 170-172.
4. W.T. Lambe. The Character and Identification of Expansive Soils. Report FHA-701. FHA, U.S. Department of Housing and Urban Development, 1960.
5. J. Kazda. Study of the Swelling Pressure of Soils. Proc., 5th International Conference on Soil Mechanics and Foundation Engineering, Paris, France, Vol. 1, 1961, pp. 140-142.
6. H.B. Seed, J.K. Mitchell, and C.K. Chan. Studies of Swell and Swell Pressure Characteristic of Compacted Clay. Bull. 313, HRB, National Research Council, Washington, D.C., 1962, pp. 12-39.
7. R.H.G. Parry. Classification Test for Shrinking and Swelling Soils. Civil Engineering and Public Works Review, London, England, No. 61, 1966, pp. 719-721.
8. R.A. Sullivan and B. McClelland. Predicting Heave of Buildings on Unsaturated Clay. Proc., 2nd International Conference on Expansive Soils, Texas A&M University Press, College Station, 1969, pp. 404-420.
9. J.E.B. Jennings and K. Knight. The Prediction of Total Heave from the Double Oedometer Test. Transactions, South African Institution of Civil Engineers, Johanne, Johannesburg, South Africa, Vol. 7, No. 9, 1957, pp. 13-19.
10. D.G. Fredlund, J.U. Hassan, and H.L. Filson. The Prediction of Total Heave. Proc., 4th International Conference on Expansive Soils, ASCE, New York, Vol. 1, 1980, pp. 1-17.
11. G.E. Blight and ESCOM-Lethabo Ad-hoc Foundation Committee. Power Station Foundations in Deep Expansive Soil. Proc., International Conference on Case Histories in Geotechnical Engineering, University of Missouri, Rolla, 1984a, pp. 77-86.
12. J.H. Schmertmann. The Undisturbed Consolidation Behaviour of Clay. Transactions, ASCE, Vol. 120, 1955, pp. 1201-1227.
13. I. Alpan. An Apparatus for Measuring the Swelling Pressure in Expansive Soils. Proc., 4th International Conference on Soil Mechanics and Foundation Engineering, London, England, Vol. 1, 1957, pp. 3-5.
14. J.W. Hilf. An Investigation of Pore Water Pressure in compacted Cohesive Soils. Report EM-761. Bureau of Reclamation, U.S. Department of the Interior, Denver, Colo., 1956.
15. R.E. Olson and L.J. Langfelder. Pore Water Pressure in Unsaturated Soils. Journal of the Soil Mechanics and Foundation Division. Proc., ASCE, New York, Vol. 91, No. SM4, 1965, pp. 127-160.

16. G. Kassiff and A. Ben-Shalom. Experimented Relationship Between Swell Pressure and Suction. Geotechnique, London, England, Vol. 21, No. 3, 1971, pp. 245-255.
17. A. Komornik, M. Livneh, and S. Smucha. Shear Strength and Swelling of Clays under Suction. Proc., 4th International Conference on Expansive Soils, Denver, Colo., Vol. 1, 1980, pp. 206-226.
18. P. Peter. Footings and Foundations for Small Buildings in Arid Climates--With Special Reference to South Australia. Chapters 4 and 8. South Australia Division, The Institution of Engineers, Adelaide, Australia, 1979.
19. D. Snethen. Characterization of Expansive Soils Using Soil Suction Data. Proc., 4th International Conference on Expansive Soils, Denver, Colo., Vol. 1, 1980, pp. 54-75.
20. R.G. McKeen. Design of Airport Pavements for Expansive Soils. Report FAA/RD-81/25, FAA, U.S. Department of Transportation, 1981.
21. D.H. van der Merwe. The Prediction of Heave from the Plasticity Index and Percentage Clay Fraction of Soils. The Civil Engineer in South Africa, Johannesburg, South Africa, Vol. 6, No. 6, 1964, pp. 203-207.
22. I.J.A. Brackley. An Empirical Equation for the Prediction of Clay Heave. Proc., 7th Asian Regional Conference on Soil Mechanics and Foundation Engineering, Haifa, Israel, Vol. 1, 1983, pp. 8-14.
23. A. Komornik and D. David. Prediction of Swelling Pressure of Clays. Proc., ASCE., Journal of Soil Mechanics and Foundation Engineering Division, New York, Vol. 25, No. SM1, 1969, pp. 209-225.
24. D. David and A. Komornik. Stable Embedment of Piles in Swelling Clay. Proc., 4th International Conference on Expansive Soils, Denver, Colo., Vol. 2, 1980, pp. 798-814.
25. R. Rama Rao and P. Smart. Significance of Particle Size Distribution Similarity in Prediction of Swell Properties. Proc., 4th International Conference on Expansive Soils, Denver, Colo., Vol. 1, 1980, pp. 96-105.
26. D.J. Henkel. Geotechnical Consideration of Lateral Stresses. Proc., ASCE, Speciality Conference on Lateral Stresses in the Ground and the Design of Earth Retaining Structures, ASCE, New York, 1970, pp. 1-49.
27. Z. Ofer. Lateral Pressure Developed During Compaction. Transportation Research Record 897, TRB, National Research Council, Washington, D.C., 1982, pp. 71-79.
28. B.O. Hardin. Plane Strain Constitutive Equations for Soils. Proc., ASCE, Journal of Geotechnical Engineering, ASCE, New York, Vol. 109, No. 3, 1983, pp. 388-407.
29. Z. Ofer. Laboratory Instrument for Measuring Lateral Soil Pressure and Swelling Pressure. Geotechnical Testing Journal, ASTM, Philadelphia, Pa., Vol. 4, No. 4, 1981, pp. 177-192.
30. E.W. Brooker and H.O. Ireland. Earth Pressure at Rest Related to Stress History. Canadian Geotechnical Journal, Vol. 2, No. 1, 1965, pp. 1-15.
31. A. Komornik and J.G. Zeitlen. An Apparatus for Measuring Lateral Soil Swelling Pressure in the Laboratory. Proc., 6th International Conference on Soil Mechanics and Foundation Engineering, Montreal, Canada, Vol. 1, 1965, pp. 278-281.
32. G. Kassiff, A. Etkin, and J.G. Zeitlen. Failure Mechanism of Canal Lining in Expansive Clay. Proc., ASCE, New York, Vol. 91, No. SM1, 1967, pp. 95-118.
33. G. Kassiff, M. Livneh, and G. Wiseman. Pavements on Expansive Soils. Jerusalem Academic Press, Jerusalem, Israel, 1969, pp. 43-158.
34. G. Kassiff and J.G. Zeitlen. Behaviour of Pipes Buried in Expansive Clays. Proc., ASCE, New York, Vol. 88, No. SM2, 1962, pp. 133-148.
35. G.E. Blight, and ESCOM-Lethabo Ad-hoc Foundation Committee. Uplift Forces Measured in Piles Expansive Clay. Proc., 5th International Conference on Expansive Soils, Adelaide, Australia, 1984b, pp. 240-244.
36. G.W. Donaldson. The Measurement of Stresses in Anchor Piles. Proc., 4th Regional Conference for Africa on Soil Mechanics and Foundation Engineering, Durban, South Africa, 1967, pp. C26-C34.
37. A. Komornik. The Effect of Swelling Properties of Unsaturated Clay on Pile Foundation. D.Sc. theses, The Technion, Haifa, Israel, 1962.
38. A.M. Robertson and F. von M. Wagener. Lateral Swelling Pressure in Active Clay. Proc., 6th Regional Conference for Africa on Soil Mechanics and Foundation Engineering, Durban, South Africa, 1975, pp. 107-114.
39. Z. Ofer, G.E. Blight, and A. Komornik. An In-Situ Swelling Pressure Test. Proc., 7th Asian Regional Conference on Soil Mechanics and Foundation Engineering, Haifa, Israel, Vol. 1, 1983, pp. 64-70.
40. Z. Ofer, G.E. Blight, and A. Komornik. Simultaneous Determination of In-Situ Swelling Pressure and Shear Strength. Proc., 5th International Conference on Expansive Soils, Adelaide, Australia, Vol. 1, 1984, pp. 80-84.

Publication of this paper sponsored by Committee on Environmental Factors Except Frost.

Prediction of Swelling Pressure and Factors Affecting the Swell Behavior of an Expansive Soil

YOUSRY M. MOWAFY and GUNTHER E. BAUER

ABSTRACT

Side friction and nonuniform distribution of moisture content over the soil specimen during saturation were the main sources of error in determining the swelling properties of an expansive soil. To decrease the frictional stresses between the soil and the confining ring of the oedometer apparatus, several techniques were used. A description of the test apparatus and the different techniques to reduce frictional effects are discussed. The merit and the theoretical background of each technique are evaluated. On the basis of experimental results of 28 soil specimens, a semiempirical equation is deduced to determine the value of swelling pressure in terms of initial dry density, initial water content, and clay content of the soil. This equation is compared with other methods of predicting swelling pressures. The semiempirical equation proposed in this paper can be used as a design guide to predict swelling pressures for the expansive soil studied.

Ramamurthy showed that side friction and nonuniform distribution of moisture over the soil specimen during saturation were the main sources of error in laboratory studies investigating the swelling properties of soil (1). By using a cylindrical soil specimen of a low height and a rubber membrane, the side friction could be considerably reduced. Laboratory research conducted by Ramakrishna showed that during the measurement of swelling percent and swelling pressure in an oedometer, the skin friction was eliminated by a thin rubber membrane between the soil and the confining ring that was coated with silicon grease (2).

El-Ramli found that the swelling pressure could be obtained from the following empirical equation (3):

$$P_s = 1{\cdot}2\ \gamma_d / w_s \quad (1)$$

where P_s is swelling pressure (kg/cm^2), γ_d is dry density (g/cm^3), and w_s is shrinkage limit. The effect of initial water content on swelling pressure is not considered in this equation.

Komornik and David proposed the following relationship to estimate the swelling pressure (4):

$$\text{Log } P_s = \overline{2}.132 + 0.0208\ w_L + 0.000665\ \gamma_d - 0.0269\ w_n \quad (2)$$

where

w_L = liquid limit,
w_n = natural water content,
P_s = swelling pressure (kg/cm^2), and
γ_d = dry density (g/cm^3).

This equation involves the main parameters that influence swelling pressure, but it is quite insensitive to variations in dry density; therefore, it should not be used if the dry density changes.

Zacharias and Ranganatham derived the following equation for the swelling pressure, p (kg/cm^2) (5):

$$P_s = a\ (SI) + b\ (w_L - w^*) + C\ (SI)\ (1/S_r) \quad (3)$$

where

SI = shrinkage index,
S_r = degree of saturation of specimen before start of test,
w^* = water content at S_r = 100 percent, and
a = -225/6.4, b = 290/6.4, and C = 1.2/6.4.

The dry density that has an important role to play in the swelling pressure is not included in this equation, and therefore the relationship is limited to dry densities ranging between 17 and 18 kN/m^3. This restricts the application of this equation considerably.

Dedier produced two equations for the relation between swelling pressure, dry density, and clay percentage as follows (6):

$$\text{Log } P_s = 2.55\ \gamma_d/\gamma_w - 1.705 \quad (4)$$

$$\text{Log } P_s = 0.0294C - 1.923 \quad (5)$$

where C is clay content (%), γ_w is density of water (g/cm^3), and P_s is given in kg/cm^2.

Neither Equation 4 nor Equation 5 considers the initial water content of the soil. Because the initial water content has a great effect on the value of both swelling percent and swelling pressure, the equations cannot be applied to soils having different initial water contents.

Rabba produced two equations for the relationship between swelling pressure, initial dry density, and clay percentage in cases of sandy-clay and silty-clay soils as follows (7):

For sandy-clay soils

$$\text{Log } P_s = 2.17\ (\gamma_d + 0.084C) - 3.91 \quad (6)$$

For silty-clay soils

$$\text{Log } P_s = 2.5\ (\gamma_d + 0.006C) - 4 \quad (7)$$

Units of P_s and γ_d are given in the previous equations. Equations 6 and 7 are limited to an initial water content of 8 percent.

The purpose of this laboratory study was to investigate the effect of side friction of the swelling behavior of an expansive soil found in Nasr City, a satellite city of Cairo, Egypt [for a detailed description of this soil see the paper titled "Treatment of Expansive Soils: A Laboratory Study" elsewhere in this record and Mowafy et al. (8)].

TEST APPARATUS AND TECHNIQUE

The ring of the oedometer used in the swelling tests had an internal diameter of 63 mm and a height of 25 mm. The swelling pressure is defined as the external pressure required to consolidate a preswelled sample to its initial void ratio.

Preparation of Test Specimens

An amount of soil was oven dried at a constant temperature (105 to 110° C) for 24 hr. The sample was mixed with the calculated amount of water to give the required initial water content, then it was kneaded thoroughly by hand until it became homogeneous (uniform color). The soil was then pressed into the mold. A pressure pad was applied at the sample surface. The specimen was then statically compacted until the required height corresponded to the specified density. Filter papers and porous plates were applied at the top and bottom of the specimen.

After preparation of the specimen, the mold containing the soil was put into the loading apparatus. An initial load of 100 kPa was applied and the reading of the dial gauge was recorded. After the pressure application, the specimen was submerged in distilled water. As soon as water was added the deformation of the specimen was recorded. The test was continued until the deformation of the specimen ceased. This generally occurred after 96 hr. After the swelling was complete the specimen was reconsolidated to its original void ratio. The corresponding pressure was termed the swelling pressure of the soil.

METHODS OF REDUCING FRICTIONAL STRESSES

There are several components of stresses that are brought into effect by the preparation of the soil sample (compaction) and by the loading procedures. The sum of the radial stresses is the confining pressure of the soil specimen that the confining ring exerts on the soil. During the compaction of the soil specimen inside a mold, a radial stress, σ_i, is exerted on it. An additional horizontal stress ($\Delta\sigma_{h1}$) will act on the circumference of the soil specimen due to the swelling of the soil. If the soil specimen is subjected to an initial preload, this again will produce a radial stress ($\Delta\sigma_{h2}$) due to the consolidation of the soil. The resultant normal stress (σ_n), when multiplied by the coefficient of friction (μ) between the soil and the confining ring material, is the tangential stress τ, that will hinder the free swell of the soil. Complete elimination of this tangential stress is not possible, but several methods were investigated to study the effect of side friction on the swelling properties of the soils investigated: These include (a) the conventional method, (b) the filter paper method, and (c) the rubber membrane method.

Conventional Method

This method did not differ appreciably from the procedure in a standard oedometer test. No attempt was made to reduce the side friction effects on the soil specimens, and the results were used as reference values to which the other test results were compared.

Filter Paper Method

Before the soil was poured into the mold, the mold was lined with filter paper. After compaction, the specimen was extracted and the filter paper was carefully removed. The extracting force was determined for the cases of no filter paper, one layer of filter paper, and two and three layers. The extracting force for the various conditions and the resulting amount of swell are given in Table 1 for one initial moisture and preload pressure. It is clear

TABLE 1 Extracting Force After Compaction

Property of Specimen	Number of Filter Papers	Extracting Force, N	Swelling Percent
γ_d = 15.9 kN/m^3	None	650	6
w_i = 15%	One	350	6.6
h_i = 15 mm	Two	73	7.2
P_o = 100 kPa	Three	40	7.3

from the results given in Table 1 that side friction has a marked effect on the free swell of the soil. The horizontal normal stress after compaction and before swelling can be given by

$$\sigma_n = K\sigma_i \tag{8}$$

The corresponding shear stress, τ, is equal to zero, because no movement (swell) has occurred to mobilize it. The value K in Equation 8 is a coefficient to incorporate the effect of the filter papers. From the results given in Table 1 and similar tests on specimens of various initial moisture contents, the K-values were determined as follows:

K = 1 (without filter paper),
K = 0.5 (with one filter paper),
K = 0.1 (with two filter papers), and
K ~ 0 (with three filter papers).

As soon as swelling of the soil begins, the confining stress, σ_n can be expressed as

$$\begin{aligned} \sigma_n &= K\,(\sigma_i - \Delta\sigma_i) + \Delta\sigma_{h1} \\ \tau &= \mu\sigma_n \end{aligned} \tag{9}$$

where $\Delta\sigma_i$ is the increment of vertical stress on the specimen due to swelling. All other terms in the preceding equations have been defined earlier. After completion of the swell test, the specimen is reconsolidated to its initial void ratio. The confining and shear stresses representing this condition can be given as

$$\begin{aligned} \sigma_n &= K\,(\sigma_i - \Delta\sigma_i) + \Delta\sigma_{h1} + \Delta\sigma_{h2} \\ \tau &= \mu\sigma_n \end{aligned} \tag{10}$$

Rubber Membrane Method

In this method the inside of the mold was lubricated with silicon grease and lined with a thin rubber membrane. Compaction was performed as outlined earlier. The soil specimen was not extracted from the mold as in the case of the filter paper method.

The confining (radial) stresses and the shear stresses at the contact surface between soil and mold can be expressed as follows:

After compaction and before swelling begins

$$\sigma_n = \sigma_i$$
$$\tau = 0 \quad (11)$$

During swelling

$$\sigma_n = \sigma_i - \Delta\sigma_i + \Delta\sigma_{h1}$$
$$\tau = \alpha\,(\mu\sigma_n) \quad (12)$$

where α is coefficient of friction between soil and membrane (for rubber $\alpha < 1$). After the specimen has been reconsolidated to its original void ratio

$$\sigma_n = \sigma_i - \Delta\sigma_1 + \Delta\sigma_{h1} + \Delta\sigma_{h2}$$
$$\tau = \alpha\,(\mu\Delta_n) \quad (13)$$

To evaluate the various radial stresses acting on the soil specimen during the several phases of a complete swelling test, a special instrumented compaction ring is needed. Such a cell has not yet been built to the knowledge of the authors.

PRESENTATION AND ANALYSIS OF RESULTS

Effect of Filter Paper on Swelling Behavior

Figure 1 shows that the relationship between the extracting force and swelling percent is linear in

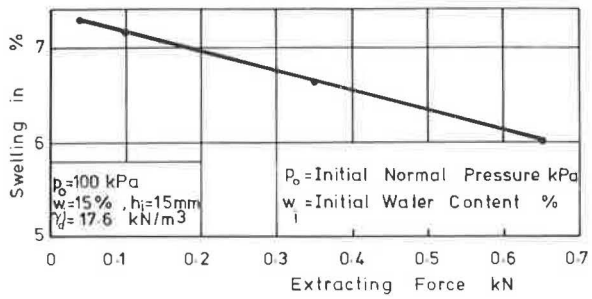

FIGURE 1 Relationship between swelling percent and extraction force.

the case where filter papers were used. Furthermore, this figure indicates that the decrease in the extracting force is accompanied by an increase in the swelling percent. Such phenomenon may be attributed to the horizontal soil stress that produces a tangential stress and that will counteract the free swell of the soil.

Figure 2 shows the relationship between swelling percent and the initial pressure for different numbers of filter papers used. It indicates that the swelling pressure decreases with the increase in the extracting force. In general, it appears that the swelling pressure increases with the number of filter papers used and the minimum swelling pressure corresponds to the case where no filter paper was used.

Effect of Rubber Membrane on Swelling Behavior

The relationship between swelling percent and water content for the conventional and the rubber membrane methods are shown in Figures 3 and 4. As expected,

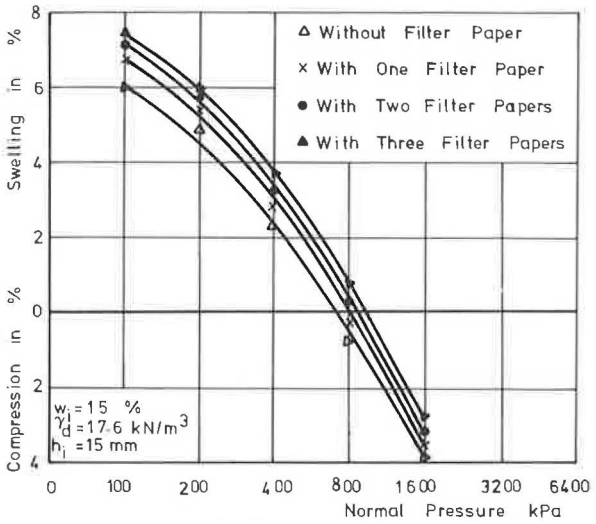

FIGURE 2 Relationship between swelling percent and normal pressure.

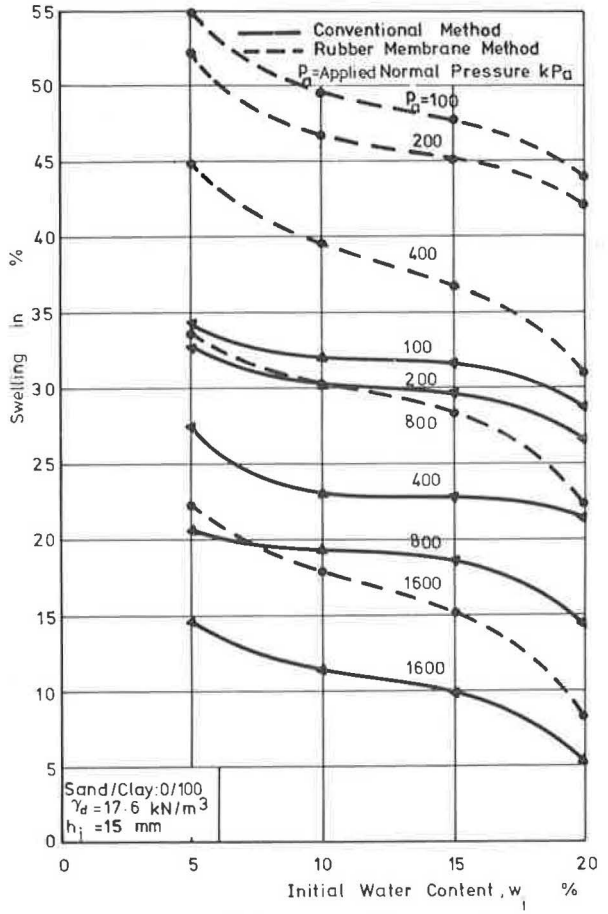

FIGURE 3 Relationship between swelling percent and initial water content.

the swelling percent is greater in the rubber membrane method than in the case where no membrane was used. For instance, at an initial water content of 5 percent and initial normal pressure of 100 kPa at a clay content of 100 percent, the increase in swelling percent is about 60 percent. Furthermore, such increase in the swelling percent is less pronounced

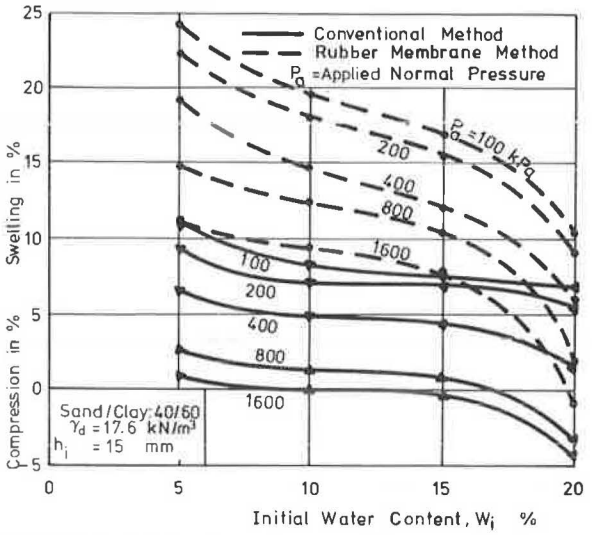

FIGURE 4 Relationship between swelling percent and initial water content.

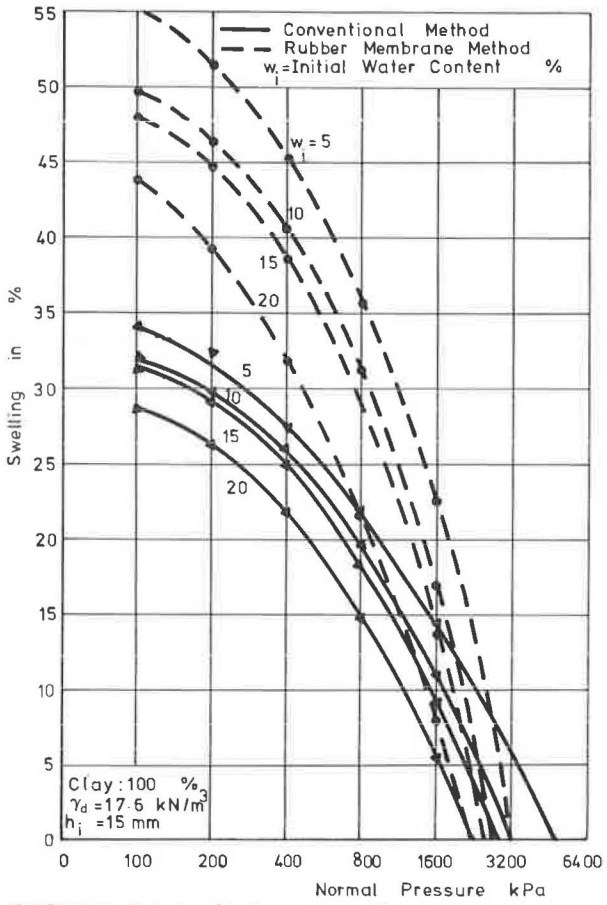

FIGURE 5 Relationship between swelling percent and normal pressure.

with the increase in initial applied load for the same initial water content. For instance, in the case of an initial water content of 10 percent, the swelling percent is 50 percent for the rubber membrane method and only 33.5 percent for the conventional method. In both cases the initial normal pressure was 100 kPa. In a similar comparison in which the normal pressure was 1600 kPa, the amount of swell was 18 percent in the case in which a rubber membrane was used compared to 11 percent when the conventional method was used.

In the case of a clay content of 100 percent, the swelling percent is considerably higher than that for a clay content of 60 percent. It is obvious that the increase in the swelling percent when the rubber membrane is used is due to the reduction of the tangential stresses.

From Figure 5, which shows the relationship between swelling percent and initial pressure, the following observations can be made. At high initial water contents there is no difference in the swelling pressure regardless if the rubber membrane or the conventional method is used. On the contrary, at low initial water contents, the swelling pressures are lower when rubber membranes were used than the corresponding values when the conventional method was used. For instance, at 20 percent initial water content, the swelling pressure is 2400 kPa for both the rubber membrane and the conventional methods, whereas at 5 percent initial water content, the swelling pressure is 3200 kPa for the rubber membrane method and 4800 kPa for the conventional method.

NEW SWELLING PRESSURE EQUATION

A general equation for the swelling pressure is proposed as follows:

$$\text{Log } p_s = A\gamma_d + Bc - Dw_n - E \qquad (14)$$

where

p_s = swelling pressure in MPa,
γ_d = dry unit weight in kN/m³,
c = clay content in percent,
w_n = initial water content in percent, and
A, B, D, and E are constants to be determined experimentally.

From the 28 specimens tested having various clay, silt, and sand contents and different dry densities and initial water contents, a multiple regression analysis was performed using the least square method. From this analysis the constants for A, B, D, and E were determined as follows:

$A = 1.366$
$B = 8.951 \times 10^{-3}$
$D = 2.179 \times 10^{-2}$
$E = 2.840$

Coefficient of correlation: $R = \sqrt{R^2} = 0.71$
Coefficient of determination: $R^2 = 0.50$
Standard deviation: $\sigma^2 = 0.071$
Standard error or regression: $\sigma = 0.27$

Substituting the values for the constants A, B, D, and E in the general relationship will yield the following equation for the swelling pressure for the soil from Nasr City:

$$\log p_s = 1.366\ \gamma_d + 8.951\ (10^{-3})\ C - 2.179\ (10^{-2})\ \omega_n - 2.840 \qquad (15)$$

This equation should be used with caution and it is recommended that it be compared to measurements from field tests.

Figures 6-8 show a comparison between the new equation and equations suggested by various researchers. It should be noted that most equations to predict swelling pressures are linear in nature and are partly empirical. Only the equation by Komornik and David and the equation proposed by the authors take the initial water content into consideration.

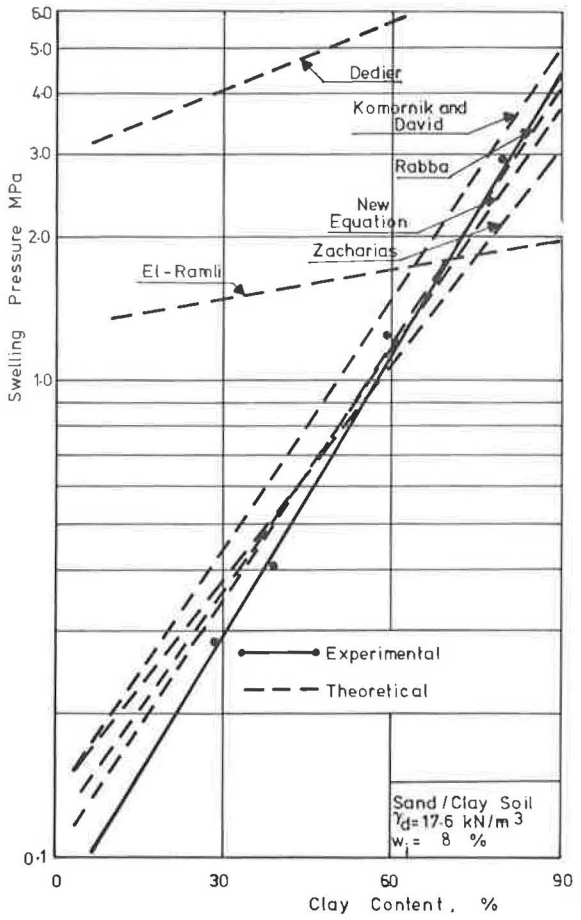

FIGURE 6 New equation plotted in relationship to other equations.

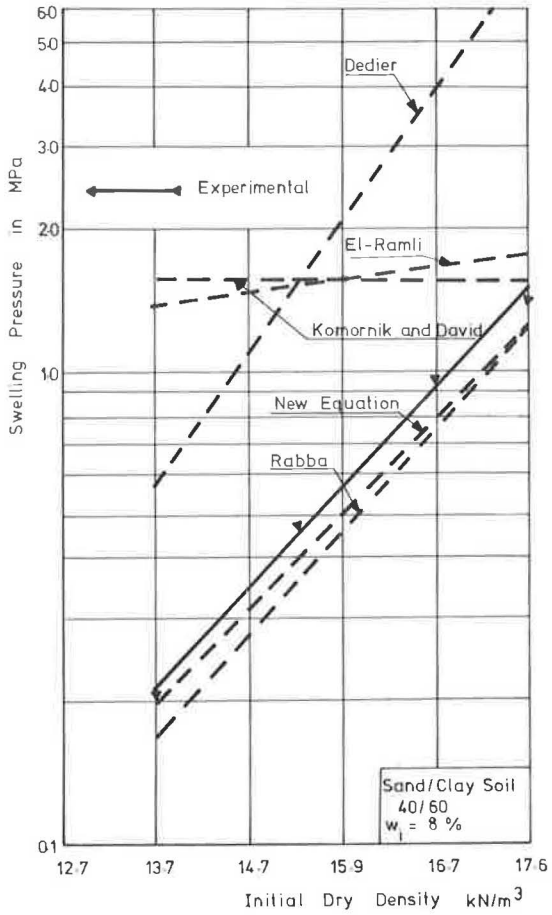

FIGURE 7 New equation plotted in relationship to other equations.

As has been shown, the initial water content has a marked effect on both the resulting swelling pressure and on the amount of swell for the soils investigated.

The proposed relationship (Equation 15) can be used in design problems to estimate the expected swelling pressures for the expansive soil found in Nasr City. It should be tested, however, for other expansive soils before a universal application can be advocated.

CONCLUSIONS

From the test results and the subsequent analysis and discussion of results, the following conclusions appear warranted.

1. Frictional stresses that are mobilized between a soil specimen and a rigid confining ring during swelling of the soil cannot be eliminated completely.
2. Side frictional effects can be reduced considerably during swelling by lining the oedometer ring with filter papers or with a thin rubber membrane. One of the two methods is therefore recommended in order to determine the swell properties of expansive soils using an oedometer ring.
3. A semiempirical relationship between the swelling pressure, the dry unit weight, the initial moisture content, and the clay content of the clay was given. This equation may be used to estimate the

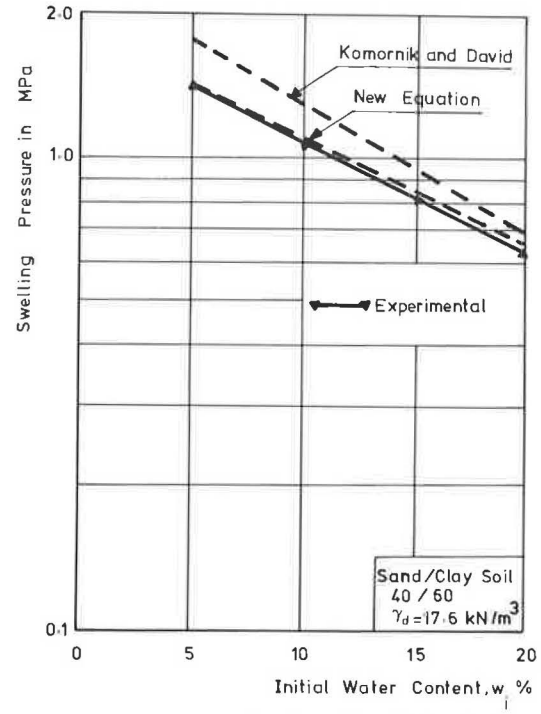

FIGURE 8 New equation plotted in relationship to other equations.

swelling pressures to be expected in the field for the soil investigated. It is speculated that the reduction of swell due to the mobilization of frictional stresses in a one-dimensional oedometer is equivalent to a reduction in soil heave in the field due to radial expansion (axisymmetric swelling).

REFERENCES

1. T. Ramamurthy. Proc., Symposium on Strength and Deformation Behaviour of Soils, Vol. 2, 1972, pp. 41-42.
2. S. Ramakrishna. Effect of Structure on Swelling and Swelling Pressure Characteristics of Black Cotton Soil. Proc., Symposium on Strength and Deformation Behaviour of Soils, 1972.
3. A.H. El-Ramli. Swelling Characteristics of Some Egyptian Soils. Journal of the Egyptian Society of Engineering, Vol. 4, No. 1, 1965.
4. A. Komornik and D. David. Prediction of Swelling Pressure of Clays. Proc., Journal of Soil Mechanics and Foundation Engineering Division, ASCE, New York, Vol. 95, No. 1, 1969, pp. 209-225.
5. G. Zacharias and B.V. Ranganatham. Swelling and Swelling Characteristics of Synthetic Clays. Proc., Symposium on Strength and Deformation Behaviour of Soils, Vol. 1, 1972, p. 129.
6. G. Dedier. Prediction of Potential and Swelling Pressure of Soils. Proc., 8th International Society for Soil Mechanics and Foundation Engineering, Vol. 22, 1973, p. 67.
7. S. Rabba. Factors Affecting Engineering Properties of Expansive Soils. M.S. thesis, Al-Azhar University, Cairo, Egypt, 1975.
8. Y.M. Mowafy. Study of Some Engineering Properties of Swelling Soils. M.S. thesis, Al-Azhar University, Cairo, Egypt, 1978.

Publication of this paper sponsored by Committee on Environmental Factors Except Frost.

Role of Mineralogical Composition in the Activity of Expansive Soils

MOHAMED A. EL SOHBY, SAYYED A. RABBA, and OSSAMA MAZEN

ABSTRACT

Heave-susceptible soils often contain swelling clay minerals. Knowledge of the mineralogy of soils and rocks plays a large part in understanding the mechanical behavior of these materials. This knowledge is used to the best advantage when it is combined with information about the engineering properties and geological history of the deposits. The object of this paper is to use the knowledge of microstructure and composition of expansive clayey soils to evaluate the activity as defined by various researchers. Therefore, different kinds of clayey soils were investigated for their index properties, activities, and mineralogical compositions. Samples for study were taken from Madinet Nasr, an area in the suburbs of Cairo where expansive soil deposits predominate. The activities of soil samples were determined by using formulae proposed by different researchers. The values of activities were then correlated to the mineralogical compositions of tested soils. The study indicated that the activity is a property of clay mineral rather than a property of whole sample and confirmed the effect of nonclay mineral or coarse-grained fraction on activity values of expansive soil deposits.

MINERALOGY OF EXPANSIVE SOILS

Expansive clays and clay bed rock formations are made up of several mineral constituents. In Egypt the responsible clay minerals are generally detrital and have been inherited from older rocks. Elsewhere swelling clay minerals have formed by in situ weathering of parent rocks as, for example, in South Africa. The amount of potential volume change is dependent on the mineralogical composition: clay mineral type, clay mineral content, and exchangeable ion.

Kerr has indicated that approximately 15 minerals are ordinarily classed as clay minerals (1). These minerals possess in common an extraordinary ability to attract to their surface dipolar water molecules and various cations. Lambe and Whiteman found that swellability varies with the type of clay mineral; it decreases in the order montmorillonite, illite, attapulgite, and kaolinite (2). Mitchel found that

most expansive soils contain montmorillonite and vermiculite (3).

Many investigators studied the effect of the amount of clay on swelling (3-7) and agreed that the amount of swell and swelling pressure increases with the increase of clay content.

The effect of exchangeable ion on swellability was also studied by various researchers whose work many be summarized as follows (2,8-11). For soils containing expansive clay minerals, the type of exchangeable ion exerts a controlling influence over the amount of expansion that takes place in the presence of water. Therefore, researchers are in complete agreement in considering the mineralogical identification as the primary method for classifying potentially expansive soils. The techniques for mineralogical identification vary. They include microscopic examination, x-ray diffraction, differential thermal analysis, dye adsorption, and chemical analysis.

ACTIVITY OF EXPANSIVE SOILS

Tests for mineralogical identification are generally elaborate; the specialized apparatus required are costly, and test results require expert interpretation. Therefore, a substantial amount of research has been conducted to replace the mineralogical identification with indirect methods for the evaluation of swelling potential of expansive soils. This could be achieved by using some simple soil property tests as primarily indicators of the presence of expansive clay minerals. Such tests may include Atterberg limits, free swell, and colloid content.

The activity method of evaluating the swelling potential of expansive soils appears to be an improvement over the preceding indicators in that the effect of both plasticity index and clay content enter in the identification of different clay minerals and the indirect evaluation of swelling potential.

Measurement of Activity

Skempton defined the activity as the ratio of the plasticity index to the abundance of clay content expressed as the percent dry weight of the minus 2 micron fraction of the sample (4). Therefore the activity A = PI/C, where PI is the plasticity index and C is the clay content.

Seed, Woodward, and Lundgren conducted further studies on a large number of artificially prepared sand clay mineral mixtures (12-14). They found that the line representing the relationship between the plasticity index and percent clay size does not always pass through the origin. It may intersect the percent clay size axis at values as high as 10 percent. Thus they introduced a modification to Skempton's definition in the form of A = PI/C-n, where n is approximately equal to 5 for natural soils and equal to 10 for artificial soils.

El Sohby, while studying a large number of samples with different contents of clay, silt, and sand (7), noted the same observations made by Seed et al. However, he found that the PI-C relationship may intersect either the PI-axis or the C-axis according to the grain fraction coarser than 2 micron in the soil sample. Thus the deviation from the origin of the straight line representing the PI-C relationship was attributed to the effect of coarse-grained fraction.

To incorporate the effect of coarse-grained fraction, El Sohby presented a new modification of the definition of activity as follows:

$$A = PI\ (100 \pm n)/100\ (C \pm n)$$

where n is the intercept of the clay percent axis.

CURRENT STUDY

The aim of this study is to analyze the factors that affect activity values and to evaluate the different methods for their measurement in the light of the mineralogical composition.

Therefore, a number of clayey soil samples representing different mineralogical compositions were investigated. First, the activities of the clayey soil samples were determined according to each of the previously mentioned three formulas. Then these activities were correlated to the mineralogical compositions as determined by the use of x-ray diffraction analysis.

Test Program

The investigation was carried out on 11 clayey soil samples selected from different locations and depths in Madinet Nasr, an arid, newly developed area located 8 km north-east of Cairo. Expansive clayey soils were found to occur with a relatively high frequency in this area.

Specimen Preparation

Two groups of specimens were tested during the investigation: (a) specimens of samples in their natural state and (b) prepared specimens consisting entirely of clay fraction (particles less than 2 micron). The second group was obtained by separation after deposition in distilled water of the clay fraction from soils of the first group.

Testing

The two groups of soil specimens were tested for the following properties (see Table 1 and Figure 1):

1. Mineralogical composition,
2. Atterberg limits for whole sample,
3. Atterberg limits for particles less than 2 micron, and
4. Grain size distribution and clay content.

TEST RESULTS AND ANALYSIS

Activity and Clay Mineral Type

Various researchers have correlated the activities with the type of clay mineral (2-4,15). In this study, the mineralogical types of tested soils were correlated with their activities as determined by each of the three formulas given by Skempton, El Sohby, and Seed et al. (4,7,13) (Table 2).

Comparing the mineralogical composition of each sample with its activity as determined from each of the previously mentioned formulas, it was found that the formula proposed by El Sohby is the only one that can provide a good correlation between type of clay mineral and activity.

For example, Soils G1, C, and G3 have identical mineralogical compositions (Table 2). Their activities, when estimated according to the El Sohby formula, are 0.78, 0.80, and 0.84, respectively. However, their activity values become 0.0, 0.93, and 0.73, respectively, when estimated according to Skempton, and 0.0, 0.79, and 1.07 when estimated

TABLE 1 Summary of Mineralogical Composition of Tested Soils

Sample Number	Clay content (particles less than 2 micron)	Clay mineral	Non-clay mineral	
			Silicate	Salt & metal minerals
B	20%	Sodium (M-V) 20%	25%	55%
G3	62%	Calcium (M-V) 62%	16%	22%
G1	46%	Calcium (M-V) 46%	25%	29%
A	59%	Calcium (M-V) 42% + Kaolinite 17%	24%	17%
C	6%	Calcium (M-V) 6%	31%	63%
G2	44%	Potassium (M-V) 44%	26%	30%
E	50%	Potassium (M-V) 39% + Kaolinite 11%	34%	16%
F	5%	Potassium (M-V) 5%		
H2	48%	Potassium (M-I) 41% + Kaolinite 4% + Illite 3%	26%	26%
H1	34%	Potassium (M-I) 26% + Kaolinite 3% + Illite 6%	26%	30%

(M-V): Montmorillonite - Vermiculite

(M-I): Montmorillonite - Illite

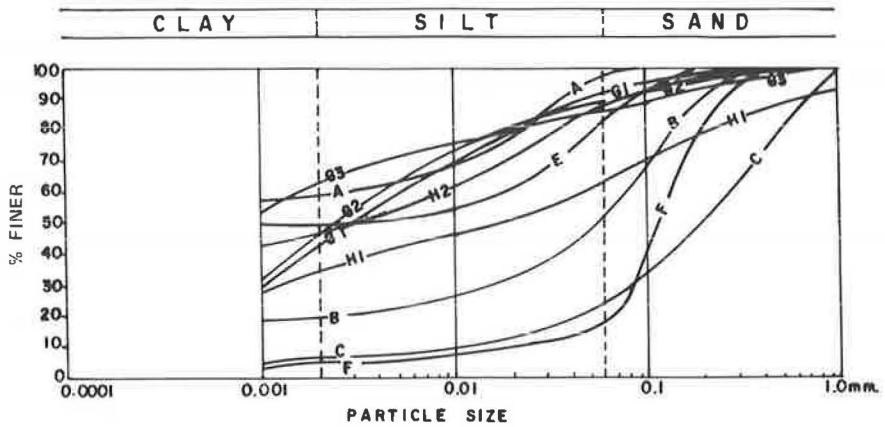

FIGURE 1 Grain size distribution curves of tested samples.

according to Seed et al. Also, the mineralogical composition of Soils F and G2 is the same, but their activity values are only similar if calculated on the basis of the El Sohby formula--they are 0.73 and 0.71, respectively. On the other hand, these values are 0.0 and 0.89 when determined by the Skempton formula, and 0.0 and 1.0 when determined using Seed et al. (Table 2).

Furthermore, a good interpretation of results could be achieved when the El Sohby formula was used. For example, Soils G1, C, and G3 consist of 100 percent calcium (montmorillonite-vermiculite); their average activity is 0.81. Soil A consists of 71 percent calcium (montmorillonite-vermiculite) plus 29 percent kaolinite; its value of activity is 0.75. Also, Soil F consists of 100 percent potassium (montmorillonite-vermiculite), and its value of activity is 0.73. When, in Soil E, the 21 percent

TABLE 2 Clay Mineralogy and Activity of Tested Soils

Soil No.	Mineralogical Composition	Clay Content "C" % < 2um	Plast. Index "PI"	PI of Part <2um	Activity "A"		
					Skempton (1953)	Seed et al (1962)	El Sohby (1981)
B	Sodium (Mont-Verm)	20	16	153	0.80	1.07	1.53
G3	Calcium (Mont-Verm)	62	45	84	0.73	0.79	0.84
C		6	0	80	0	0	0.80
G1		46	43	78	0.93	1.05	0.78
F	Potassium (Mont-Verm)	5	0	73	0	0	0.73
G2		44	39	71	0.89	1.0	0.71
A	Calcium (Mont-Verm) 71% + Kaolinite 29%	59	54	75	0.90	1.0	0.75
E	Potassium (Mont-Verm) 79% + Kaolinite 21%	50	36	57	0.72	0.80	0.57
H1	Potassium (M-I) 75% +Illite 16% +Kaolinite 9%	34	43	60	1.26	1.48	0.60
H2	Potassium (M-I) 85% +Illite 7% +Kaolinite 8%	48	39	70	0.81	0.91	0.70
D	-	13	24	76	1.86	3.0	0.76

kaolinite existed in addition to the 79 percent potassium (montmorillonite-vermiculite), the activity was reduced to 0.57 (Table 3).

Activity and Exchangeable ion

Researchers appear to be in complete agreement with the contention that ion hydration plays a large part in water uptake by clay mineral (2-4,8,9).

Skempton stated that the activity of sodium montmorillonite is about five times greater than the activity of calcium montmorillonite (4). Lambe and Whiteman found that swellability depends considerably on the exchangeable ion, but not in the same way with each mineral; lithium (Li^+) and sodium (Na^+) clays are the more expansive from (2). Rosenqvist indicated that lithium and sodium montmorillonites have abnormally high power because their cations cannot keep the single sheets of the lattice together (8). In the larger alkali ions, namely potassium, the internal swelling property is absent. Gillot stated that calcium montmorillonite commonly takes up only two layers of water, whereas sodium montmorillonite imbibes more water, in variable amounts.

This was only confirmed in this study when the El Sohby formula was used for activity values of tested soils (Table 4). For example, Soils B, G1, C, G3, F, and G2 are mixed layers of montmorillonite-vermiculite, but the exchangeable ion varies. It was found that the results of activities vary with the variation of the cation as cited in the literature. The activity of 1.53 of Soil B with sodium as the cation is the highest value compared with 0.78, 0.8, and 0.84 for Soils G1, C, and G3 with calcium as the cation, and 0.73 and 0.71 for Soils F and G2 with potassium as the cation.

On the other hand, when the values of activity were obtained using Skempton's formula or the modified Seed et al. formula, the effect of exchangeable ion on the value of activity could not be verified. As indicated in Table 2, the activity of Soil B with sodium as the cation is less or almost the same as the activity of Soil G1 with calcium as the cation. Also, the activity of Soil C with calcium as the cation is zero, whereas the activity of Soil G2 with potassium as the cation is 0.89 and 1.0.

Activity and Non-Clay Mineral

Because the plasticity index reflects the capability of a certain soil to absorb water, which, in turn, is affected by the surface area of soil particles, it may be expected that silts need a smaller amount of clay than sands to develop plasticity.

TABLE 3 Effect of Presence of Kaolinite on Activity of Tested Soils

Mineralogical composition	Calcium (Mont-Verm) 100%			Calcium (Mont-Verm) 71% + Kaolinite 29%	Potassium (Mont-Verm) 100%	Potassium (Mont-Verm) 79% + Kaolinite 21%
Soil sample	G1	C	G3	A	F	E
Activity	0.78	0.8	0.84 (average 0.81)	0.74	0.73	0.57

Mont.: Montmorillonite

Verm.: Vermiculite

TABLE 4 Activity and Exchangeable Ions

Type of clay mineral	(Montmorillonite - Vermiculite) mixed layers					
Type of Exchangeable cation	Sodium Na^+	Calcium (Ca^{++})			Potassium K^+	
Activity	1.53	0.78	0.80	0.84	0.73	0.71
Average value	1.53	0.81			0.72	
Soil No.	B	G1	C	G3	F	G2

El Sohby, by studying a large number of prepared soils consisting of different percentages of clay, silt, and sand, noticed that a straight line representing the PI-C relationship may intersect the clay content percent axis at either a positive or a negative value depending on the type of the non-clay mineral (coarse-grained fraction) in the soil (7).

It is observed in this study that the lines representing the PI-C relationship intersect the C-axis at points of ±n (see Figure 2). It is noted

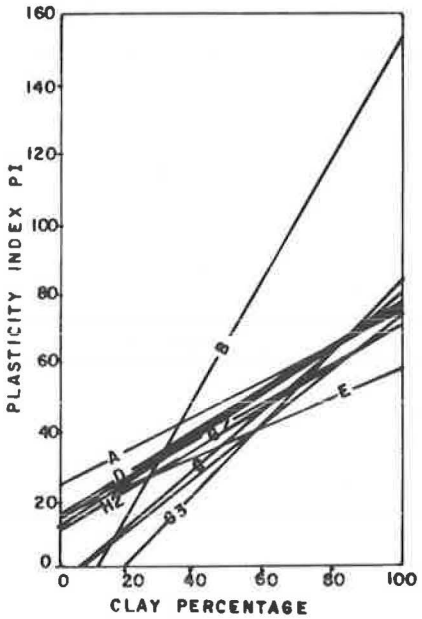

FIGURE 2 Relationship between plasticity index and clay percentage.

that for soils with relatively high percentages of sand (Figure 3), these lines intersect the C-axis at points of +n, whereas for soils with relatively low percentages of sand the lines intersect the C-axis at points of -n (see Figure 4).

Figure 5 shows the relationships between plasticity index of clay mineral and clay content for idealized soils of different mineralogical composition. In this case these relationships are represented by straight lines passing by the origin. The slope of each line represents the activity of the clay mineral.

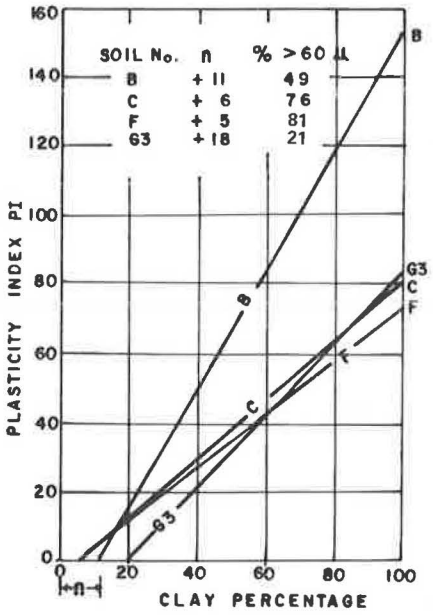

FIGURE 3 Influence of coarse-grained fraction on the relationship between plasticity index and clay percentage (soils of relatively high percentage sand).

CONCLUSIONS

From the foregoing study of the mineralogical composition of clayey soil deposits and their relationships to their activity values as measured using formulas given by different investigators, the following conclusions may be drawn.

1. The role of mineralogical composition of expansive soils (clay minerals and non-clay minerals) in the values of activity is evidenced and available knowledge is confirmed.
2. There are two criteria for activity values of clayey soils: (a) activity values of the 100 percent clay content soils and (b) activity values of natural soils.
3. The formula proposed by Skempton is directly related to the 100 percent clay content soils (4). The blind use of this formula could yield unreliable activity values.
4. For natural soils, the incorporation of the coarse-grained fraction (as an important parameter) in the determination of activity is an essential

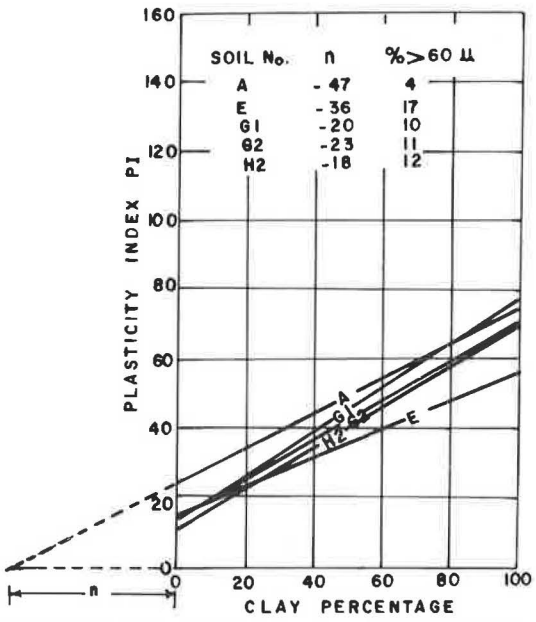

FIGURE 4 Influence of coarse-grained fraction on the relationship between plasticity index and clay percentage.

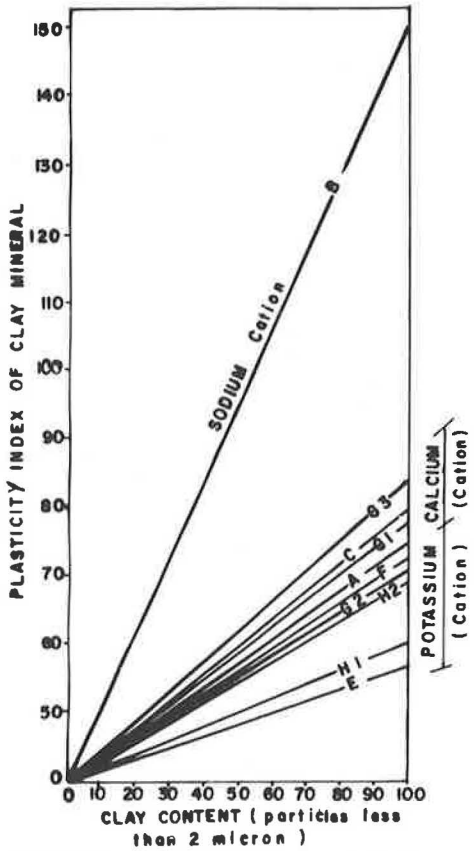

FIGURE 5 Relationship between plasticity index of clay mineral (particles < 2 um) and clay content (idealized soil).

prerequisite to developing accurate values. In this study, this could only be achieved when the formula proposed by El Sohby was used (7).

5. It is suggested that charts based on activity for the determination of potential expansiveness of clayey soils be reevaluated with the effect of coarse-grained fraction parameter considered (4,15-17).

REFERENCES

1. P.F. Kerr. Physico-Chemical Properties of Soils: Clay Minerals. Journal of the Soil Mechanics and Foundations Divisions, ASCE, Vol. 85, No. SM2, 1959, pp. 73-78.
2. T.W. Lambe and R.V. Whiteman. The Role of Effective Stress in the Behavior of Expansive Soils. Quarterly of the Colorado School of Mines, Vol. 54, No. 4, 1959, p. 39.
3. J.K. Mitchel. Fundamentals of Soil Behaviour. John Wiley and Sons, New York, 1976.
4. A.W. Skempton. The Colloidal Activity of Clays. Proc., 3rd International Conference on Soil Mechanics and Foundation Engineering, Vol. 1, Zurich, Switzerland, 1953, pp. 57-67.
5. W.G. Holtz. Expansive Clays--Properties and Problems. Quarterly of the Colorado School of Mines, Vol. 54, No. 4, 1959, p. 89.
6. S.A. Rabbaa. Factors Affecting Engineering Properties of Expansive Soils. M.S. thesis, Al-Azhar University, Cairo, Egypt, 1975.
7. M.A. El Sohby. Activity of Soils. Proc., 10th International Conference on Soil Mechanics and Foundation Engineering, Vol. 1, Stockholm, Sweden, 1981, pp. 587-591.
8. I.Th. Rosenqvist. Physico-Chemical Properties of Soils: Soil Water Systems. Journal of the Soil Mechanics and Foundation Division, ASCE, Vol. 85, No. SM2, 1959, pp. 31-53.
9. J.E. Gillot. Clay in Engineering Geology. Elsevier Publishing Co., Amsterdam, The Netherlands, 1968.
10. R.E. Grim. Clay Mineralogy. McGraw Hill, New York, 1968.
11. M.A. El Sohby and S.O. Mazen. Mineralogy and Swelling of Expansive Clayey Soils. Geotechnical Engineering, Journal of the Southeast Asian Society of Soil Engineering, Thailand, Vol. 14, 1983, pp. 79-87.
12. H.B. Seed, R.J. Woodward, and R. Lundgren. Prediction of Swelling Potential for Compacted Clays. Journal of the Soil Mechanics and Foundations Division, ASCE, Vol. 88, No. SM3, 1962, pp. 53-87.
13. H.B. Seed, R.J. Woodward, and R. Lundgren. Clay Mineralogical Aspects of the Atterberg Limits. Journal of the Soil Mechanics and Foundations Division, ASCE, Vol. 90, No. SM4, 1964a, pp. 107-131.
14. H.B. Seed, R.J. Woodward, and R. Lundgren. Fundamental Aspects of Atterberg Limits. Journal of the Soil Mechanics and Foundations Division, ASCE, Vol. 90, No. SM6, 1964b, pp. 75-105.
15. D.H. van der Merwe. The Prediction of Heave from the Plasticity Index and Percentage Clay Fraction of Soils. The Civil Engineer in South Africa, Vol. 6, No. 6, 1964.
16. C.M.A. De Bruyn, L.E. Collins, and A.A.E. Williams. The Specific Surface, Water Affinity and Potential Expansiveness of Clays. Clay Minerals Bulletin, Vol. 3, 1957, pp. 120-128.
17. D.H. van der Merwe. Current Theory and Practice for Building on Expansive Clays. Proc., 6th, Regional Conference for Africa on Soil Mechanics and Foundation Engineering, Durban, South Africa, Vol. 2, 1975, pp. 166-167.

Publication of this paper sponsored by Committee on Environmental Factors Except Frost.

Treatment of Expansive Soils: A Laboratory Study

YOUSRY M. MOWAFY, GUNTHER E. BAUER, and FAHIM H. SAKER

ABSTRACT

Excessive heave and settlements that are associated with the volume changes of expansive soils can cause considerable distress to civil engineering structures. Even structures such as highway embankments and roadways that are generally insensitive to small vertical movements are subject to high maintenance costs if constructed on expansive soils. It has been reported that a small amount of settlement or heave over a short length of road is intolerable for high-speed highways (1-5). A laboratory investigation to reduce the swelling properties of the expansive soils found in Nasr City, a satellite community of Cairo, Egypt, is reported in this paper. Three techniques to reduce the amount of swelling and the associated swelling pressures were studied: (a) complete saturation of the expansive soil specimens after they had been compacted at various initial water contents, (b) mixing of the expansive soil with various proportions of sand to study the effect of grain size distribution on the swelling potential, and (c) use of various salt concentrations of the pore fluid to show its effectiveness in reducing the overall swelling property. All three techniques were found to be effective in reducing the swelling behavior of soils to various degrees as discussed in this paper.

Volume changes of clayey soils due to change in their water content represent one of the most serious problems in the field of foundation engineering because of unpredictable upward movement of structures that are founded on such soils. Many researchers investigated the effect of initial water content on the amount of swelling and swelling pressures (6-11). They noticed that swelling and swelling pressures were inversely proportional to the initial water content for disturbed and undisturbed specimens of clay. They also observed that there was a certain initial water content for a particular expansive soil at which no swelling occurred.

Other investigators (9,12-14) showed that the swelling phenomenon was dependent, to a certain degree, on the salt concentration of the pore fluid. Their results indicated that the percentage of swelling was inversely proportional to the concentration of salt in the solution. Grim found that lime acted as a stabilizing agent and greatly improved the soil subgrade containing high percentages of expansive clays (15). In addition, this also reduced the plasticity index and increased the bearing capacity of these soils.

The purpose of this study was to investigate in the laboratory three different techniques that can be used to reduce the swelling behavior of the soil found in Nasr City, a satellite community of Cairo, Egypt. The first technique consisted of completely saturating the expansive soil specimens after they had been compacted at various initial water contents. In the second technique the expansive soil was mixed with various amounts of sand. In the third technique various salt concentrations of the pore fluid were used.

TEST APPARATUS AND TECHNIQUE

The test apparatus and the technique that were used throughout this study are described in detail by Mowafy and thus are only summarized here (16).

The mold of the oedometer used in the swelling tests had an internal diameter of 63 mm and a height of 25 mm. After preparation of the specimen, the mold containing the soil was put into the loading apparatus. An initial load was applied and the reading of the dial gauge was recorded. After a normal pressure application, the specimen was submerged in distilled water. The dial readings were recorded at intervals of 1/4, 1/2, 1, 2, 4, 8, 24, 48, 72, and 96 hr. The test was continued until the deformation of the specimen ceased.

Swelling pressure is defined as the external pressure required to consolidate a preswelled sample to its initial void ratio. To decrease the frictional stresses between the specimen and the oedometer ring, either a filter paper or a rubber membrane was placed around the wall of the compaction mold. The results of this investigation have been discussed elsewhere in this Record. It is therefore recommended that to investigate the swelling potential of soils in an oedometer, side friction effects should be minimized.

To study the effect of initial water and sand contents on swelling percent and swelling pressure, the clay was mixed with the following percentages of sand: 0, 10, 20, 30, 40, 50, 60, 70, 80, 90, and 100 percent. For each subgroup, four specimens each of initial water contents 5, 10, 15, and 20 percent were tested.

To study the effect of salt concentration on the swelling properties, the soil was permitted to swell by wetting it with different concentrations (20, 30 and 60 g/L) of a sodium chloride solution.

SOIL PROPERTIES

Physical Properties

The natural moisture content of the soil was 18.9 percent; the specific gravity was 2.7; the unit weight was 16.8 KN/m^3; and the dry unit weight was 14.5 KN/m^3. The soil had a liquid limit of 86 percent, a plastic limit of 43 percent, and a plasticity index of 43 percent. It also had a free swell of 90 percent. A grain-size distribution curve of

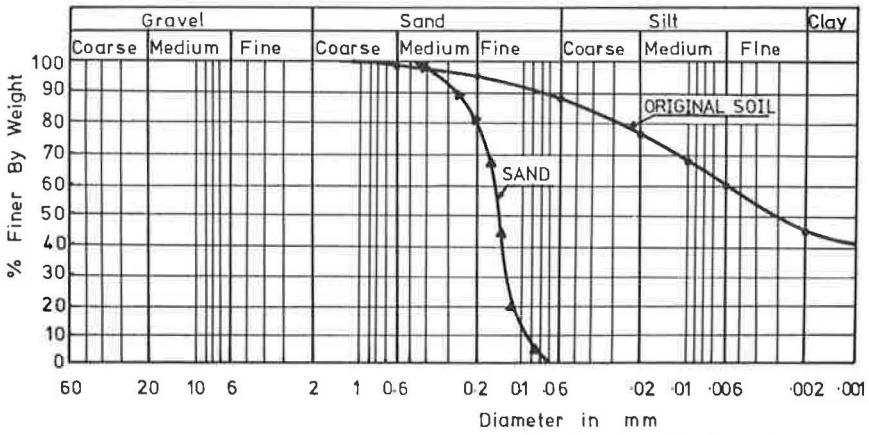

FIGURE 1 Grain size distribution curve for original soil and sand used in the testing program.

TABLE 1 Summary of Soil Properties

Physical Property	Value
Depth of sampling	3.00 m
Natural moisture content (w_n), %	18.9
Specific gravity (G_s)	2.7
Unit weight (γ)	16.8 KN/m^3
Voids ratio (e)	0.61
Liquid limit (w_L), %	86
Plastic limit (w_p), %	43
Plasticity index (PI), %	43
Shrinkage limit (w_s), %	14
Sand percentage	
Coarse (2 - 600 micron), %	1
Medium (600 - 212 micron), %	3
Fine (212 - 75 micron), %	6
Silt percentage (% > 2 micron), %	44
Clay percentage (% < 2 micron), %	46
Liquid limit of particles < 2 micron, %	128
Plastic limit of particles < 2 micron, %	50
Plasticity index of particles < 2 micron, %	78
Activity of clay mineral (A)	0.93
Dry unit weight (γ_d), %	14.5 KN/m^3
Free swell, %	90

the original soil is shown in Figure 1. Table 1 gives a summary of the soil properties.

Mineralogical Composition

The mineralogical composition of the tested soil was found by x-ray, and the results are given in Table 2.

TABLE 2 Mineralogical Composition

Mineral	Percentage
Percentages of non-clay minerals	
Alpha quartz (α si 0_2)	13.6
Orthoclase (KAl si $3O_8$)	32.6
Calcite [ca Mg $(co_3)_2$]	11.3
Dolomite [ca Mg $(co_3)_2$]	4.7
Anhydrite (ca so_4)	7.9
Geothite [Fe (oH)]	10.2
Ilmenite (Fe Tio_3)	2.7
Magnetite (Fe_3 0_4)	6.8
Alpha manganese (α Mn)	3.4
Beta manganese (β Mn)	6.6
Clay minerals	
Ca(montmorillonite, vermiculite) mixed layer (46%)	
Montmorillonite: $[(0H)_4\ Al_4\ Si_8\ 0_{20}\ nH_{20}]$	
Vermiculite: $[(0H)_4(Mg{\cdot}Ca)\ (Si_{8-X}\ Al_X)\ (Mg{\cdot}Fe_X\ 0_{20}\ Y\ H_20)]$	
where X = 1.0 to 1.1 and Y = 8	

The grain-size distribution curve for the sand that was used in mixing with the clay is also shown in Figure 1. The uniformity coefficient for the sand was 1.7 and its specific gravity was found to be 2.71.

PRESENTATION AND ANALYSIS OF RESULTS

The most pertinent information that resulted from this investigation is shown in Figures 2-10.

EFFECT OF INITIAL WATER CONTENT ON SWELLING VALUES

Figures 2-5 show the relationship between the swelling percent and the clay content at initial water

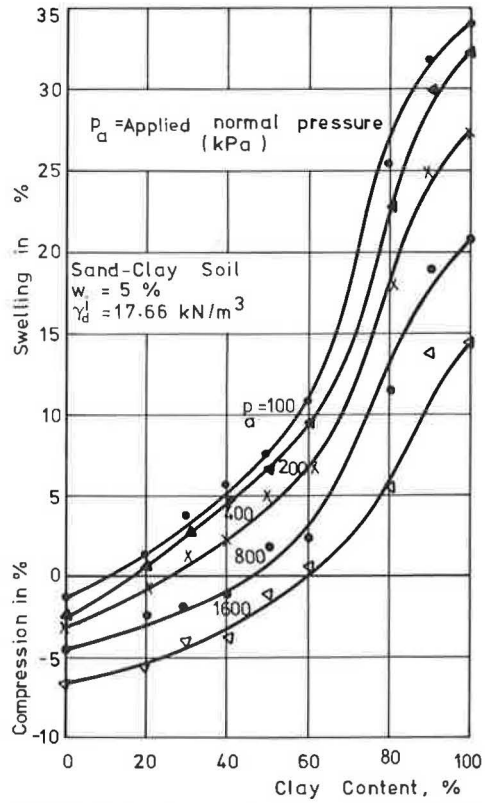

FIGURE 2 Relationship between swelling percent and clay content.

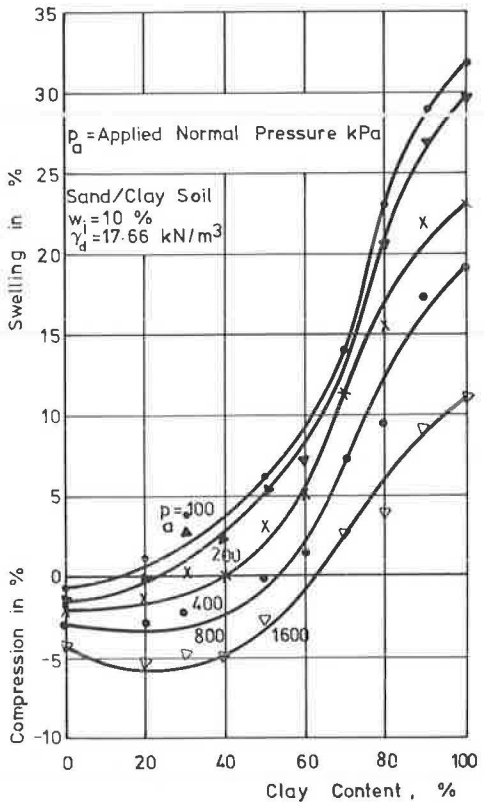

FIGURE 3 Relationship between swelling percent and clay content.

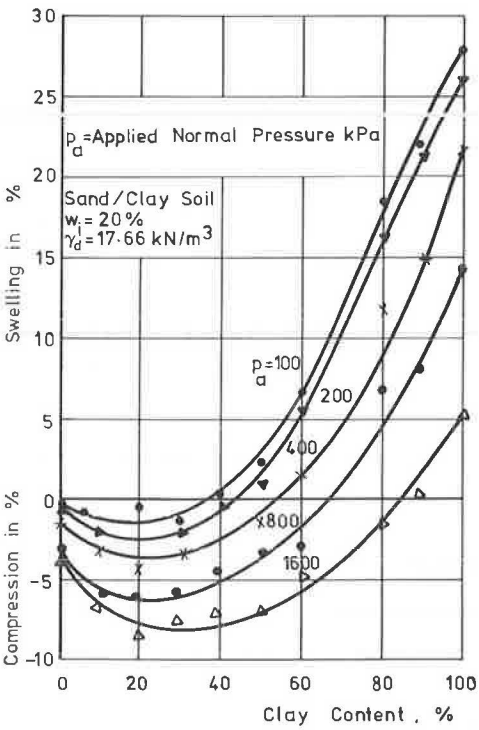

FIGURE 5 Relationship between swelling percent and clay content.

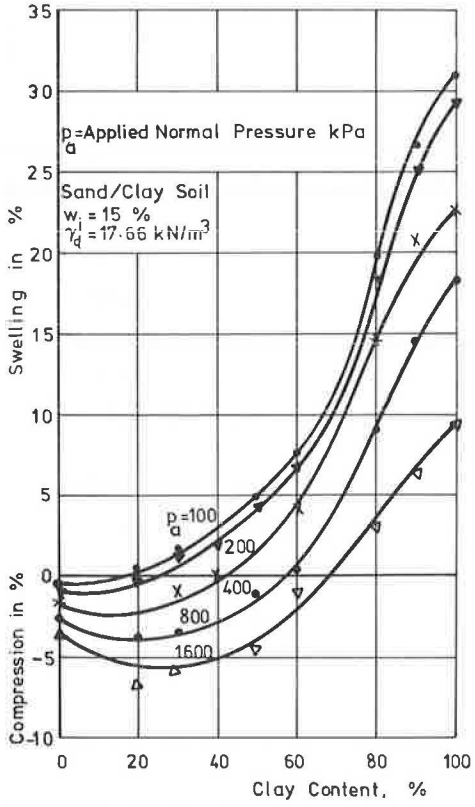

FIGURE 4 Relationship between swelling percent and clay content.

contents of 5, 10, 15, and 20 percent, respectively. The normal pressure varied from 100 to 1600 kPa. From the four figures it can be observed that the amount of swell decreased with increasing initial water content. For a low initial normal pressure of 100 kPa and a clay content of 100 percent, the swelling percent decreased by 15 percent if the initial water content was increased from 5 to 20 percent. For a high normal pressure of 1600 kPa, the amount of swell decreased by 64 percent as the initial water content was increased from 5 to 20 percent for 100 percent clay content.

Figure 6 shows the amount of swelling pressure to clay content. Curves for 5, 10, 15, and 20 percent initial water content are given. The amount of swelling pressure is clearly influenced by the initial water content of the soil. For example, the swelling pressure decreased by 50 percent when the initial water content was increased from 5 to 20 percent at a clay content of 100 percent.

EFFECT OF THE AMOUNT OF SAND ON SWELLING PROPERTIES

The effect of the amount of sand on swelling percent and swelling pressure is shown in Figures 2-6. From these figures the following observations can be made:

1. Clay content has a great influence on the magnitude of swell (swelling percent) of the soil.
2. For a given initial water content and normal pressure, there is a "critical" clay content at which the amount of swell is zero. Below that critical value the soil will compress, and above that the soil is susceptible to swelling.
3. Swelling potential is increased considerably as the clay content is increased. For example, at an initial water content of 5 percent, a normal pressure of 100 kPa, and a clay content of 20 percent,

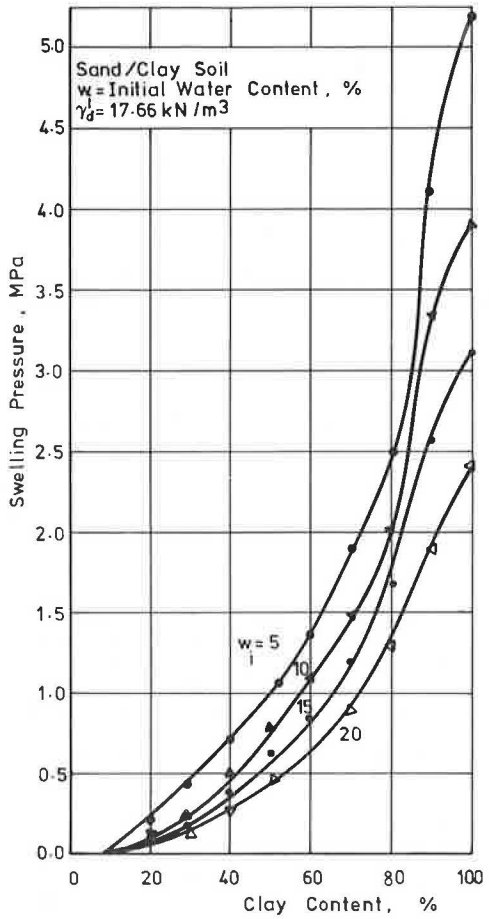

FIGURE 6 Relationship between swelling percent and clay content.

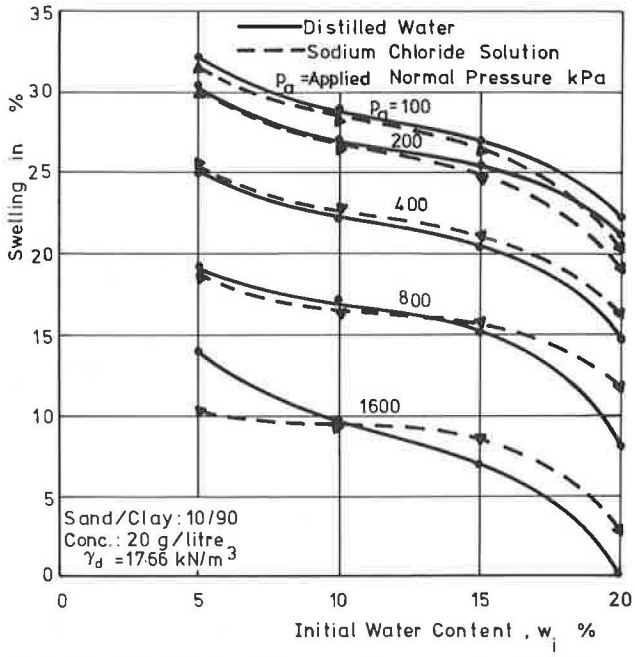

FIGURE 7 Relationship between swelling percent and initial water content.

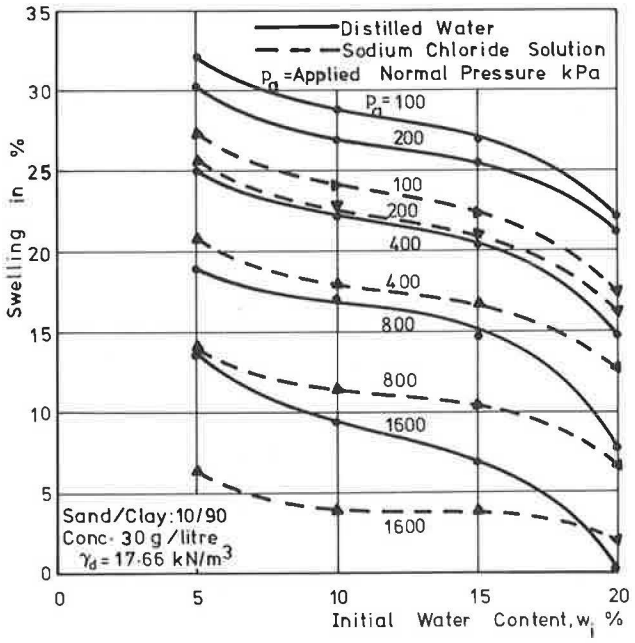

FIGURE 8 Relationship between swelling percent and initial water content.

the amount of swell is 1.2 percent. As the clay content is increased to 60 percent, keeping all other conditions the same, the amount of swell increases to 11.5 percent.

4. Swelling pressure increases dramatically as the clay content is increased at the same initial water content (Figure 6). At a clay content of 10 percent (critical clay content), the swelling pressure is zero regardless of the initial water content. As the clay content is increased to 60 percent, the swelling pressure increases to 1.4 MPa for 5 percent initial water content and to 52 MPa at a clay content of 100 percent.

5. A higher proportion of sand content, and corresponding lower clay content, will reduce the tendency of the clay to swell due to the larger capillary canals in the soil pores and the corresponding reduction in soil suction.

6. The addition of sand to the swell-susceptible clay increased the rate of deformation considerably due to the corresponding increase of soil permeability.

EFFECT OF SALT CONCENTRATION IN THE PORE FLUID ON SWELLING BEHAVIOR

The effect of salt concentration of pore fluid on swelling percent and swelling pressure are shown in Figures 7-10. Figures 7-9 show the relationship between the swelling percent and the initial water content. All specimens had a sand-to-clay ratio of 10 to 90. The normal pressures varied from 100 to 1600 kPa. The salt concentration varied from 20 to 60 g/L. A study of these figures reveals that as the concentration of sodium chloride increases, the swelling percent decreases for the same conditions of initial water content, initial normal pressure, and clay content. At a concentration of 20 g/L, for a high applied initial normal pressure and a high initial water content, the swelling percent due to wetting by sodium chloride solution is greater than that due to wetting by distilled water. For concentrations greater than 20 g/L, the swelling per-

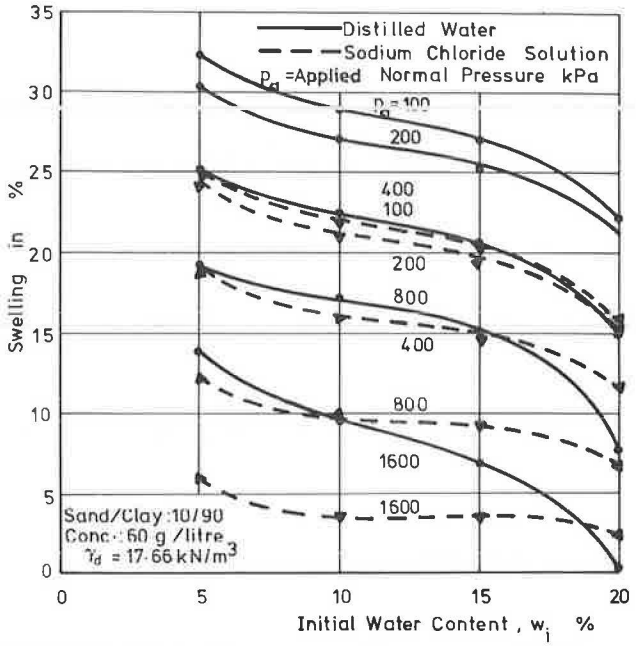

FIGURE 9 Relationship between swelling percent and initial water content.

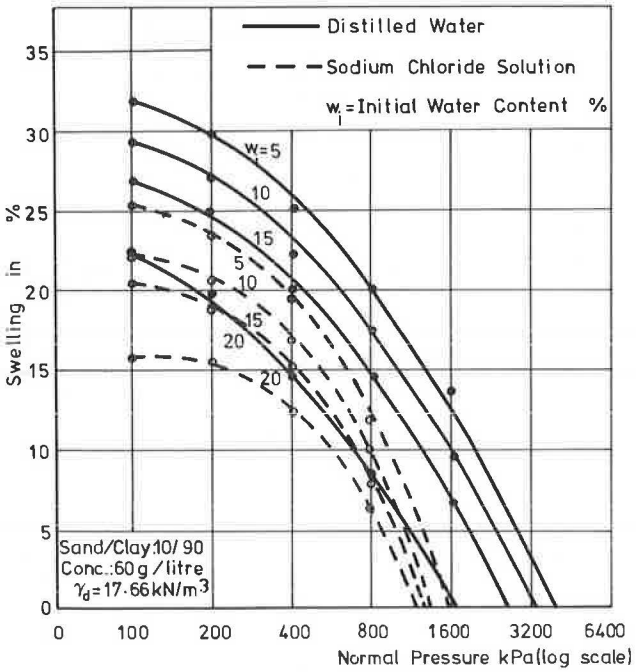

FIGURE 10 Relationship between swelling percent and normal pressure.

cent for sodium chloride solution is lower than the value obtained with distilled water. However, the increase in the swelling percent decreases with the increase of the initial water content.

Figure 10 shows the relationship between the initial normal pressure and the swelling percent. All specimens had a sand-to-clay ratio of 10 to 90 by weight. Curves for 5, 10, 15, and 20 percent initial water contents are given. As shown in Figure 10, when a sodium chloride solution is used, the swelling pressure is lower than the corresponding value for distilled water. Such a decrease in swelling pressure is more pronounced at higher concentrations of sodium chloride. As the initial water content is increased, the addition of sodium chloride has a minor effect on reducing the swelling properties of the soil. This phenomenon can be explained as follows:

1. The charges on the surface of the particles of the clay play an important role in the stability of colloids that require the presence of small concentrations of electrolytes. The addition of sodium chloride produces a large amount of electrolytes that precipitate in the colloids with the effect of rapidly flocculating the colloids (17). The increase in the size of particles leads to a decrease in the total surface area and hence, the amount of absorbed water will decrease and in turn the swelling will diminish.
2. The sodium chloride in solution is ionized into Na^+ and Cl^-. Cation exchange occurs between the Na^+ and Ca^{++} ions of the calcium montmorillonite, while the chloride ions are absorbed between the sheets of the montmorillonite to form calcium chloride between the sheets. The calcium chloride prevents water from entering and thus decreases the swelling ability of the montmorillonite.
3. Owing to the high osmotic pressure of the sodium chloride solution, dehydration of soil particles occurs and thereby decreases the amount of retained water and the swelling potential.

CONCLUSIONS

The investigation of swelling properties of Nasr City soils warrants the following conclusions:

1. All of the three techniques, that is, variation of initial water content, increasing the proportion of sand content, and using different salt concentrations of the pore fluid, were found to be effective in reducing the swelling behavior of expansive soil to various degrees.
2. The amount of swell and swelling pressure increases with the amount of clay content of the soil.
3. An increase in initial water content will cause a reduction in the magnitude of swell and in the swelling pressure. Therefore, in order to reduce both these properties, compaction of these soils in the field should occur at high moisture contents.
4. A reduction of swelling potential can also be achieved by decreasing the clay content. This can be accomplished in the field by mixing coarse fractions of granular material with swell-susceptible soils.
5. In general, the presence of sodium chloride in the pore fluid caused a decrease in swelling and swelling pressure. Therefore, the injection of a salt solution into swell-susceptible soils could be a possible method of overcoming this problem, if the soil permeability is sufficiently high.
6. It may be more convenient to use more than one technique in order to reduce the swelling potential of the expansive soil.

ACKNOWLEDGMENTS

This paper is based on the results of a research project carried out in the Laboratory of Soil Mechanics, Civil Engineering Department, Al-Azhar University. The helpful discussion and encouragement of S. Tahir, Professor of Soil Mechanics and Foundation Engineering at Al-Azhar University, is grate-

fully acknowledged. The authors also wish to express their thanks to the technicians in the Soil Mechanics Laboratory at Al-Azhar University for their help.

REFERENCES

1. G. Baldovin and D. Santovito. Tunnel Construction in High Swelling Clays. Proc., 8th International Conference on Soil Mechanics and Foundation Engineering, Moscow, USSR, 1973, pp. 13-16.
2. A.W. Bishop and G.A. Blight. Some Aspects of Effective Stress in Saturated and Partially Saturated Soils. Geotechnique, Vol. 13, No. 3, 1963, pp. 177-197.
3. G.E. Blight. The Time-Rate of Heave of Structures on Expansive Clays. Symposium on Moisture Equilibria and Moisture Changes in Soils Beneath Covered Area. Butterworths, Sydney, Australia, 1965, pp. 78-88.
4. G.A. Blight and J.A. Dewet. The Acceleration of Heave by Flooding. Symposium on Moisture Equilibria and Moisture Changes in Soils Beneath Covered Area. Butterworths, Sydney, Australia, 1965, pp. 89-92.
5. J.B. Burland. Some Aspects of the Mechanical Behaviour of Partly Saturated Soils. Symposium on Moisture Equilibria and Moisture Changes in Soils Beneath Covered Areas, Butterworths, Sydney, Australia, 1965, pp. 270-278.
6. A.H. El-Ramli. Swelling Characteristics of Some Egyptian Soils. Journal of the Egyptian Society of Engineering, Vol. IV, No. 1, 1965.
7. D. Mohan and B.G. Rao. Moisture Variation and Performance of Foundations in Black Cotton Soils in India. Symposium on Moisture Equilibria and Moisture Changes in Soils Beneath Covered Areas, Butterworths, Sydney, Australia, 1965, pp. 175-183.
8. J.V. Parcher and P. Lin. Some Swelling Characteristics of Compacted Clays. Proc., ASCE, Vol. 91, 1965, pp. 1-17.
9. R. Pietkowski and R.C. Boiarski. Absorbed Water in Soils. Proc., 3rd Budapest Conference on Soil Mechanics and Foundation Engineering, 1968, pp. 221-226.
10. E.S.A. Rabba. Factors Affecting Engineering Properties of Expansive Soils. M.S. thesis, Al-Azhar University, Cairo, Egypt, 1975.
11. H.L. Uppal. Field Study on the Movement of Moisture in Black Soils Under Road Pavements. Symposium on Moisture Equilibria and Moisture Changes in Soils Beneath Covered Areas. Butterworths, Sydney, Australia, 1965, pp. 165-173.
12. B.V. Ranganatham and N.S. Pandian. Strength-Gain in Thermally Cured Lime Stabilized Clays. Proc., 4th Conference on Soil Mechanics, Budapest, 1971, pp. 263-272.
13. B.P. Warkentin. Water Retention and Swelling Pressure of Clay Soils. Canadian Journal of Soil Science, Vol. 42, 1962, p. 189.
14. I. Goldberg and A. Klein. Some Effects of Treating Expansive Clays with Calcium Hydroxide. American Society for Testing and Materials, Special Technical Publication, Vol. 142, 1952, pp. 53-67.
15. R.E. Grim. Applied Clay Mineralogy. McGraw-Hill, New York, 1962, pp. 204-277.
16. Y.M. Mowafy. Study of Some Engineering Properties of Swelling Soils. M.S. thesis. Al-Azhar University, Cairo, Egypt, 1978.
17. B. Mason. Principles of Geochemistry. John Wiley and Sons, Inc., New York, Jan. 1958, pp. 155-169.

Publication of this paper sponsored by Committee on Environmental Factors Except Frost.

Foundation Design of an Industrial Plant in Stillwater, Oklahoma

VIRENDRA SINGH

ABSTRACT

The geotechnical considerations in the design and construction of an industrial plant in an expansive soil environment are discussed in this paper. The soils at the site exhibited a high swelling potential that necessitated a defensive design approach. The behavior of these soils was quantified from a limited number of controlled swelling tests. The data were supplemented by using published correlations between the swelling behavior of soils and the results of soil index tests that are routinely performed during soil investigations. Correlations were found very useful in corroborating quantitative test results from controlled tests. Several measures were included in the design to protect the foundations and the structure against the potentially damaging effects of subgrade swelling. One of these measures included the use of a collapsible fiberboard carton under the slabs to accommodate expansion of subgrade soil without exerting any significant upward pressure. The collapse mechanism of this fiberboard carton was determined in the laboratory under simulated field conditions by using a simple, practical test setup. The test results confirmed that the fiberboard would collapse before swelling pressures reached the acceptable design pressure. The test results show that relatively easy-to-perform tests and routine soil index tests can be very useful in developing an understanding of the behavior of swelling soils and in selecting the proper design details that will minimize the potential problems associated with such soils.

Certain clay-rich soils in temperate and tropical climates undergo volume change with change in water content. When this volume change is appreciable, foundation design deserves special attention in order to protect the foundation and the structure from damage. This can be achieved in two ways: the foundation system may be designed to accommodate the anticipated heave or the structure and the foundation may be designed to withstand pressures that can be caused by this swelling. A combination of the two approaches may be used to achieve an economy in the design.

Irrespective of the design approach, it is essential to understand the behavior of the soil and to make quantitative estimates of anticipated heave and pressures that swelling can cause on the structure foundation. Further, it is advantageous if such estimates can be derived from soil properties that are easily determined with a reasonable degree of reliability using simple, routine tests.

Similarly, it is important to know how the defensive measures included in the design will ameliorate the effects of swelling under actual field conditions. Because these measures are implemented beneath the foundation, their performance can be evaluated either by observation of adjacent similar constructions or by simulation in the laboratory.

Geotechnical considerations in foundation design for a recently constructed industrial plant in Stillwater, Oklahoma, are presented in this paper. The plant is founded on swelling soils with design parameters derived from a limited number of controlled swelling tests and correlations with results of soil index tests. Several defensive measures were included in the design to minimize the potential effects of swelling on the structure, including the placement of a fiberboard carton form under the slabs to accommodate anticipated heave. Performance of the cardboard was evaluated by using a simple laboratory test that proved to be extremely useful in the design.

SITE CONDITIONS

Moore Business Forms, Incorporated, owns an industrial plant facility located in the town of Stillwater, Oklahoma. A portion of the plant was constructed several years ago, and new facilities were added to it to expand the firm's manufacturing capabilities. Located adjacent to the existing plant structures, the new plant includes a process building, a tank farm, and other appurtenant structures (Figure 1).

The site is located in a temperate climate with a mean annual temperature of 60.8° F and a mean annual precipitation of 32.18 in. (1). The maximum reported mean temperature is 94° F for the month of July, and the bulk of the rainfall occurs from May through August.

The soils on the site consist of approximately 28 ft of sandy, silty, reddish-brown clay that overlies a heavily overconsolidated thick stratum of clay known locally as "red-bed." The upper clay soils exhibit swelling tendencies when wet and have been overconsolidated through a desiccation process. The heavily overconsolidated red-bed behaves similarly to a soft rock and shows no perceptible swelling tendencies.

GENERAL DESIGN CONSIDERATIONS

The project design criteria established a number of specific requirements for acceptable foundation performance. Some of these requirements, which in-

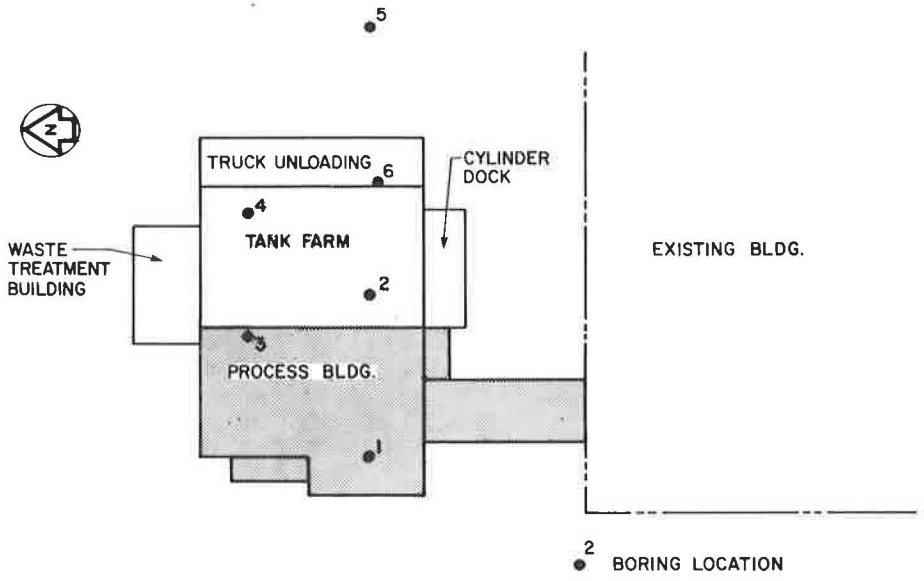

FIGURE 1 Site plan.

fluenced geotechnical investigations and design, are as follows:

1. The finished grade elevation for the process building was established several feet above the existing ground; this required structural fill under the foundation. Cost comparisons indicated that use of the on-site clay soils would be preferred because any granular soil had to be imported from a source away from the site at a significantly higher cost.
2. The process building housed sensitive and heavy equipment, which required that foundation movements be minimal, if any, and that the effect of unknown movements associated with swelling or shrinkage be minimized.
3. It was determined feasible to support the tank farm foundation directly on subgrade. Any differential movement caused by seasonal swelling and shrinking or gradual cumulative swelling could be accommodated by the flexibility inherent in the metal structures and piping with no distress or impact on the performance.

It should be pointed out that the existing plant structure was supported on belled caissons founded in red-bed.

Subgrade Soil Investigations

Several borings were drilled in the general site area during the preliminary planning stage of the project. Once the structure layout was prepared, nine additional borings were drilled to define the soil conditions under the planned structures and to collect soil samples for laboratory tests; the location of six of these borings is shown in Figure 1. The drilling was performed during December 1982, using a 4.5-in. inside-diameter continuous flight hollow stem auger. Standard penetration tests were performed in all borings at 5-ft intervals, and intact soil samples were collected using thin-walled Shelby tubes. The drill cuttings were removed by forced air, and the samples were wrapped in plastic to minimize any change in natural moisture content on exposure. Each boring was advanced a minimum of 5 ft into the underlying red-bed, and the rock cores were recovered for inspection and laboratory testing. Several grab samples were collected to determine compaction requirements for the soil proposed for the structural fill.

Laboratory Tests on Soils

A laboratory testing program with a limited scope was undertaken to determine swelling characteristics and other soil properties. A list of tests that were performed on soil samples, which were conducted using standard test procedures, is given in Table 1.

TABLE 1 Laboratory Test Program

Test Type	No. of Tests	
	Soil	Red-Bed
Water content	15	6
Unit weight	7	6
Atterberg limits	12	
Shrinkage limit	1	
Grain size	6	
Specific gravity	1	5
Free-swell index	13	
Controlled swelling	2	
Consolidation	1	
Unconfined compression		4
Triaxial compression	4	2

The test results are included in Tables 2 and 3 and in Figures 2 through 4. Free-swell index tests and controlled swelling tests were performed according to Bureau of Reclamation practice (2). A brief description of test procedures is presented here. No swelling tests were performed on red-bed as it showed no perceptible swelling tendency upon wetting.

Free-Swell Test

This test was performed by slowly pouring 10 cm^3 of dry soil passing a Number 40 sieve into a graduate filled with water. The soil mixture was allowed to come to rest at the bottom, and the swollen volume was noted. The free-swell index value was determined

TABLE 2 Summary of Test Results

Sample No.	Soil Type	Fines (%)	Sand (%)	Colloids (%)	Liquid Limit (%)	Plasticity Index (%)	Free-Swell Index (%)	Potential Degree of Expansion	Water Content (%)	Dry Density, lb/ft^3
BH1-1							40			
BH2-2	CH	90	10	40	76	51	80	Very high	19.0	
BH2-4	CH				59	40	50	Very high	17.3	114.7
BH3-2	CH	83	17	32	60	41	50	Very high	12.0	
BH3-4	CH				63	41	50	Very high	15.0	117.9
BH4-2	CL	82	18	27	42	25	30	High	11.0	115.0
BH4-3	CL	70	30	26	40	24	20	Medium high	12.0	
BH5-1	CH				71	51	60	Very high	15.6	
BH5-3	CH				59	37	40	Very high	13.8	
BH7-2	CH	91	8	40	80	57	50	Very high	17.3	
BH8-2	CH	93	6	31	61	38	60	Very high	18.1	
BH9-2	CH				73	52	60	Very high	23.0	
BH9-4	CL				37	21	0	Medium high	9.1	130.5

TABLE 3 Summary of Expansion and Uplift Tests

	Sample No.			
	BH1-1	BH1-1	BH2-2[a]	Remarks
Soil type	CH	CH	CH	
Dry density (lb/ft^3)	124.1	115.9	109.5	
Water content (%)	11.9	15.7	17.4	
Saturation (%)	84.4	88.7	90.1	
Expansion when wetted (%)	4.69		–[b]	Seating load of 1.13 psi
Load to consolidate to original height (psi)	55.0			
Swelling pressure when wetted (psi)		8.3	53	Sample BH1-1 expanded 1.13 percent under 8.3 psi
		(55)		Swelling pressure (55 psi) interpolated graphically
Expansion when load released (%)		2.77		

[a]Sample BH2-2 was tested for consolidation using ASTM procedure. A load of 53 psi represents the total incremental load when sample showed an expansion of about 0.5 percent and started consolidating under higher loads.
[b]No test data available.

as the ratio of increase in the volume and initial dry volume.

Load Expansion Test

This test was performed by using a standard consolidometer with a porous stone at each end. The specimen, prepared from a Shelby tube intact sample, was placed in the consolidometer and loaded to 1 psi. The sample was saturated under this load, and the increase in height (volume) was recorded. When the swelling was complete, additional loads were applied in increments to determine the load required to bring the specimen to its original height. The data give an indication of the potential expansion under a nominal load of 1 psi.

The second specimen was tested to determine the maximum load required to prevent expansion. The sample was placed in the consolidometer and sufficient load was added during sample saturation to prevent an increase in volume. Because of difficulties experienced during testing, a small volume increase was noted and the results were extrapolated to estimate the maximum potential swelling pressure corresponding to a zero increase in volume. When further swelling under the load (8.3 psi) ceased, the sample was unloaded in decrements to allow expansion and the increase in volume was recorded.

The third sample was loaded in the consolidometer to determine its compression characteristics. The sample exhibited strong swelling tendency when exposed to water and continued swelling under each increment of load until a load of 53 psi was reached. The test proved to be very useful in estimating maximum swelling pressure.

Because only one test was performed for each set of conditions, data were correlated with index test results using published correlations by others (2) and are shown in Figures 3 and 4. In view of the large variations normally encountered in soil properties, the correlations between the index tests and the swelling tests were quite encouraging.

LABORATORY TEST ON CARDBOARD CARTON FORM

A 4-in. high, wax-impregnated fiberboard carton was provided under the grade beam supported slab to accommodate expansion of subgrade soils without exerting large pressures against the slab. According to the fiberboard manufacturer, the carton had a puncture strength of 275 psi and could support up to 1,000 psf of distributed load when dry. (Although these are desirable characteristics for handling, supporting of workmen, and the weight of wet concrete, there was a genuine concern about the fiberboard's collapsibility under limited moisture exposure conditions and a load of 3 psi or less that could be safely resisted without any distress by the 12-in. thick slab.)

A relatively simple test was devised to study the collapse mechanism of the fiberboard carton. A 12- x 12-in. rectangular cell 36 in. high, was constructed of 1/4-in. thick acrylic plastic (Figure 5). The cell was supported on a wooden base and reinforced at the bottom. A 6-in. thick layer of soil was placed at the bottom of the acrylic container. The soil was reddish-brown clay obtained from the site and was placed and compacted in four layers at the field placement water content. A dry density of 111.5 pcf was achieved at a moisture content of 18 percent using standard proctor compaction effort. A piece of fiberboard carton, 12 x 12 in. in size, was placed over the compacted soil layer. The two open sides of the carton were protected against excessive

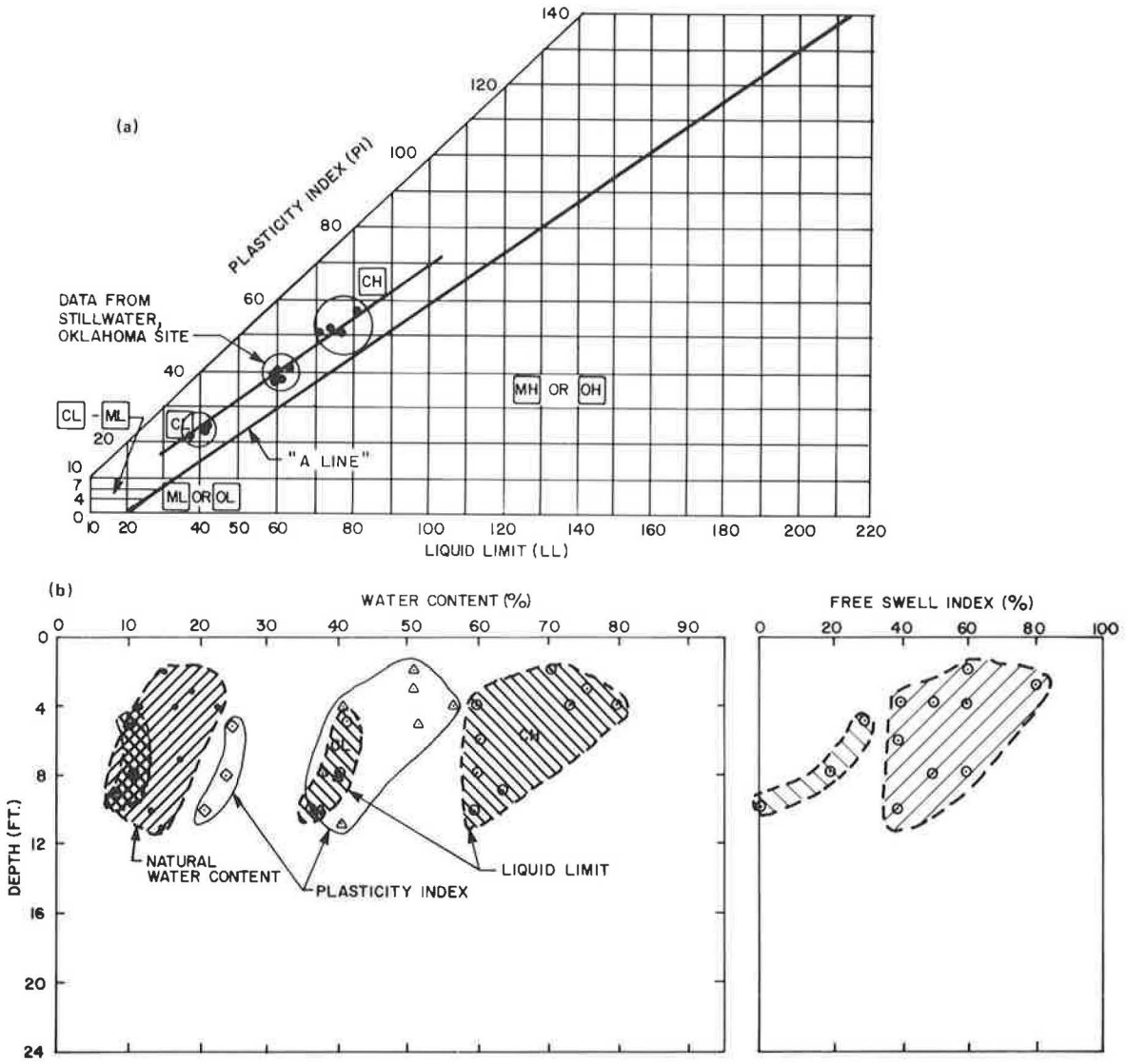

FIGURE 2 Index test results: (a) plasticity chart and (b) depth profile.

moisture soaking by a 2-in. plastic sheet taped to the top of the carton. Next, 12-in. thick concrete was poured on the carton form using a concrete mix similar to the design mix (water/cement ratio of 0.54). The setup represented the site conditions fairly well. A 4 mil plastic sheet was placed between the concrete and the acrylic container to eliminate bonding and friction. The four sides were also coated with white petroleum jelly so that the 4 mil plastic sheet would not adhere to the acrylic walls (Figure 6).

The deformations of the cardboard were observed under the weight of wet concrete for the next 6 days. The measured deformation and the shape of the deformed carton are given in Table 4 and shown in Figure 7a, respectively. On the 6th day, additional load was placed on the concrete to bring the total load on the carton to 2.16 psi. No additional deflection was noticed during the next 2 hours, and it was decided to expedite the test by increasing the load to a final value of 3 psi. The load was increased to 3.16 psi (the maximum acceptable upward pressure on the foundation slab was 3 psi). Within 20 minutes of the loading, the deflections increased suddenly and approached 3 in. within 4 hr of loading; these data are given in Table 5. The observations continued for the next 8 days at which time the test was terminated when further increase in deflection was small. The final collapsed shape of the carton is shown in Figure 7b.

The test was considered successful and demonstrated that the fiberboard would support the wet reinforced concrete until such time that the concrete gains sufficient strength to support itself, but would collapse if the load increased to 3 psi. The collapsed carton will continue to accommodate as much as 3.5 in. of swelling.

FOUNDATION DESIGN

The foundation for the process building consists of grade beams supported on belled caissons seated in firm red-bed. The grade floor slab that supports heavy and sensitive equipment is designed as a two-way slab supported on grade beams. The slab in the remaining areas is supported directly on subgrade and is free to move upward or downward with subgrade. This slab may experience some differential

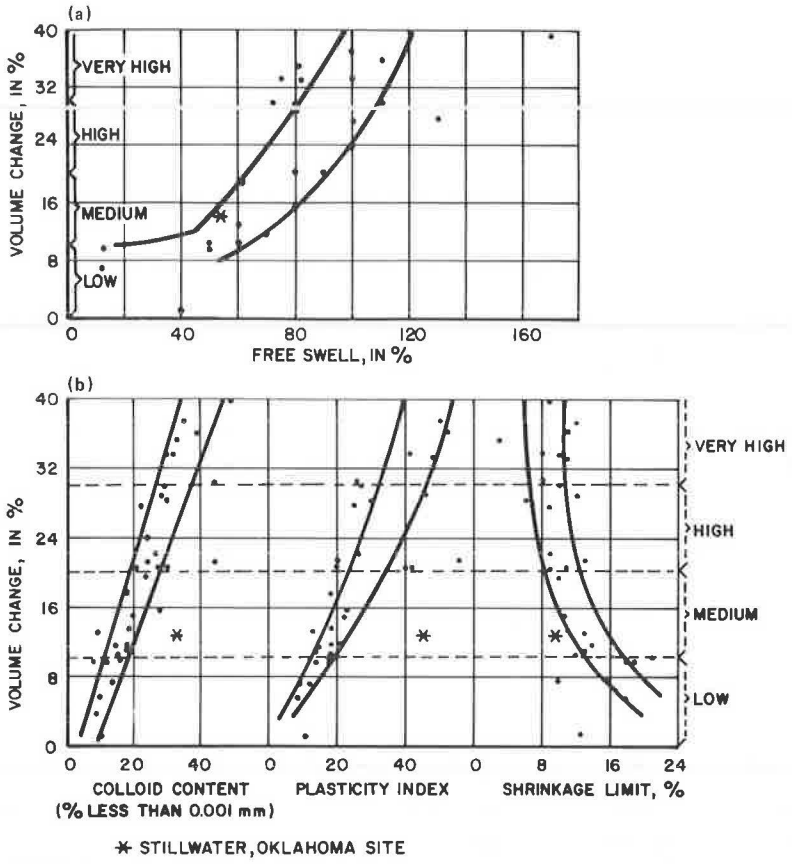

FIGURE 3 Swelling potential related to index properties.

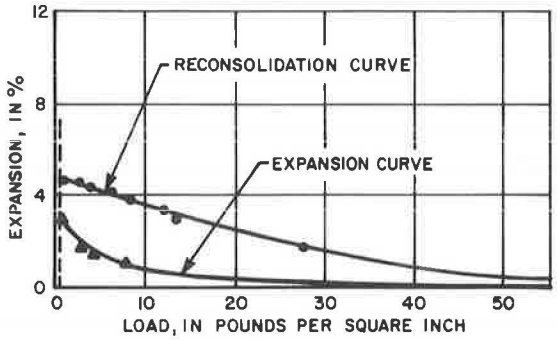

FIGURE 4 Effect of sequence of loading and wetting on expansion.

movement and does not support any equipment that will be affected by these movements.

The net bearing capacity for caissons was estimated to be 27.36 kips/ft^2 using a cohesion value of 3,040 psf and a bearing capacity factor of 9.0 (the contribution of skin friction was ignored for conservatism). Using a maximum allowable design load of 10 ksf, this resulted in a safety factor of 2.74. An upper limit of uplift force on caisson was estimated as follows (3):

$$Q \text{ uplift} = (\Pi)\ (d_s)\ (L)\ (Ca) \quad (1)$$

where d_s is the diameter of the caisson shaft, L is the length of the caisson shaft, and Ca is the average adhesion value between the soil and the caisson.

An adhesion value of 2,000 psf was considered a reasonable upper limit assuming the soil absorbed sufficient moisture during swelling and, thus, softened. For a 20-ft long shaft, this provides an uplift force of 40 Πd kips per caisson. The diameter of the bell was checked to assure sufficient resistance against uplifts as follows:

$$Q \text{ uplift} - Q \text{ dead} = q_d/F)\ \Pi/4\ (d_b^2 - d_s^2) \quad (2)$$

where

q_d = net bearing capacity = C.Nc. (cohesion x bearing capacity factor)
d_b = diameter of the caisson bell,
d_s = diameter of the caisson shaft,
F = safety factor, and
Q dead = permanent dead load.

The diameter of the caisson shafts varied from 24 to 36 in. and the bell diameter varied from 4 to 8 ft. The total length of caissons, including the belled portion, varied from 9 to 21.5 ft. A layout plan for the cassions, which were reinforced for the entire length, is shown in Figure 8.

An estimate of the heave under the foundation was made using data from laboratory tests under different in situ confining pressures. It was estimated that the soils could heave as much as 1.3 in. under the foundation. Such a heave would have no effect on the two-way supported slab because the fiberboard carton form would accommodate up to 3.5 in. of heave. It was estimated that the grade beams could experi-

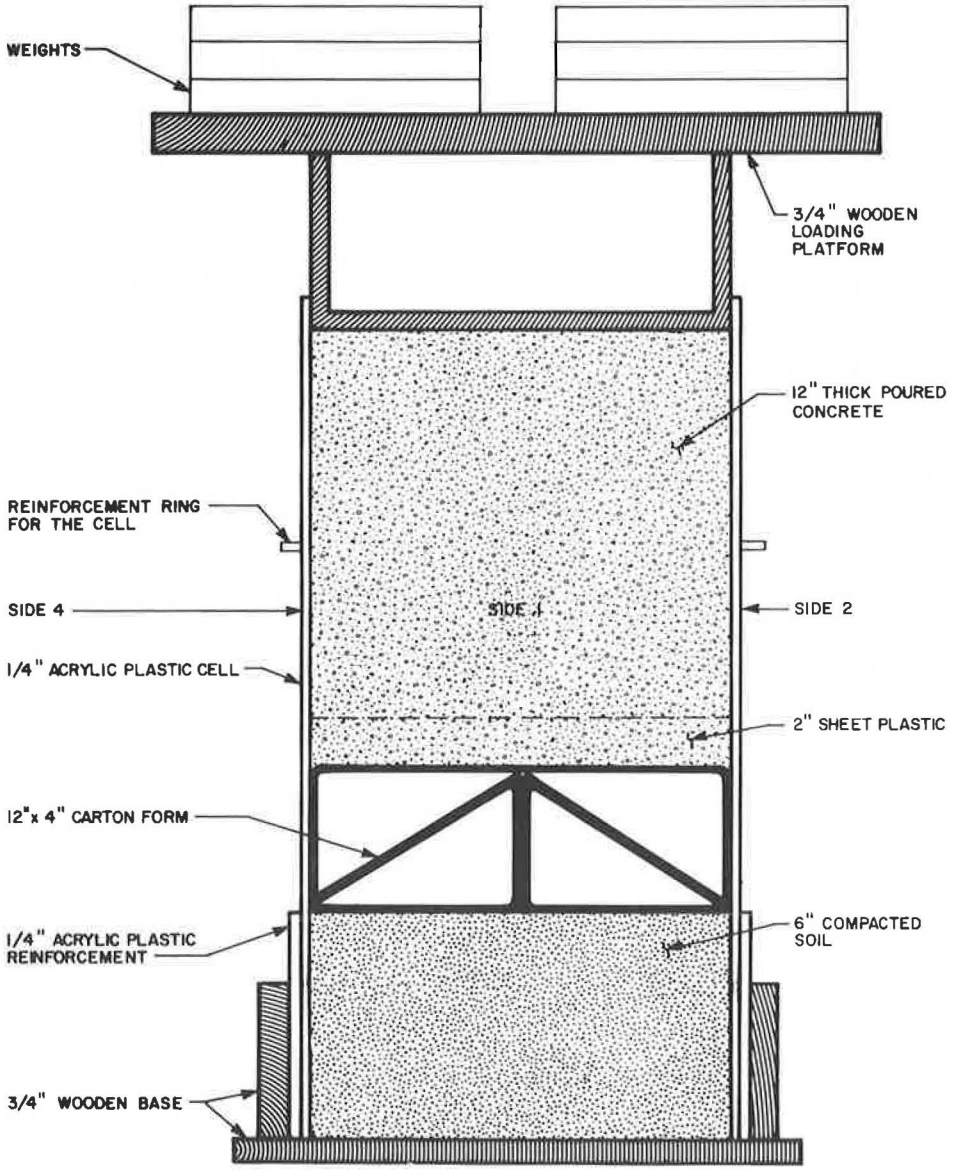

FIGURE 5 Carton form test setup.

TABLE 4 Fiberboard Carton Test Load, 1.16 psi (Weight of Concrete)

		Maximum Deflection of Carton Form, in.				
Date	Time	Side 1	Side 2	Side 3	Side 4	Remarks
June 23, 1983	8:45 a.m.					Placed concrete
	9:15 a.m.	0.45	0.12	0.5	0.12	
	9:45 a.m.	0.52	0.12	0.62	0.20	
	4:00 p.m.	0.52	0.20	0.67	0.20	
June 24, 1983	8:30 a.m.	0.63	0.25	0.75	0.25	
	4:30 p.m.	0.63	0.25	0.75	0.25	
June 26, 1983	12:00 noon	0.67	0.30	0.80	0.30	
June 27, 1983	11:00 a.m.	0.67	0.30	0.80	0.30	
June 29, 1983	9:05 a.m.	0.72	0.32	0.82	0.32	At 11:30 a.m., load increased to 3.26 psi

FIGURE 6 Deformation of carton form—test setup before placing of concrete.

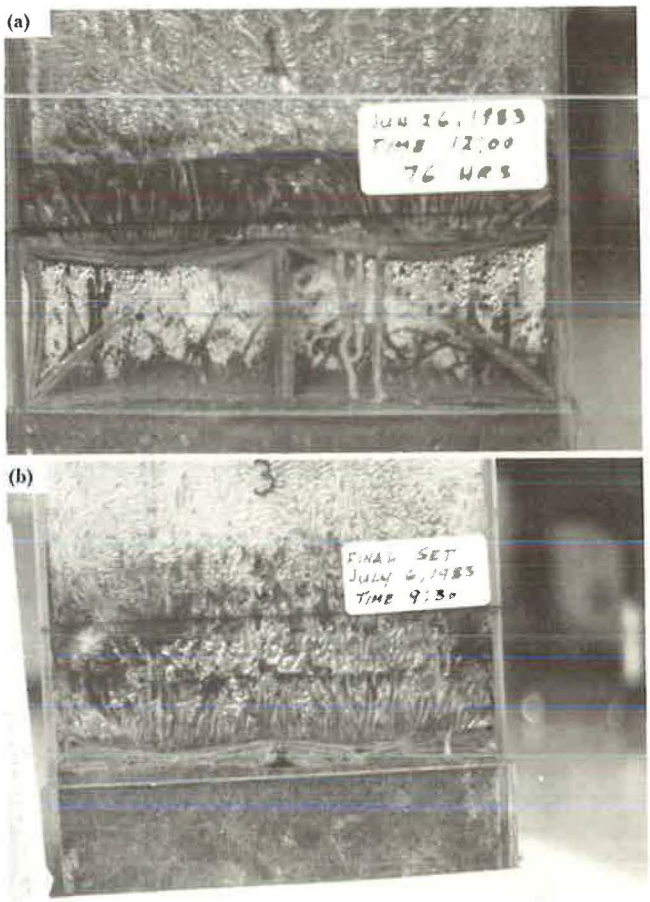

FIGURE 7 Deformation of carton form under a load of (a) 1 psi and (b) 3 psi.

TABLE 5 Fiberboard Carton Test Load, 3.16 psi

Date	Time	Maximum Deflection of Carton Form, in. Side 1	Side 2	Side 3	Side 4	Remarks
June 29, 1983	11:50 a.m.	2.90	2.55	2.92	2.52	
	11:55 a.m.	2.95	2.55	3.00	2.52	
	12:40 p.m.	2.95	2.55	3.05	2.52	
	4:30 p.m.	3.00	2.62	3.07	2.60	
July 4, 1983	9:00 a.m.	3.30	3.00	3.47	3.10	
July 6, 1983	9:25 a.m.	3.32	3.05	3.52	3.15	Test terminated

ence as much as 6 to 10 psi of upward pressure during extreme conditions, but those conditions are unlikely to occur due to other defensive measures included in the design.

The following features were included in the design to further protect the structure against harmful effects of swelling and shrinkage:

1. All exterior grade beams were placed 4 ft below grade. This depth was judged to be slightly more than the depth of seasonal moisture variation. Thus, the subgrade soil is reasonably well protected from the seasonal change in the environment.

2. All floor slabs not supporting critical equipment were designed to be independent of grade beams and can move up or down with the subgrade soil.

3. The structural fill placed under the structures was compacted at a moisture content that will result in minimum or no swelling. This moisture content was close to the natural moisture content of site soils but considerably higher than the optimum moisture content.

4. General drainage around the facilities was designed to drain away any precipitation rapidly and efficiently. Thus, subgrade soil was protected against saturation from extended ponding or rainfall.

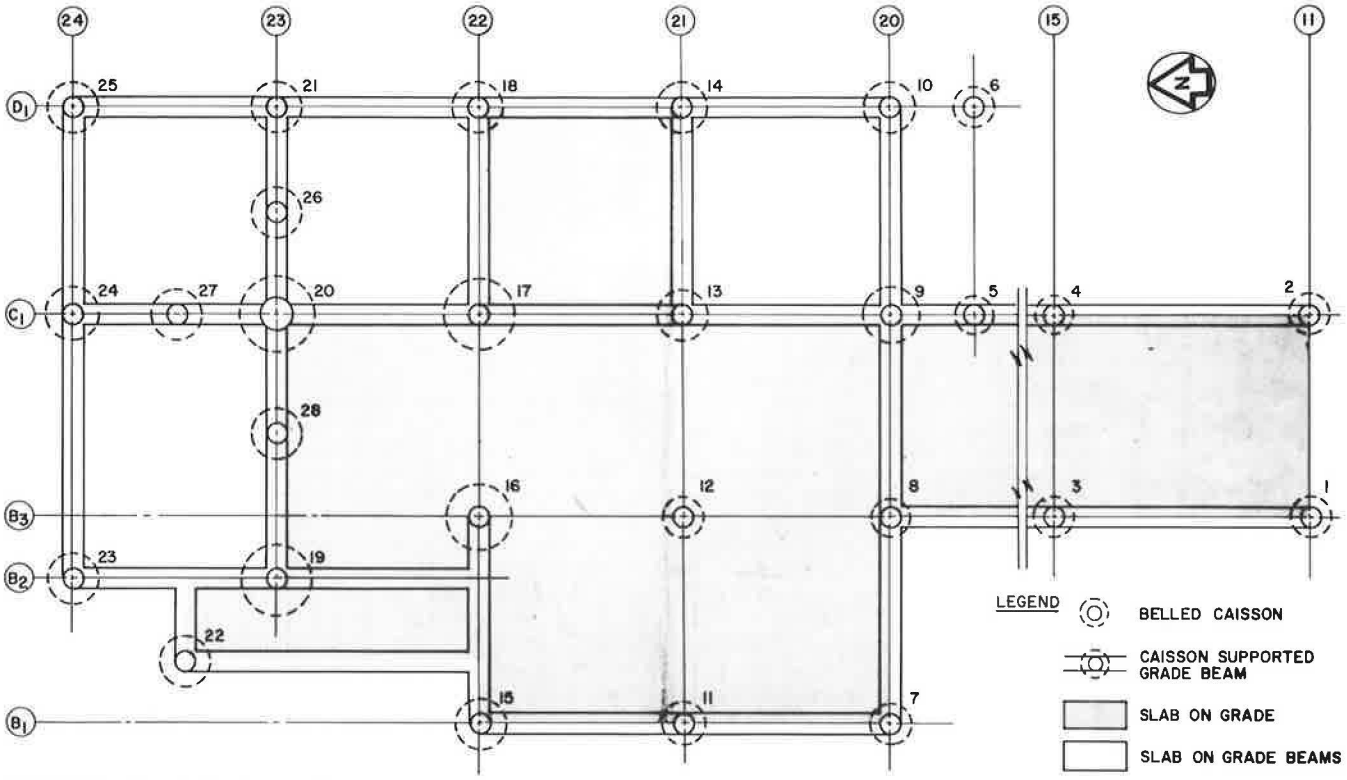

FIGURE 8 Foundation layout plan.

CONCLUSIONS

The soil properties were determined using a limited number of controlled tests supplemented with a sufficient number of simpler tests that can be performed much more rapidly and economically. Agreement was found between the correlations for the site soil and the published data. Performance of a fiberboard carton form was studied in the laboratory under simulated conditions. The tests were relatively simple and provided valuable information on the expected behavior of the fiberboard. Several defensive design features were included at a relatively minor cost that added much to protect the structure against the potential harmful effect of swelling soil.

ACKNOWLEDGMENT

The author is grateful to Moore Business Forms, Inc. for granting permission to publish these data. Financial support and encouragement were provided by Acres American Incorporated. Thanks also to Acres' geotechnical engineering and laboratory staff whose contributions to the project were innumerable.

REFERENCES

1. The States Climatologist Program, 1954-1973. Climate of the States, Vol. 2, Gale Research Company, Detroit, Mich., 1978.
2. W.G. Holtz and H.J. Gibbs. Engineering Properties of Expansive Clays. Papers in Geotechnical Engineering 1950-1959, ASCE, 1977.
3. R.B. Peck, W.E. Hanson, and T.H. Thornburn. Foundation Engineering. Second Edition, John Wiley & Sons, New York, 1974.

Publication of this paper sponsored by Committee on Environmental Factors Except Frost.

Controlling Expansive Soil Destructiveness by Deep Vertical Geomembranes on Four Highways

MALCOLM L. STEINBERG

ABSTRACT

Expansive soils are a worldwide problem. In the United States damages caused by expansive soils probably exceeded $10 billion in 1984. One-half of these damages involved highways, streets, and roads. Studies and research have been conducted by international, national, state, and educational institutions. The Texas State Department of Highways and Public Transportation has used relatively impervious fabrics (geomembranes) placed vertically along the pavement edges through the zone of moisture activity to minimize the destructiveness of expansive soils. These vertical geomembranes have been placed in sections of four highways in San Antonio, Texas, varying from 1/4 to 2 mi. Testing procedures involved measuring the smoothness of the riding surface and the cracking of the pavement surface, installing moisture sensors, and determining maintenance requirements. Two of the earlier projects had records of 4 and 5 years without significant surface cracking, which is an indication that the use of the geomembrane barrier contributed to a better riding surface and less maintenance. All four tests indicate that the fabric can be placed in a variety of ways. Conclusions to date offer guarded optimism that the deep vertical geomembrane barrier can reduce the destructiveness of expansive soils on pavement.

Expansive soils are a worldwide problem and the subject of international conferences and studies. In the United States these soils extend from coast to coast and from border to border. They were estimated to cause $2 billion in damages in 1973 (1) and $7 to $9 billion in 1980 (2), and these damages probably exceed $10 billion annually in the United States today. One-half of this destruction occurs to the nation's highways, roads, and streets (1). Additional damages are suffered by other transportation facilities such as airport runways, railroads, canals, pipelines, and sidewalks.

Controlling these soils has been the subject of studies by universities and state, national, and regional groups. The following methods have been used to control expansive soils: replacement, avoidance, chemical stabilization, electro-osmotic treatment, ponding, and membranes. A study by the U.S. Corps of Engineers Waterways Experiment Station (3) funded by the Federal Highway Administration reviews many of these methods. The encouraging results of shallow vertical barriers used in South Dakota (4) and the results of a ponding project (5) led the Texas State Department of Highways and Public Transportation (TSDHPT) to try a deep geomembrane. The ponding study showed that a zone of activity of the expansive clays in the San Antonio area is usually in the range of 6 to 8 ft below the surface. If the wide fluctuations of the moisture (from 3 to 35 percent) could be minimized, perhaps the destructive movements caused by these subgrades could be minimized.

Several questions arose: Could the geomembrane fabric be placed 8 ft deep? What kind of production of placement would be possible? How could effectiveness be measured? And would minimizing subgrade moisture change minimize pavement distortion over expansive soils?

INTERSTATE 410

The first test section of a deep vertical geomembrane on a Texas highway was part of a rehabilitation project on Interstate 410 in southwestern San Antonio (Figure 1). In this area, Interstate 410 crosses the Blacklands prairie physiographic zone, which contains Houston black clays from the Taylor and Navarro groups. These clays are firm when moist and sticky and plastic when wet. Atterberg limits included liquid limits from 50 to 79 and plasticity indices (PI) from 28 to 48. Built in 1960, the freeway section main lanes were a 4-lane divided highway with a 44-ft grass median. The main lanes contained 16 in. of foundation course, 9 in. of flexible base, and 3 in. of Type A and 2 in. of Type C asphaltic concrete. In the section where the deep vertical geomembrane was used, the main lanes transitioned from natural ground elevation to a depressed section between 20 to 22 ft below the original ground. Since their construction, the main lanes in this area distressingly revealed the destructiveness of the expansive clays. Repeated asphaltic concrete level-ups were followed by more pavement distortions, more level-ups, and heater-planer work where the "bumps" were burned off. Additional level-ups and exposed based patches indicated the need to try something different.

The Interstate 410 rehabilitation project was 15 mi long and included an asphalt seal coat, a 1 1/4-in. Type C asphaltic level-up, and a 3/4 in. Type D finish asphaltic concrete surface. In the Valley Hi area, a 1/2-mi long test section of the geomembrane barrier was placed along the inside and outside shoulders of the northbound main lane (Figure 2). The adjacent southbound main lane was to be the control section. The asphaltic concrete level-up placed varied from 1 to 12 in. thick.

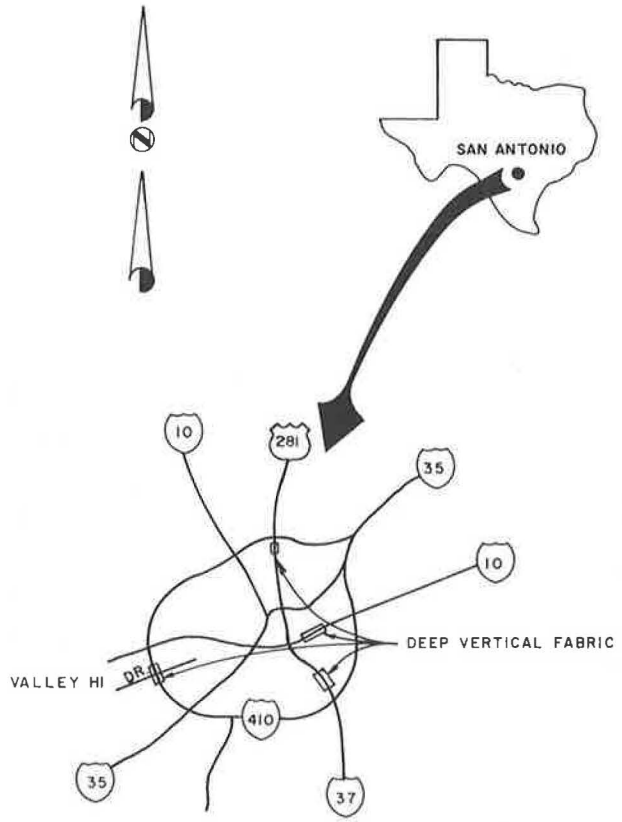

FIGURE 1 Test locations.

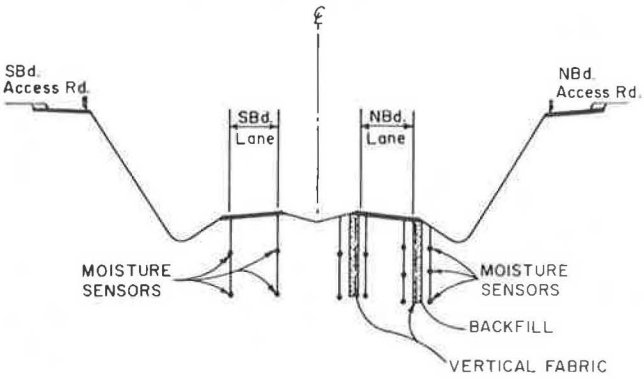

FIGURE 2 Interstate 410 section.

A spun-bonded polypropylene membrane coated with ethyl vinyl acetate (Dupont Typar T-063) 15.5 mils thick was used as the vertical geomembrane. It was placed 8 ft deep along the inside and outside shoulders of the northbound lanes with 2 ft lapped and tacked to the shoulders with an asphalt emulsion. The problem of installing the fabric after some initial sliding of the excavation was resolved by a subcontractor who used a backhoe that excavated the material and pulled a sliding shoring that held the roll of geomembrane vertically in the frame. The shoring consisted of two steel plates, each about 6 ft^2 separated by rods that held them rigid with the fabric roll held vertically between them. As the backhoe moved forward, the fabric unrolled in the trench and was tacked to the shoulder. A sand backfill was then placed in the trench. The vertical barrier work was done in February and March 1979 at rates averaging 350 to 400 ft a day.

Moisture sensors were placed inside and outside the geomembrane test section of the northbound lanes at depths of 2 to 8 ft. Sensors were also placed along the control sections of the southbound lanes adjacent to the fabric stations. Soiltest moisture cell sensors (MC374) were used following calibration under the direction of R.O. Lytton of the Texas Transportation Institute.

Sensor readings reported in detail in an earlier study (6) initially indicated greater changes in the subgrades in the unprotected southbound lanes than in the northbound lanes. These changes reflected a drying process, as indicated by the increase in resistivity in the cells, and also appeared outside the fabric along the northbound lanes. However, the irregularity and nonresponse in many cells led to abandonment of the readings.

Profilometer testing began in June 1979. These measurements were computer reduced to serviceability indices (SIs) in which 5.0 was the perfect smooth riding road with descending values indicating increasing roughness. The first SIs on the southbound lanes were 4.13 on the outside and 4.02 on the inside lane compared with 4.16 and 4.11 on the northbound lanes (Table 1). Before rotomilling in March 1981, the SIs were 3.38 and 3.17 for the southbound lanes compared with 3.72 and 3.76 for the northbound lanes.

Rotomilling was followed by an asphalt level-up. The southbound lanes received 200 tons compared with 100 tons for the northbound lanes. Following these operations, in December 1981, the SI for the southbound outside lanes was 3.57 and the SI for the inside lane was 3.56 compared with the SIs of 3.76 and 3.66 for the fabric-protected northbound lanes. By March 1984, this variation had increased again; the unprotected southbound lanes' SIs were 3.12 and 2.87,

TABLE 1 Interstate 410 Serviceability Indices

Location	June 1979	November 1979	August 1980	December 1980	March 1981[a]	July 1981[b]	December 1981	June 1982	February 1983	September 1983	March 1984
Southbound Lane (Control Section)											
Outside	4.13	3.70	3.39	3.28	3.38	3.43	3.57	3.47	3.28	3.16	3.12
Inside	4.02	3.63	3.30	3.15	3.17	3.29	3.56	3.25	2.99	2.89	2.87
Northbound Lane (Deep Vertical Fabric)											
Outside	4.16	4.03	3.83	3.55	3.72	3.74	3.76	3.66	3.57	3.47	3.49
Inside	4.11	3.99	3.83	3.57	3.76	3.61	3.66	3.67	3.55	3.50	3.59

[a]Rotomilled southbound lane March 30-April 2, 1981. Rotomilled northbound lane (isolated spots) April 3-7, 1981.

[b]Project leveled up August 1981.

TABLE 2 Interstate 410 Vertical Photologging

Location	August 1980	December 1980	June 1981	January 1982	August 1982	January 1983
Northbound Lanes						
Outside	0.07	0.08	0	0.04	0	0.19
Inside	0.01	0.24	0.08	0.34	0.03	0.37
Southbound Lanes						
Outside	0.28	0.62	0.11	0.87	0.29	0.75
Inside	0.24	1.01	0.10	0.78	0.51	0.45

while the northbound lanes' SIs were 3.49 and 3.59. The fabric-protected lanes continue to provide the smoother ride as indicated by the profilometer testing.

Photologging results indicated a similar pattern. Photologging was conducted with a camera mounted on a trailer taking pictures of 8-ft long segments and a travel lane 12 ft wide. The number of frames showing surface cracking, which may be indicative of subgrade-caused movement providing for intrusion of surface water, is expressed as a percentage of the total 8 ft segments. The first photos were taken in August 1980; the northbound lanes showed 0.07 and 0.01 percent of their area cracked whereas the southbound lanes showed as much as 0.28 and 0.21 percent of their area cracked. By 1983 cracking had increased to 0.19 and 0.37 percent in the northbound fabric-protected lanes while cracking in the southbound lanes had increased to 0.75 and 0.45 percent (Table 2).

INTERSTATE 37

Encouraged by the results on Interstate 410, a decision was made to use geomembranes in the rehabilitation of Interstate 37 in southeast San Antonio. This highway segment was constructed in 1968. South of Interstate 10, between Fair Avenue and Pecan Valley Drive, the Interstate 37 main lanes were in a depressed section usually 20 to 25 ft below natural ground. The soils are Houston black clays with PIs from 34 to 59 and liquid limits from 56 to 92. The main lane section has four northbound and four southbound lanes with a sodded median 28 to 36 ft wide. The median has a concrete ditch on a flat grade with a steel beam guardrail (Figure 3). The main lanes are four 12-ft wide lanes; 10-ft outside and 6-ft inside shoulders were built on 6 in. of lime-stabilized subgrade, 8 in. of cement-stabilized base, and 8 in. of concrete pavement. Substantial swelling clay movement had caused considerable distortion of the riding surface, the median guardrail, curbs, and slopes. Pavement maintenance for the 2-mi section cost an estimated $50,000 each year. (Communication with W.B. Collier, District Maintenance Engineer, TSDHPT).

Work on the 2.1-mi rehabilitation project began in October 1979 and included placement of 23,750 yd^2 of geomembranes 10 ft wide. The vertical geomembrane was placed 8 ft deep with backfill of gravel topped by 3 ft of cement-stabilized base. The decision to use this method was partly motivated by the experience on Interstate 410 of having two vehicles go axle deep in the sand backfill within a 6-month period. This process has not been repeated in the past 5 years. The fabric was placed along the outside shoulders of the southbound and northbound lanes. The project also included a rubberized asphalt seal, an asphaltic concrete level-up, and overlay. The median was reconstructed by removing the ditch and using positive drainage to the outside shoulders (Figure 4).

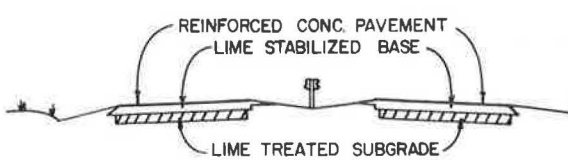

FIGURE 3 Existing Interstate 37 section before rehabilitation.

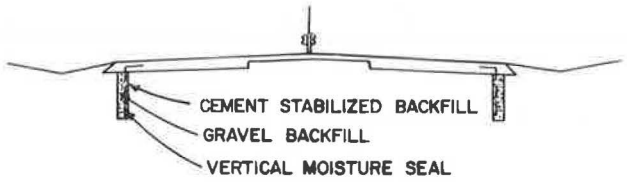

FIGURE 4 Proposed Interstate 37 section following rehabilitation.

The same subcontractor who used the backhoe on the Interstate 410 project was employed to place the geomembrane on the Interstate 37 rehabilitation project. However, the subcontractor used a trenching machine on the Interstate 37 project. The trenching machine pulled the sliding shoring with the fabric roll held vertically. A boom from the trenching machine deposited the excavated material into a dump truck. The cement-stabilized base was batched in a portable paving machine that followed the trenching and backfilling with the gravel. Polypropylene spunbonded fabric coated with ethyl vinyl acetate (Dupont Typar T-063) was placed in February and March 1980. A maximum of 485 ft of fabric was placed in 1 day, and an average of 385 ft was placed daily. Generally when 400 ft was placed, the day's operation ended; frequently this occurred by 2 p.m.

The first profilometer tests were conducted in November 1979, before placement of the geomembrane. The control sections were usually embankments to the north and south of the depressed section being rehabilitated. The initial SIs in the control sections varied from 3.33 to 3.15. The lanes to be improved had SIs ranging from 2.92 to 2.79 (Table 3).

In December 1980 following the rehabilitation, the fabric-protected lanes had SIs of 3.81 and 3.68 while the SIs in the control section varied from 3.30 to 2.97. This pattern of higher SI readings for the lanes with geomembranes placed continued through August 1983, with the fabric-protected lanes showing SIs of 3.72 and 3.64 compared with SIs of 3.26 and 3.04 in the control sections.

By March 1984, an asphalt level-up was applied to

TABLE 3 Interstate 37 Serviceability Indices

Location	November 1979[a]	December 1980[b]	July 1981	December 1981	June 1982	February 1983	August 1983	March 1984
Southbound lane								
North control	3.22	2.97	2.79	2.99	3.04	3.09	3.04	2.96
Fabric section	2.79	3.68	3.72	3.67	3.69	3.61	3.64	3.75
South control	3.33	3.18	3.20	3.22	3.22	3.19	3.19	2.36
Northbound lane								
North control	3.15	3.09	3.02	2.93	3.12	3.01	3.05	4.24
Fabric section	2.92	3.81	3.84	3.75	3.80	3.68	3.72	3.83
South control	3.24	3.30	3.30	3.28	3.33	3.29	3.26	2.31

[a]November 1979 testing before rehabilitation work.
[b]December 1980 and later tests after work completed.

the northbound lanes' north control section, which raised its SI to 4.24. Otherwise the fabric-protected lanes continued to show higher SIs than the lanes in the control section, 3.83 and 3.75 compared with 2.31, 2.36, and 2.96.

Photologging has revealed little surface cracking. In this testing, two 1,750-ft sections of both the northbound and southbound lanes were used to compare the fabric-protected lanes with the adjacent control sections. In general, there was very little cracking of any type. The initial photologging in June 1981 indicated cracking only in the northbound lane pavement with 0.15 percent in the fabric-protected section and 0.04 percent in the control section. A year and a half later, only the northbound control pavement showed any cracking, and it was a minimal 0.07 percent.

Moisture sensors installed on Interstate 37 have proven more reliable than those installed on Interstate 410. Reported fully in a paper by Picornell, Lytton, and Steinberg (7), these thermal block sensors were model MCS 6000. Ten sensors were installed at four locations in two areas within the lanes rehabilitated with geomembranes. Two of the locations were inside the fabric and two were outside. Periodic readings within a 90-week period indicated a uniformity of high moisture levels at the time of initial placement. However, the sensors placed outside the fabric, while showing this high matrix potential or high moisture readings initially, showed substantial change. All five sensors inside the fabric showed a uniform matrix potential over a 2-yr period, whereas those outside indicated considerable change. Several of the sensors have since become nonoperational. The sensors continuing to function indicated that inside the fabric the subgrade moisture remained relatively uniform whereas outside the fabric more significant changes occurred.

US-281

In 1983 two other highways built over expansive soils were contracted for pavement rehabilitation: US-281 in the north-central section of San Antonio and Interstate 10 between Pine and Amanda Streets on San Antonio's east side. The US-281 rehabilitation project is discussed next. On US-281, finished roadway elevations varied from original ground level to an excavation of about 20 ft below natural ground in 0.4 mi. The subgrade is an Austin Tarrant clay association. Atterberg limits indicated PIs from 25 to 58 and liquid limits from 47 to 80. Potential vertical rise values were calculated to range from 4 to 5 in. The freeway was built between 1970 and 1975, having sustained a 3-year period of construction. The main lanes included 6 in. of lime-stabilized subgrade, 6 in. of base, an asphalt seal coat, and 8 in. of continuously reinforced concrete pavement. In the rehabilitation area, the southbound lane was showing surface signs of significant distress. Rehabilitation of the southbound lane, beginning 0.3 mi south of Interstate 410, included applying an asphaltic seal coat, an asphaltic concrete level-up, and finish course with the geomembranes placed 8 ft along the inside and outside shoulders, similar to the Interstate 410 section (Figure 5). The fabric was to be lapped approximately 2 ft over the paved shoulder. A Class A gravel backfill was used in the trench with 12 in. of cement-stabilized base on top of the trench. Geomembranes were used again because of the favorable results on the Interstate 410 and Interstate 37 improvements.

The contractor used a gradall to excavate the trench. Progress was not rapid; an average of 50 to 120 ft of material was excavated per day. As time became shorter, suggestions to accelerate this operation resulted in excavation being done by two gradalls, and placement increased by 225 to 250 ft per day. The contractor experienced no sliding of the trench and no sloughing, and only saw cutting of the shoulders was necessary. The geomembrane, a composite system of woven polypropylene fabric with polypropylene film bonded 20 mils thick (a Mirafi MCF 500) was unrolled by hand and placed in the trench. The backfill operation followed. Profilometer testing followed the completion of the project in January 1984. The adjacent northbound lane, which had no rehabilitation work, was used as the control section (Table 4). Data are limited, but the initial

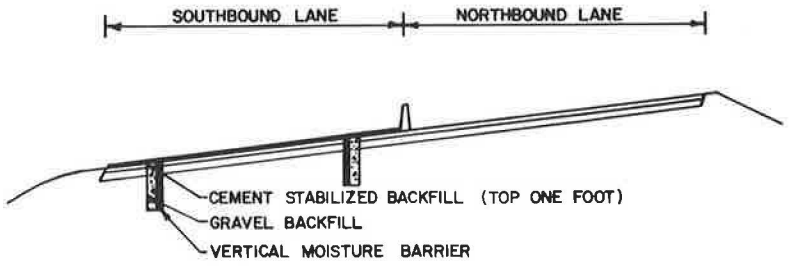

FIGURE 5 US-281 section following rehabilitation.

TABLE 4 US-281 Serviceability Indices

Date	Outside	Center	Inside
Southbound Lane (Geomembrane)			
July 1983	2.42	2.35	1.31
March 1984	3.08	3.07	3.00
Northbound Lane (Control)			
July 1983	2.90	2.86	2.72
March 1984	2.84	2.91	2.55

tests in July 1983 substantiated the decision to repair the southbound lane first. The asphalt level-up and finish course made the lane a smoother ride. However, it is too early to determine the impact of the geomembrane.

INTERSTATE 10

The final rehabilitation project in which geomembranes were used was Interstate 10 between Pine and Amanda Streets on the east side of San Antonio. Here the clays are Houston blacks with PIs of 35 to 55 and liquid limits from 65 to 75. During construction of Interstate 10 in 1968, problems arose with springs and water in the subgrade. This section of Interstate 10 has three eastbound and three westbound travelway main lanes separated by a sodded median. The pavement sections consist of 6 in. of lime-stabilized subgrade, 6 in. of lime-stabilized flexible base, an asphalt seal coat, and 8 in. of continuously reinforced concrete pavement. Usually the main lanes between Pine and Amanda Streets are in a depressed section, frequently 20 ft below natural ground.

Rehabilitation plans called for a rubber asphalt seal, asphaltic concrete level-up, and finish course. Plans also included placement of a vertical geomembrane 8 ft deep along the outside shoulders of the main lanes. The geomembrane will lap 2 ft over the paved shoulder. Its placement trench is approximately 2 ft wide with Class B gravel backfill, and the top 18 in. is a cement-stabilized base.

As in the US-281 rehabilitation project, the TSDHPT's generic specification and the supplier's low bid resulted in the Interstate 10 contractor using a Mirafi MCF 500 fabric. The estimated 24,745 yd^2 of geomembrane was placed by a trenching machine that excavated the material and also pulled a sliding steel shoring frame 7 ft at the top and tapered to 5 ft at the bottom and 8 ft deep. The sliding steel shoring frame held the fabric roll vertically in the trench, feeding the material out as the trenching machine moved forward. As on Interstate 37, the trenching machine had a conveyor belt on a boom that deposited the excavated material into a dump truck. The gravel was backfilled in the trench following placement of the fabric. The cement-stabilized base material was delivered to the site in transit mix trucks. The contractor experienced considerable sliding behind the trench excavation on this project. This resulted in the fabric placement being moved 6 to 8 ft out beyond the shoulder and extra geomembrane emulsion had to be tacked to the fabric placed in the trench to permit the "tie" to the paved shoulder. Despite this problem, on several days the contractor succeeded in placing more than 700 ft of the geomembrane.

Profilometer testing was conducted before construction and will continue at regular intervals when the project is completed. This project will also be monitored with moisture sensors and photologging. No test data are currently available.

OBSERVATIONS

The four different contractors on these pavement rehabilitation projects used three different methods to place the 8-ft deep geomembrane. Despite difficult sliding conditions on the Interstate 10 project, placement has exceeded 700 ft a day. A variety of testing procedures has been used. Perhaps the first test section on Interstate 410, which has a 5-year record of results, offers the best comparison. Adjacent lanes were compared: one lane with the fabric and one lane without the fabric. The lane with the fabric had consistently higher serviceability indices, indicating a smoother riding surface with less pavement cracking. When asphalt level-up was applied, twice as much was required on the southbound nonfabric-protected lane as on the northbound geomembrane lane. On the Interstate 37 project, a section that had maintenance costs of $50,000 a year has had no expenditure in 4 1/2 years. No doubt removing the median ditch and adding the rubberized asphalt surface seal have also contributed to this improvement. Research by others (8) and a small horizontal fabric project (9) in San Antonio has emphasized the effectiveness of minimizing the intrusion of surface water into the subgrade. Other research indicates that geomembranes can provide added strength to sections when used horizontally. Moisture sensors show that the geomembrane deep vertical protection may minimize subgrade moisture change. However, the need for greater sensor longevity remains.

A look at costs is worthwhile. On the first deep fabric placement on Interstate 410, the low bid price was $20 per lineal foot along the pavement, which included all materials, excavation, placement, backfilling, and disposition of excavated materials. The bid price on Interstate 37 was $21 per lineal foot. The US-281 contract plans contained separate pay items for the fabric, the gravel backfill, and the cement-stabilized base. The low bidder's price totaled $15.66 per lineal foot for the fabric placement and related items. On Interstate 10, which had the same range of separate bid items, the low bidding contractor's price was $27.15 per lineal foot. With fabric prices from suppliers probably ranging from $1.25 to $1.75 per lineal foot, some further economies can be expected.

CONCLUSION

Deep vertical geomembranes can be placed in expansive soils 8 ft deep. A substantial number of feet of geomembrane can be placed in 1 day. Lanes with geomembranes can be considered to result in a generally smoother riding surface than unprotected lanes. Geomembranes appear to minimize the destructive impact of swelling subgrades on highway pavements and to reduce moisture change in the soils beneath the pavements; this may contribute to the reduced destructive movement. Further use of both vertical and horizontal geomembranes is worthy of serious consideration.

ACKNOWLEDGMENT

The author expresses thanks to R.E. Stotzer, G.H. Wilson, G.K. Hewitt, R.L. Lytton, Consuelo Flores,

Ken Hankins, John Nixon, W.C. Garbade, A.O. Hilgers, T.J. Walthall, R.H. Magers, M.H. Hardy, M. Picornell, D.R. Snethen, R.D. Lockhart, Pablo De Arkos, and Rick Norwood.

REFERENCES

1. D.E. Jones and W.G. Holtz. Expansive Soils--The Hidden Disaster. Civil Engineering Magazine, Aug. 1973, pp. 49-51.
2. J.P. Krohn and J.E. Slosson. Assessment of Expansive Soils. Proc., 4th International Conference on Expansive Soils, Denver, Colo., ASCE, New York, Vol. 1, June 1980.
3. D.R. Snethen et al. A Review of Engineering Experiences with Expansive Soils in Highway Subgrades. Report FHWA-RD-75-48. FHWA, U.S. Department of Transportation, 1978.
4. E.B. McDonald. Experimental Moisture Barrier and Waterproof Surface. Report HR 0200(3645). South Dakota Department of Transportation, Pierre, Oct. 1973.
5. M.L. Steinberg. Ponding on Expansive Clay Cut: Evaluations and Zones of Activity. Transportation Research Record 641, TRB, National Research Council, Washington, D.C., 1978, pp. 61-66.
6. M.L. Steinberg. Deep Vertical Fabric Moisture Barriers in Swelling Soils. Transportation Research Record 790, TRB, National Research Council, Washington, D.C., 1981, pp. 87-94.
7. M. Picornell, R.L. Lytton, and M.L. Steinberg. Assessment of Effectiveness of a Vertical Moisture Barrier. 5th International Conference on Expansive Soils, Adelaide, Australia, 1984.
8. B.J. Dempsey and O.L. Robnett. Influence of Precipitation Joints and Sealing or Pavement Marriage. Transportation Research Record 705, TRB, National Research Council, Washington, D.C., 1979, pp. 13-23.
9. M.L. Steinberg. Horizontal Placement of a Geotextile on a Subgrade to Control a Swelling Soil. Research Report 187-9. Texas State Department of Highways and Public Transportation, Austin, Feb. 1983.

Publication of the paper sponsored by Committee on Environmental Factors Except Frost.

Long-Term Behavior of a Drilled Shaft in Expansive Soil

LAWRENCE D. JOHNSON and WILLIAM R. STROMAN

ABSTRACT

A vertical load test was performed in November 1982 on an instrumented 30-in. diameter drilled shaft 36 ft long with a 4-ft underream. Shaft LAFB-2 was constructed at Lackland Air Force Base, Texas, during July 1966, in stiff, expansive clay soil that contained a perched water table in a clayey gravel stratum. Soil adjacent to LAFB-2 had heaved 7.7 in. at the ground surface by September 1981, while the shaft had heaved 3.4 in. Because soil within 3 ft of the shaft base had heaved only 1.8 in., LAFB-2 had stretched or fractured along the shaft length. Results of the vertical load test indicated a discontinuity in the load-displacement curve that separated the observed skin friction resistance of 250 tons from the end bearing resistance of 130 tons. Uplift thrust of the adjacent swelling soil mobilized skin friction and tensile forces in the shaft equivalent to the shear strength of the adjacent soil times the total shaft surface area. Long-term end bearing capacity was reduced to about 75 percent of short-term capacity because of long-term wetting of soil beneath the shaft base.

In July 1966 seven test shafts were constructed at Lackland Air Force Base to study the performance of drilled shafts in expansive soil. The test site was instrumented with porous stone piezometers, free-standing benchmarks, and two deep reference benchmarks to provide accurate pore water pressure and elevation profiles. Pressure heads recorded in the piezometers indicated a perched water table 8 ft below ground surface extending down to about 50 ft. A deep water table was observed 80 ft below ground surface.

A vertical load test was performed on shaft LAFB-2 in November 1982 to investigate the long-term performance of a drilled shaft in expansive soil. This 2.5-ft diameter by 36-ft long shaft, including a 4-ft diameter bell, is located in the southeast corner of a 100 x 100-ft covered area constructed in 1974 to observe trends in long-term heave in expan-

sive soil beneath lightly loaded areas (1). LAFB-2 was instrumented with 21 strain gauges secured on steel reinforcement and distributed in groups of three at periodic intervals along the full shaft length. Steel reinforcement is 3 number 14S bars tied with number 4 bars at 12-in. centers for 6.75 in.^{2} or 1 percent of the shaft cross section. LAFB-2 was also instrumented with eight Carlson earth pressure cells that were mounted in specially prepared holes cut into undisturbed soil on opposite sides of the shaft perimeter at depths of 2.4, 6, 15, and 32 ft below ground surface. Compressive strength tests performed on 3-in. diameter concrete core samples taken from the adjacent shaft (LAFB-1) in 1982 at 3.8 and 11.5 ft deep indicated a Young's modulus of 216,00 tsf and compressive strength of about 400 tsf (2,3).

DESCRIPTION OF SOILS

The overburden material consists of about 8 ft of expansive black to gray CH clay and 4 to 5 ft of GC clayey gravel with caliche. The primary material encountered below the gravel is fissured expansive CH clay shale of the Upper Midway group of the Tertiary system. The soils are uniform within the test area. Laboratory tests to classify the soil and to evaluate strength and consolidation parameters were performed on 6-in. diameter undisturbed samples obtained between 1966 and 1982 by Shelby tube or piston samplers. Relatively undisturbed samples could not be obtained from the clayey gravel. Details of the results of these soil tests and site layout are described elsewhere (2,3).

HEAVE PROFILE

The soil heave profile measured from the freestanding benchmarks, PSTBM, shown in Figure 1 relative to July 1966 indicate the least measured vertical swell at the test site. Heave recorded at the ground surface by the PSTBM was about 3 in. in 1981. Soil heave of about 1 in. occurred less than 5 ft below ground surface, 0.9 in. between 15 and 25 ft in the fissured clay shale of the Upper Midway group, 0.6 in. from 25 to 40 ft, and 0.4 in. below 40 ft. Soil adjacent to LAFB-2 had heaved 7.7 in. by 1981, considerably more than the freestanding benchmarks. Soil near the base of shaft LAFB-2 at 35 ft had also heaved about twice that of the 35-ft benchmark. Shaft LAFB-2 had heaved 3.4 in. by 1982, much more than the 1.8 in. of soil heave observed near the shaft base; therefore, the shaft appeared to stretch 1.6 in. Because LAFB-2 is underreamed, it may have fractured at one or more locations along the shaft length.

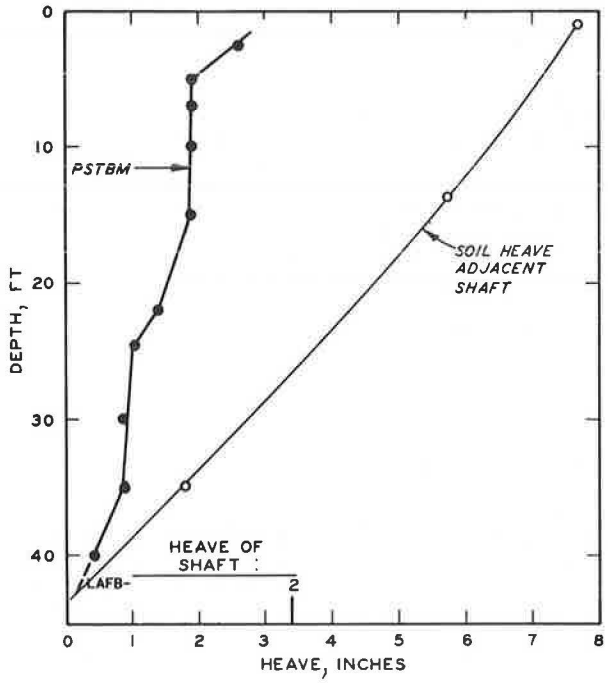

FIGURE 1 Heave profile of LAFB-2 in September 1981.

THEORETICAL MODELS

Vertical axial loads are resisted by skin friction along the shaft-soil interface and by end bearing capacity of the soil beneath the shaft base. The ultimate capacity Q_u of the shaft is commonly given by

$$Q_u = Q_{su} + Q_{bu} \tag{1}$$

$$Q_{su} = \pi D_s \int_0^L \bar{f_s} \, dL \tag{2}$$

$$Q_{bu} = q_{bu} A_b \tag{3}$$

where

Q_{su} = ultimate mobilized skin resistance, tons;
Q_{bu} = ultimate end bearing resistance, tons;
D_{su} = shaft diameter, ft;
$\bar{f_s}$ = full mobilized skin friction, tsf;
dL = increment of shaft length L, ft;
q_{bu} = ultimate base resistance pressure, tsf; and
A_b = base area, ft^2.

The ultimate capacity Q_u is normally reduced to an allowable bearing capacity Q_a for design by selection of suitable factors of safety.

End Bearing Capacity

Shaft foundations normally fail by punching shear in which the shear surface is not well defined and failure is progressive with continuing downward movement or punching of the soil. The end bearing capacity, q_{bu}, for deep foundations may be given by

$$q_{bu} = cN_c + \sigma_v' N_q \tag{4}$$

where c is the cohesion, tsf; σ_v' is the effective vertical overburden pressure, tsf; and N_c, N_q is the bearing capacity factors. Factor N_c equals 9 and N_q equals 1 for total stress (undrained) analysis. σ_v is equally ignored to compensate for the shaft weight. The cohesion c equals the undrained shear strength C_u.

The bearing capacity factor N_q for effective stress (drained) analysis has been evaluated by a variety of useful procedures in which cohesion is normally ignored. Two procedures for local and general shear failure are

$$\text{Local (4): } N_q = (1 + \tan\phi')e^{\tan\phi' \tan^2(45 + \phi'/2)} \tag{5a}$$

$$\text{General (5): } N_q = [e^{(270-\phi')\pi\tan\phi'/180}] \div [2\cos^2(45 + \phi'/2)] \tag{5b}$$

where ϕ' is the effective friction angle. Settlements required to achieve ultimate end bearing vary widely, but practical estimates for drilled shafts are up to 25 percent of the shaft diameter.

Skin Friction

The development of skin friction f_s in deep foundations depends on the relative displacement between soil and shaft. The full mobilized skin friction $\bar{f_s}$ occurs at relative displacements much less than those usually required to achieve full end bearing and often less than 0.5 in. of total shaft head displacement. Cylindrical shear models are considered most appropriate for analysis of skin friction resistance as used in Equation 2. The magnitude of ultimate skin friction for practical design applications may be computed by the same cylindrical shear model for applied structural loads, pullout loads, downdrag forces from consolidating soil, and uplift thrust from swelling soil. The maximum uplift thrust developed in swelling soil is considered in this paper.

Methodology for evaluating $\bar{f_s}$ by undrained analysis is

$$\bar{f_s} = \alpha\, C_u \tag{6}$$

where α is a factor relating adhesion along the soil-shaft interface to the undrained cohesion C_u. The factor α appears to vary with the type of soil and is on the order of 0.5 for the stiff clays of this test site (6); however, α for modeling uplift thrust from expansive soil may be larger than 0.5 and could approach 1.0 because the soil expands tightly against the shaft perimeter over the full length of the swelling soil.

Methodology for evaluating the full mobilized skin friction by drained analysis is given by

$$\bar{f_s} = \beta\, \sigma_v' \tag{7}$$

where β is the lateral earth pressure and friction angle factor. Among the models available for evaluating β, the model (7)

$$\beta = K_o \tan \delta' \tag{8}$$

is commonly used where K_o is the coefficient of lateral earth pressure at rest. In practice the most appropriate effective friction angle δ' appears to be several degrees (≈ 5 degrees) less than the measured angle ϕ' or about $0.8\phi'$.

The uplift thrust from swelling of expansive soil is expected to increase the actual coefficient of lateral earth pressure toward the passive coefficient K_p, which could be modeled by the Rankine passive state ignoring cohesion and $\delta' = \phi'$. The uplift thrust Q_{us} may also be modeled by (8,9)

$$Q_{us} = 1.3\pi D_s \int_0^L \sigma_s \tan \phi'_{residual}\, dL \tag{9}$$

where σ_s is the swell pressure, tsf, and ϕ' residual is the residual effective friction angle, degrees. Possible explanation for the factor 1.3 in Equation 9 are that measured swell pressures may be less than actual swell pressures, and the friction angle may be between the peak and residual friction angle.

Load-Displacement Behavior

The load-displacement behavior may be estimated by a variety of techniques. Results of several elastic and load transfer models applied to LAFB-2 are described elsewhere (3). The finite element method using computer program AXIPLN (10) and load transfer functions programmed into a computer code AXILTR (2) are applied in this paper to evaluate load-displacement behavior of LAFB-2. Load transfer functions programmed into AXILTR are discussed next.

Shaft Load Transfer Functions

The load transfer function or t-z curve defined by Seed and Reese (11) uses a shape function that depends on the type of soil. Experimental data (11) indicated the load transfer (or normalized t-z) function for normally consolidated soil shown in Figure 2a. Kraft, Ray, and Kagawa (12) also developed a load transfer hyperbolic t-z function after Randolph and Wroth (13) that leads to the normalized

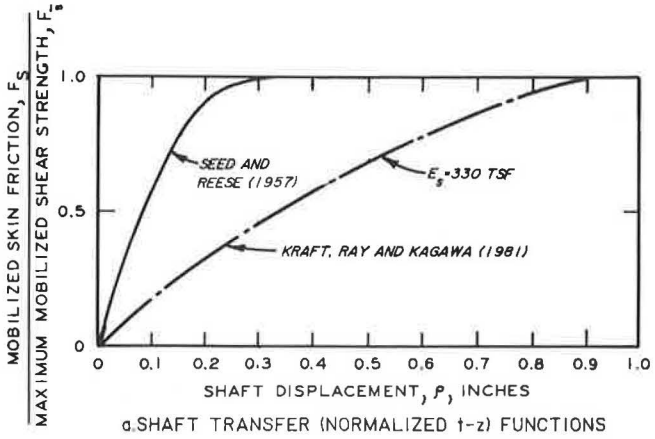

a. SHAFT TRANSFER (NORMALIZED t-z) FUNCTIONS

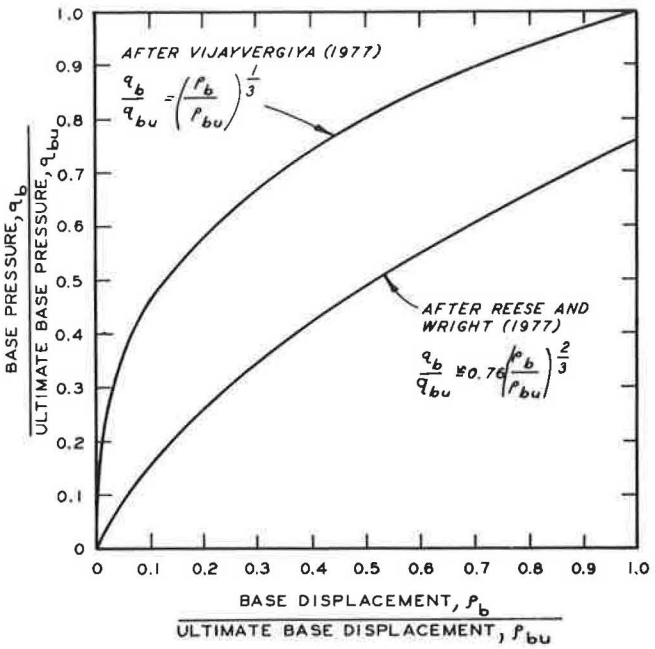

b. BASE TRANSFER (NORMALIZED q-z) FUNCTIONS

FIGURE 2 Normalized load transfer functions.

load transfer function (Figure 2a) for the following parameters consistent with shaft LAFB-2:

Soil Young's modulus, E_s = 330 tsf
Soil Poisson's ratio, ν_s = 0.3
Soil shear modulus, G = 127 tsf
Soil shear strength, f_s^- = 1.5 tsf
Shaft diameter, D_s = 2.5 ft
Shaft length, L = 36 ft
Curve fitting constant, R_f = 0.96

This load transfer function is less stiff than the empirical function of Seed and Reese (11) for the preceding parameters.

Base Load Transfer Functions

Transfer functions have also been developed for load transfer to the soil beneath the shaft base. Figure 2b shows two (normalized q-z) base functions after Reese and Wright (14) and Vijayvergiya (15). The ultimate base settlement ρ_{bu} has been related to the strain in laboratory tests by (14)

$$\rho_{bu} = 2D_b\varepsilon_{50} \quad (10)$$

where D_b is the base diameter in feet and ε_{50} is the strain at 1/2 maximum deviator stress of undrained Q triaxial test. Confining pressure during the Q test was not specified. In the interest of simulating in situ conditions, the confining pressure should be similar to the in situ soil overburden pressure. Vijayvergiya (15) assumed ρ_{bu} is about 4 to 6 percent of the base diameter, D_b. The ultimate base pressure, q_{bu} (Figure 2b) is taken as $9C_u$ where C_u is the undrained shear strength. Figure 2b shows that the data after Vijayvergiya (15) indicate substantially stiffer soil than the mean data after Reese and Wright (14).

RESULTS AND ANALYSIS OF VERTICAL LOAD TEST

The vertical load test was performed in November 1982 using a 1,250-ton capacity loading frame supported by two 3-ft diameter shafts 36 ft long with 7-ft, 6-in. diameter bells. Each anchor shaft contained ten 1 3/8-in. diameter, 150,000 psi high-strength bars equally spaced around a 28-in. diameter ring. Vertical loads were applied with a calibrated and electronically operated loading jack of 1,200 ton capacity. Displacements were measured by two dial gauges, sensitive to 0.001 in., positioned on each side of the test shaft and mounted on a wood frame independent of the shaft. Backup ruler and wire gauges were also in position. The load test was conducted in accordance with ASTM Standard Test Method D1143 (16).

Results of Load Test

The shaft experienced an intermediate plunging failure at 250 tons causing rapid displacement to 1.5 in. (Figure 3). This intermediate failure was attributed to applied loads exceeding the maximum skin resistance and the presence of a void or soft soil, or both, beneath the base. Because LAFB-2 had heaved

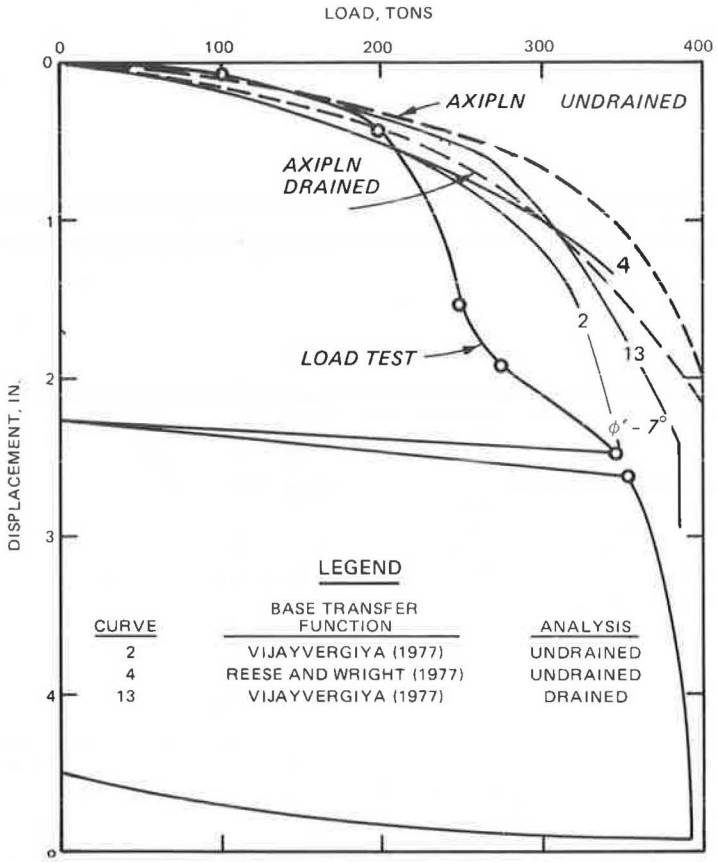

FIGURE 3 Comparison of observed with calculated load-displacement behavior by programs AXILTR and AXIPLN.

1.6 in. more than the soil had heaved near the vicinity of the base, a gap had occurred in the shaft and could have been caused by tensile fracture near the base. The strain gauge data (2) indicated negligible elastic modulus in the shaft near the shaft base and the strain gauge data also had shown that the shaft had compressed about 1 in. during the load test, mostly below 20 ft. Therefore, a fracture in the shaft appears to have existed near the base, and 0.6 in. of possible space may have existed beneath the base. The shaft held an additional 130 tons after the intermediate plunging failure, which is attributed to the end bearing capacity. The failure load of 380 to 400 tons was maintained for 8 hr with a creep rate of 0.001 in./min. Loads exceeding 400 tons significantly increased the creep rate and could not be maintained.

An analysis of the skin friction distribution with depth (2,3) indicated that the α factor at maximum skin resistance relative to the undrained shear strength is about 0.85 and 1.0 from 0 to 16 ft and 16 to 34 ft, respectively (Figure 4). These α factors are larger than those expected in nonswelling soil, indicating intimate contact at the soil-shaft interface. The skin friction distribution is bounded by the Seed and Reese (11) and Kraft, Ray, and Kagawa (12) load transfer models. The large magnitude of skin friction observed over the full length of the shaft indicates that any fracture in the shaft must have occurred near the base. Strain gauge readings (2,17) show that large tensile strains had developed in the lower portion of the shaft.

The maximum end bearing load, Q_{bu}, was 130 tons at a displacement of 4.9 in. A plot of the normalized base transfer q-z functions in Figure 5 shows that the load test results are between the functions after Vijayvergiya (15) and Reese and Wright (14)

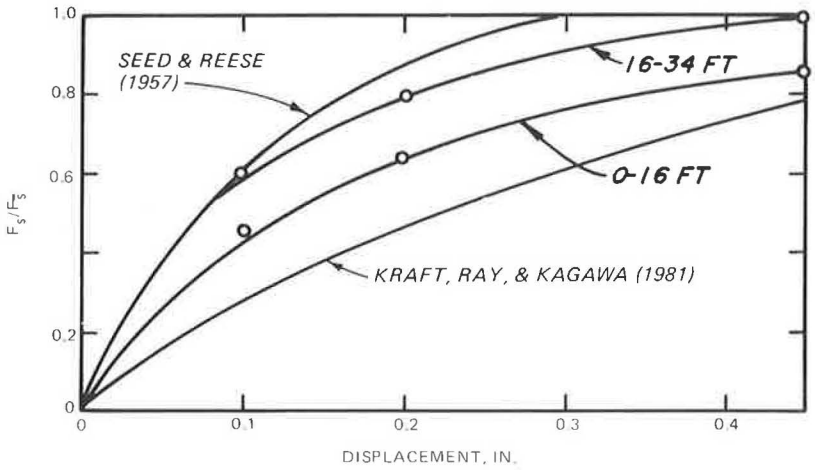

FIGURE 4 Normalized t-z skin friction curves of shaft LAFB-2.

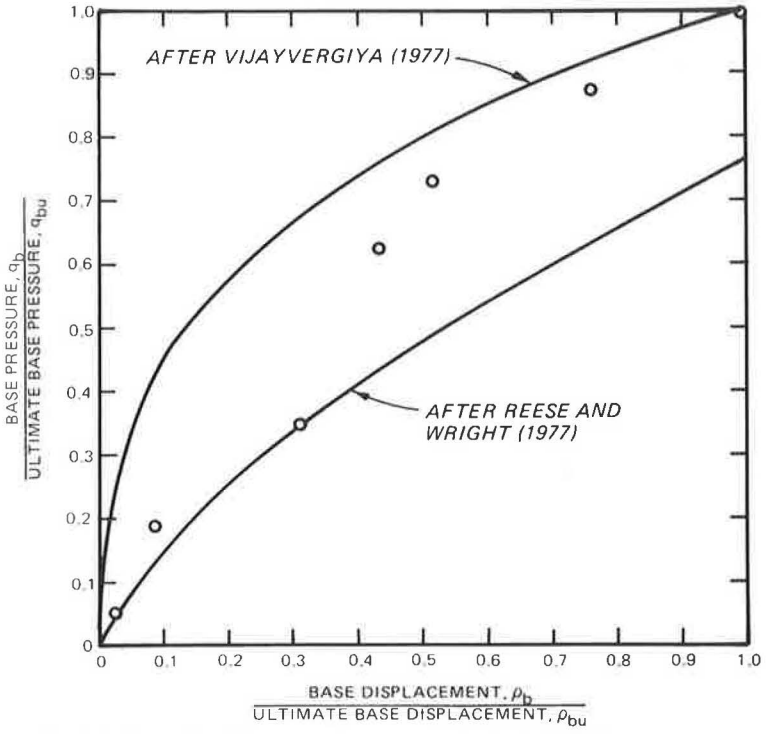

FIGURE 5 Normalized base transfer q-z curve for shaft LAFB-2.

shown in Figure 2b. The ultimate base displacement, ρ_{bu}, estimated by Equation 10 is 0.6 in., which is much less than observed even excluding the 1.5 in. of rapid drop at 250 tons. The value of ρ_{bu} after the criterion of 4 to 6 percent of D_b (15) is 2 to 3 in., which reasonably simulates the observed ρ_{bu} if 1 to 2 in. of displacement are subtracted from the observed 4.9 in. to compensate for crack closure in the shaft.

The skin friction model used to calculate curves 2, 4, and 13 in Figure 3 was after the load-transfer skin friction model of Kraft, Ray, and Kagawa (12). The general shear Equation 5b was used to compute ultimate base capacity, Q_{bu}, for the drained analysis of curve 13, and N_c = 9 was used to compute Q_{bu} for the undrained analysis. The shaft modulus was 108,000 tsf, simulating a long-term concrete modulus. The input parameters used in programs AXIPLN and AXILTR are given in Tables 1 and 2. The calculated curves tend to underestimate displacements for loads exceeding mobilization of skin friction. Skin friction parameter α = 0.45 for undrained analysis of curves 2 and 4 is too low. The finite element drained (C_u = 0) and undrained (ϕ' = 0) results from AXIPLN; both overestimate end bearing capacity similar to results of AXILTR.

Ultimate Capacity

End bearing capacity, Q_{bu}, for undrained analysis using N_c = 9 is 170 tons, which exceeds the actual end bearing capacity by 40 tons. A bearing capacity factor N_c = 7 reasonably consistent with a recommended value of 7.4 (18) properly simulates end bearing, Q_{bu}, for drained analysis using ϕ' = 27 degrees, and the general shear model for N_q grossly overestimates end bearing at 278 tons. N_q approximated by local shear failure from Equation 5a reasonably simulates actual end bearing resistance.

Skin resistance was underestimated for α = 0.45 and should have been near 1.0 for undrained analysis consistent with results in Figure 4. Skin resistance for drained analysis is properly calculated using the measured effective friction angle ϕ' from results of $\bar{R}$ tests with pore pressure measurements and a coefficient of lateral earth pressure K approaching 3.0. The measured earth pressure distribution on LAFB-2 (2,3) indicates lateral pressures about three times the vertical pressure. The Rankine friction model or the swell pressure model given by Equation 9 using ϕ' residual = 9 degrees and 1966 swell pressures both lead to skin frictions comparable to those measured during the 1982 load tests.

CONCLUSIONS

The α factor for skin friction resistance by total stress (undrained) analysis in expansive soil is larger than may occur in nonswelling soils. It can approach 1.0 over the entire length of the shaft subject to lateral thrust from swelling soil.

End bearing capacity for LAFB-2 was less than expected and approximately given by N_c = 7 for undrained analysis and N_q given by local shear failure for drained analysis. The reduced end bearing capacity is attributed to shaft heave, which lifted the base off the soil contributing to a possible void and soil heave with softening beneath the base and shaft fracture near the base.

Load-displacement behavior may be modeled by a variety of methods of which load transfer functions appear practical. Skin friction was bounded by the Seed and Reese (11) and Kraft, Ray, and Kagawa (12) models and end bearing by the Vijayvergiya (15) and Reese and Wright (14) models.

Drilled shaft foundations for supporting permanent structures in expansive soil should be loaded near the allowable bearing capacity assuming a minimum factor of safety consistent with good engineering practice. The amount of reinforcement steel required to resist uplift thrust caused by swelling soil should be based on the maximum shear strength of the adjacent soil. Reinforcement should be full length extending into any existing underream and well secured in the underream. Elements of deep foundations

TABLE 1 Soil Parameters for Analysis of Vertical Load-Displacement Behavior, AXILTR

Depth, ft	Specific Gravity	Poisson's Ratio	Void Ratio	Water Content (%)	Shear Strength Parameters			Soil Modulus, tsf
					C_u, tsf	ϕ', deg.	K_o	
0-10	2.72	0.3	0.90	29.0	0.8	25	0.7	150
10-20	2.75	0.3	0.90	29.0	0.8	27	0.7	150
20-34	2.77	0.3	0.88	30.5	1.5	34	1.5	400
34-40	2.77	0.3	0.88	30.5	1.5	35	1.5	700

Note: Concrete modulus = 108,000 tsf; ϵ_{50} = 0.006; R_f = 0.97; soil shear modulus = 58 tsf; α = 0.6.

TABLE 2 Soil Parameters for Analysis of Vertical Load-Displacement Bheavior, AXIPLN

Depth, ft	Poisson's Ratio	Unit Weight tons/ft^3	Shear Strength Parameters			Hyperbolic Parameters			
			C_u tsf	ϕ' deg	K_o	R_f	K_i	K_{ui}	n
0-10	0.3	0.059	0.8	18	0.7	0.97	190	380	0.64
10-20	0.3	0.059	0.8	20	0.7	0.97	190	380	0.64
20-80	0.2	0.060	1.5	28	1.5	0.90	380	760	0.28
Concrete	0.2	0.075	1.0						
Interface element	0.495		0.8	20		0.97			0.64

Note: Concrete modulus = 108,000 tsf, K_j = 6440.

should not penetrate through perched water tables into deeper desiccated soil if practical.

ACKNOWLEDGMENT

This load test and analysis were supported by a grant to the Waterways Experiment Station from the Office, Chief of Engineers, and conducted in cooperation with the U.S. Army Engineer District, Fort Worth, Texas.

REFERENCES

1. L.D. Johnson. Field Test Sections on Expansive Soil. Proc., 4th International Conference on Expansive Soils, Denver, Colo., ASCE, New York, 1981.
2. L.D. Johnson. Methodology for Design and Construction of Drilled Shafts in Cohesive Soils. Technical Report GL-84-5. U.S. Army Engineer Waterways Experiment Station, Vicksburg, Miss., 1984.
3. L.D. Johnson and W.R. Stroman. Vertical Behavior of Two 16-Year Old Drilled Shafts in Expansive Soil. Analysis and Design of Pile Foundations. J.R. Meyer, ed., ASCE, San Francisco, Calif., 1984, pp. 154-173.
4. A.S. Vesic. Design of Pile Foundations. NCHRP Synthesis of Highway Practice 42, TRB, National Research Council, Washington, D.C., 1977.
5. J.E. Bowles. Foundation Analysis and Design. McGraw-Hill, New York, 1968, pp. 607-609.
6. L.C. Reese, F.T. Touma, and M.W. O'Neill. Behavior of Drilled Piers Under Axial Loading. Journal of the Geotechnical Engineering Division, ASCE, Vol. 102, No. GT5, 1976, pp. 493-510.
7. R.J. Chandler. The Shaft Friction of Piles in Cohesive Soils in Terms of Effective Stress. Civil Engineering and Public Works Review, Vol. 63, 1968, pp. 48-51.
8. W.P. Jobes and W.R. Stroman. Structures on Expansive Soil. Technical Report M-81. Construction Engineering Research Laboratory, Champaign, Ill., 1974.
9. M.W. O'Neill and N. Poormoayed. Methodology for Foundations on Expansive Clays. Journal of the Geotechnical Engineering Division, ASCE, Vol. 106, No. GT12, 1980, pp. 1345-1357.
10. J.L. Withiam and F.H. Kulhawy. Analytical Modeling of the Uplift Behavior of Drilled Shaft Foundations. Report B-49(3). School of Civil and Environmental Engineering, Cornell University, Ithaca, N.Y., Niagara Mohawk Power Corporation, Syracuse, N.Y. 1978.
11. H.B. Seed and L.C. Reese. The Action of Soft Clay Along Friction Piles. Transactions ASCE, Vol. 122, pp. 731-753.
12. L.M. Kraft, R.P. Ray, and T. Kagawa. Theoretical t-z Curves. Journal of the Geotechnical Engineering Division, ASCE, Vol. 107, No. GT11, 1981, pp. 1543-1561.
13. M.F. Randolph and C.P. Wroth. Analysis of Deformation of Vertically Loaded Piles. Journal of the Geotechnical Engineering Division, ASCE, Vol. 104, No. GT12, 1978, pp. 1465-1488.
14. L.C. Reese and S.J. Wright. Drilled Shaft Design and Construction Guidelines Manual, Construction of Drilled Shafts and Design for Axial Loading. Vol. I, FHWA, U.S. Department of Transportation, 1977.
15. V.N. Vijayvergiya. Load-Movement Characteristics of Piles. Proc., Port '77 Symposium, Long Beach, Calif., ASCE, New York, 1977, pp. 269-284.
16. Piles Under Axial Compressive Load. ASTM D 1143, Part 19, ASTM, Philadelphia, Pa., 1981.
17. Investigations for Building Foundations in Expansive Clays. Vols. I and II, U.S. Army Engineer District, Fort Worth, Texas, 1968.
18. Procedures for Foundation Design of Buildings and Other Structures (Except for Hydraulic Structures). Technical Manual 5-818-1. Department of the Army, Washington, D.C., 1983.

Publication of this paper sponsored by Committee on Environmental Factors Except Frost.

Experience With Roads and Buildings on Expansive Clays

G. WISEMAN, A. KOMORNIK, and J. GREENSTEIN

ABSTRACT

The procedures used for designing safe and economic structures to resist load-induced deformation are inadequate for the design of roads and buildings on expansive clays. For these clays, increase in moisture causes not only a decrease in strength but also volume expansion that results in cracked buildings and rough pavements. A method of quantifying the amount of heave expected (depending on surcharge pressures), the depth of replacement with nonswelling materials, and the final equilibrium suction values are presented. The procedure is based on one-dimensional laboratory swelling curves. Since time, site, and budget limitations frequently do not allow for complete laboratory testing, commonly used empirical correlations are discussed. A method of calibrating these correlations, which are usually based on simple index tests is presented. The importance of post construction observations and comments on increased interest in the legal aspects of the problem are presented. A review of some early publications is included along with flow charts and a program written in BASIC for computing heave.

Engineers have considerable experience in designing safe and economic structures to resist load-induced deformation. For example, engineers use a pavement design procedure that accounts for possible softening of subgrade clays due to moisture increase within the design life of the pavement. However, for swelling clays, increase in moisture causes not only a decrease in strength, but also volume expansion and hence increased pavement roughness that is not load induced. Similarly, for building foundations on expansive clays, the use of an adequate factor of safety against bearing capacity failure, with due consideration for seasonal variations in strength, is an inadequate design procedure for assuring that deformation of the structure stays within safe limits.

A brief review of some of the literature published more than 25 years ago is presented next. Despite the progress that has been made in recent years, those associated with design and construction on expansive clays would do well to remember the complexity of the problems and the limitations on the ability to accurately predict performance. The legal aspects of the problem are, therefore, becoming increasingly important. In 1983 a symposium on the Influence of Vegetation on the Swelling and Shrinking of Clays was sponsored by the British journal Geotechnique. One of the many interesting papers presented at the symposium dealt with the legal aspects of the problem (1). The Fourth International Conference on Expansive Soils held in Denver, Colorado, also included a paper on the legal aspects of design and construction on expansive clays as observed by a consulting engineer (2). The proceedings of both meetings contain many interesting technical papers; however, the two papers on the legal aspects should be considered compulsory reading because premature distress is a common feature of roads and buildings built on expansive clay subgrades.

This paper includes guidelines for identifying a swelling clay problem, a discussion of laboratory swelling curves, and a method of calibrating commonly used empirical equations for predicting the parameters necessary to describe the laboratory swelling curve. A computational routine for computing surface heave is also presented.

REVIEW

Two interesting papers (by Porter and Wooltorton) draw attention to swelling clay problems (3,4). These papers were published in the Proceedings of the First International Conference on Soil Mechanics and Foundation Engineering held at Harvard University in 1936. Porter reported movement observations on a 1,500-ft long concrete pavement laid in Texas in 1931 (3). Cracks 15 cm wide and 3.5 m deep were observed in the pavement shoulders, and seasonal fluctuations in elevation of 12 cm at the pavement edge and 6 cm at the pavement centerline were measured. The subgrade soils at the site were reported to have a liquid limit of about 80 to 100, a plasticity index (PI) of 52 to 74, and a shrinkage limit of from 8 to 10. It is worth noting that on the basis of Atterberg limits alone, the subgrade soils at the site would be identified today as a highly plastic clay (CH) probably exhibiting large volume change if climatic conditions were such that large variations in subgrade moisture content were to be expected.

Wooltorton describes in detail damage to numerous buildings in the Mandalay District of Burma caused by vertical and horizontal soil movements. The climate of the Mandalay District is characterized by high rainfall, but it also has an extended dry season. Seasonal moisture variations were measured at depths of 3.5 m, and cracks in the soil were measured at even greater depths. About 100 damaged buildings were examined in detail. The conclusion drawn was that the damage to the structures was due not to inferior workmanship or low bearing value of the soil as was presumed at the time, but to seasonal soil movement. Computations are presented showing that swelling pressures on the order of 1.0 ton/ft^2

developed against foundation elements in which movements were restrained. Wooltorton recommended extending foundations to depths at which moisture fluctuations are minimal by using drainage and impervious aprons to control the moisture regime in the vicinity of buildings, designing the structure to resist unbalanced forces due to subgrade soil swelling pressures, and not using contact pressures (from dead load and normal live load) of less than 1.0 ton/ft^2. Wooltorton drew attention to the fact that similar soils and associated foundation problems existed in India, South Africa, and Sudan (4).

Twenty years later, two papers were published that dealt with the identification of swelling clays, laboratory testing, and the prediction of surface heave as a function of restraining load. These two papers, one by Holtz and Gibbs (5) published in the Transactions of the American Society of Civil Engineering (ASCE) and the other by McDowell (6) published in the Proceedings of the 35th Annual Meeting of the Highway Research Board, in addition to providing practical guidance on design and construction, strongly influenced subsequent research on the subject of swelling clays.

Holtz and Gibbs presented a classification of expansive clays based on the percent swell of air-dried undisturbed samples when allowed to swell upon saturation (under a vertical pressure of 1.0 psi) in a rigid ring consolidometer. In addition to plasticity index and shrinkage limit, they suggested the use of the "free-swell test" to identify possible troublesome soils. The free-swell value is the percent increase in volume when 10 cc of air-dry soil passing the Number 40 sieve is slowly poured into a 100 cc graduate filled with distilled water. They suggested the use of laboratory tests in the rigid ring consolidometer on compacted or undisturbed samples to determine quantitative uplift values for anticipated load conditions. Holtz and Gibbs drew attention to the importance of the sequence of loading and saturation and suggested duplicating as closely as possible in the laboratory anticipated field conditions. They also presented interesting results showing that, although index tests can be useful in identifying potentially troublesome soils, the actual degree of swelling or swelling pressure developed depends on the initial conditions of moisture content and dry density before wetting.

McDowell (6) presented in considerable detail his method of computing "potential vertical rise" on the basis of an assumed fixed relationship of one-third between linear swell and volumetric swell and on the basis of a family of universal curves for the relationship between volumetric swell and load upon saturation (i.e., free access to water). The curves are identified by their percent volume change at zero load and cover the complete range of vertical load from zero load to the load required for no volume change (i.e., swelling pressure). The curves are the result of measuring percent swell on submergence of individual specimens tested at various loads in a rigid ring consolidometer.

For this type of test, the volume change is equal to the change in height. McDowell, however, assumed that in the field, restraint conditions are such that the vertical rise would be only one-third the volume change measured for full restraint in the laboratory. This overly optimistic assumption is no doubt offset by his implied assumption of zero suction over the entire depth of the swelling clay profile. McDowell presented data that enabled the estimation of expansion characteristics and initial moisture conditions from the plasticity index. However, he recommended testing of undisturbed samples of foundation soils at some convenient surcharge in order to identify the swell versus load curve pertinent to the problem at hand. The potential vertical rise is then computed considering the thickness of the clay layer, gravity loading, and surcharge loadings due to any structure. McDowell developed a slide rule for computing potential vertical rise as a function of percent volume swell at a load of 1 psi--the clay layer thickness and surcharge loadings were based on the universal family of swelling curves presented in the 1956 paper.

The international soil mechanics community continued to show an interest in the problem of expansive soils. The Proceedings of the Third International Conference on Soil Mechanics and Foundation Engineering held in Switzerland in 1953 contains eight papers by authors from seven countries dealing with the measurement of building movement, laboratory measurement of swelling pressure and soil suction, field measurement of the distribution of soil moisture, and the influence of vegetation.

In 1953 extensive research was initiated by Zeitlen in Israel where serious problems with the performance of building foundations, retaining walls, pipelines, and pavements had been identified as associated with expansive clays.

The group in Israel hosted a First International Colloquium on expansive clays in Haifa, in 1961. It was attended by a small group of researchers from all over the world (India, the United States, Spain, Canada, Australia, South Africa, and the United Kingdom). Five full-fledged international conferences have since been held at Texas A&M University in 1965 and 1969; Haifa, Israel, in 1973; Denver, Colorado, in 1980; and Adelaide, Australia, in 1985.

IDENTIFICATION OF THE PROBLEM

The existence of a combination of all or some of the following factors usually gives rise to a swelling clay problem:

1. A soil type that exhibits considerable volume change on changes in moisture content;
2. Climatic conditions, extended wet and dry seasons;
3. Possible changes in moisture content, due to changes in micro-climatic conditions, man-made, or due to vegetation; and
4. Structures (buildings, roads, etc.) sensitive to differential movement.

The authors have found that simple index tests have generally been adequate to identify soil types that are potentially troublesome as indicated in the following table:

	Usually No Problems	Almost Always Problematic
Plasticity index	<20	>32
Shrinkage limit	>13	<10
Free swell (5)	<50	>100

The remaining factors are location and job dependent and require on-site inspection by experienced geotechnical engineers. Much useful information can be gained from examining test pits and from observing the depth of cracking and slickensides. Moisture content profiles as related to the plastic limit, preferable for both wet and dry seasons, can be an indication of the depth of seasonal moisture variations.

The single most important factor with respect to buildings is an adequate depth of foundation (remembering the importance of isolation of grade beams). Though this is closely related to the depth of moisture variation (seasonal or man-made) it is more

fundamentally related to the swelling pressure profile with depth (7,8). All pertinent information with respect to successful foundation experience should be examined in the published literature and at the site.

LABORATORY SWELLING CURVES AND EMPIRICAL CORRELATIONS

The most commonly used laboratory test method for quantifying the swelling behavior of an expansive clay is to study the volume change upon wetting in a one-dimensional consolidation apparatus. Test results are usually presented on arithmetic scales as percent volume change versus vertical applied stress. The test method has been standardized (ASTM D 3877-80) allowing for different sequences of loading, wetting, and expansion control of volume change. The test results depend on the stress path followed and on the details of the test procedure. The soil water suction is presumed to be zero, at equilibrium. Considering how difficult it is to saturate clay samples, even using a back-pressure, it is more probable that even at equilibrium there is a small pore-water tension associated with consolidometer type testing.

The complete curve of swelling, $\Delta V/V$ versus applied pressure, is characterized by its end points and the shape of the curve between these two end points. The end points are:

1. S_o, the ratio in percent of $\Delta V/V$ for zero applied pressure. S_o is sometimes defined as $\Delta V/V$ for an applied pressure of 1.0 psi (i.e., atmospheric pressure divided by 14.2); and
2. The applied pressure required to prevent volume expansion known as the swelling pressure (P_o).

Even for well-funded projects there are objective difficulties associated with sampling, laboratory testing, and estimating final design equilibrium conditions. Preliminary designs are frequently prepared based on a knowledge of the soil profile and the results of index tests such as Atterberg limits and in situ moisture and density only. Laboratory swelling studies on undisturbed samples are sometimes performed only in the final design stages, if at all. It is therefore not surprising that numerous efforts have been made to attempt to find useful correlations between index properties of swelling soils and their swelling characteristics (9,10).

Various correlations have been suggested for predicting the swelling pressure for zero movement (P_o) or percent swell for zero load (S_o), as measured in a rigid consolidometer, from a knowledge of the liquid limit of the soil, its initial moisture content, and dry density (11,12). A generalized form of the equations may be written as follows:

$$\text{Log}(P_o/P_a) = a_o + a_L \cdot (LL) + a_d \cdot (\gamma_d/\gamma_\omega) + a_\omega \cdot (\omega_o) \quad (1)$$

$$\text{Log}(S_o) = b_o + b_L \cdot (LL) + b_d \cdot (\gamma_d/\gamma_\omega) + b_\omega \cdot (\omega_o) \quad (2)$$

where

P_o = swelling pressure,
P_a = atmospheric pressure,
S_o = percent swell for zero load (%),
LL = liquid limit (%),
γ_d = dry density of soil,
γ_ω = unit weight of water, and
ω_o = in situ moisture content (%).

The coefficients "a. . . ." and "b. . . ." are determined by using techniques of multiple regression. This was once a tedious job but with increased access to computers, statistical analysis is now easily performed. The technical literature is being flooded with new expressions having varying degrees of reliability as described by their correlation coefficients. These expressions are usually adequate for a particular set of data but frequently do rather poorly for predicting swelling behavior for another data set.

If heave predictions must be developed for a particular site and no test data exist, then there is no alternative but to use one of the published correlations considered most pertinent. However, if even a limited amount of test data are available then it is a great improvement if the coefficients are adjusted to match the available data. Now examine the preceding expression for estimating the swelling pressure and observe how the coefficients might be developed from a limited amount of data.

By illustration the data taken from the paper by Komornik and David will be used. The statistical analysis of all their data gave the following results (11):

$a_o = -1.868$

$a_L = 0.0208$

$a_d = 0.665$

$a_\omega = -0.0269$

First examine the influence of initial density and moisture content on the swelling pressure for a soil of a given liquid limit. Rewriting Equation 1

$$(\gamma_d/\gamma_\omega) = [\text{Log}(P_o/P_a) - a_L \cdot (LL) - a_o/a_d] - [a_\omega/a_d] \cdot (\omega_o) \quad (3)$$

It can be observed from Equation 3 that contours of equal swelling pressure drawn with moisture content-dry density coordinates should be parallel straight lines with a slope of $(-a_\omega/a_d)$. In the absence of sufficient data, the value of $-a_\omega/a_d = 0.040$ (obtained from the Komornik data) will be used (see Figure 1).

Rewriting Equation 1 again

$$\text{Log}(P_o/P_a) = [a_o + a_L \cdot LL] + a_d \cdot \{\gamma_d/\gamma_\omega + [a_\omega/a_d] \cdot (\omega_o)\} \quad (4)$$

If test results are plotted for the log of the swelling pressure versus $\{\gamma_d/\gamma_\omega + [a_\omega/a_d] \cdot (\omega_o)\}$ using the value of a_ω/a_d determined above, parallel straight lines may be fitted through the data points for each liquid limit to give the value for a_d. The intercept of each line on the zero axis will give the value for $[a_o + a_L \cdot LL]$ (see Figure 2).

The use of Equation 1 implies that the values for a_ω/a_d and for a_d will be the same for soils having different liquid limits. If the data that are available for a particular site tend to support this assumption then the final step can begin by examining other data sets with different liquid limits and $[a_o + a_L \cdot (LL)]$ versus LL can be plotted. The slope of the line will give the value of a_L and the zero intercept will give the value of a_o (see Figure 3).

The percent swell at zero load (S_o) was used by McDowell (6) to characterize a family of swelling curves. Examination of these curves shows the following relationship:

$$S_o(\%) = 6.8(P_o/P_a) \quad (5)$$

The test results are for individual specimens tested in rigid ring consolidometers.

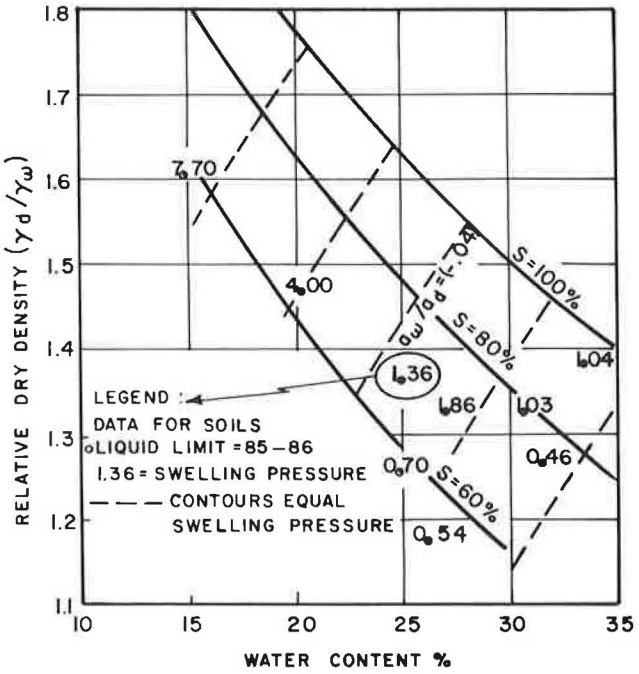

FIGURE 1 Determination of (a_ω/a_d) for swelling pressure correlations.

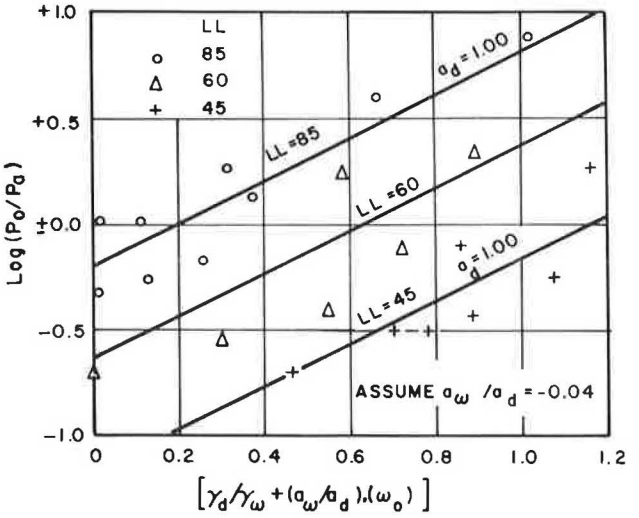

FIGURE 2 Determination of (a_d) for swelling pressure correlations.

An examination of the data presented by others (11,12) for the measured rebound swell, also measured in rigid ring consolidometers at 1.0 psi load (after performing a swelling pressure test), shows the following approximate relationship:

$$S_o(\%) = 3.0(P_o/P_a) \quad (6)$$

This result is reasonable because the 1 psi seating load and the measurement of the percent swell after first performing a swelling pressure test would reduce the expected value of S_o for a particular value of P_o.

Analysis of data presented by Holtz (5) shows that the ratio of S_o for 1.0 psi to P_o/P_a for a particular soil depended on the degree of saturation and was equal to 3.5 for a degree of saturation equal to 85 percent and increased to 7.0 for a degree of saturation of 70 percent.

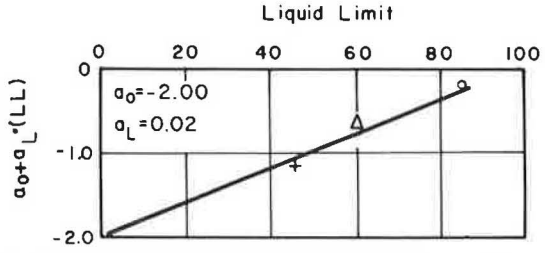

FIGURE 3 Determination of (a_o and a_{LL}) for swelling pressure correlations.

Equation 5 can be written in more general terms as follows:

$$S_o(\%) = S_R \cdot (P_o/P_a) \quad (7)$$

In the preceding paragraphs methods of predicting values of the percent swell at zero load (S_o) and the pressure required for zero swell, that is, swelling pressure (P_o) have been examined. Now it is time to examine the shape of the curve (of percent swell versus applied pressure) joining these two end points. On the basis of an examination of numerous laboratory swelling tests, McKeen (13) has suggested that there is a unique shape to all swelling curves if normalized values of swelling (S_p/S_o) are plotted versus normalized values of applied pressure (P_p/P_o), where S_p is the percent swell for an applied stress of P_p. Following one of the more commonly used formulations relating volume change to applied vertical stress in one-dimensional consolidation:

$$S_p/S_o = \Delta\ell/1 + \ell_o \cdot 100/S_o = -CR \cdot \text{Log}[(P_p/P_o)] \quad (8)$$

where $\Delta\ell$ and ℓ_o are the change in void ratio and initial void ratio, respectively. The test data published by McKeen are consistent with a constant value of $C_R = 0.45$, where S_o is the percent swell for a vertical stress of 1.0 psi and all swell values (S_o and S_p) are for rebound on a single specimen after performing a swelling pressure test. (Note that Equation 8 is valid only for values of $P_p/P_o > 0.01$ and $P_p > 1.0$ psi.)

The master swelling curves published by McDowell (6) are consistent with a higher value of $C_R = 0.54$ where S_o is the percent swell under zero load and all percent swell values (S_o and S_p) are for individual test specimens at a constant vertical stress. (Note that Equation 8 is a reasonable description of McDowell's master curves.)

A complete family of swelling curves can then be described as follows:

$$S_p/S_o = -C_R \cdot \text{Log}[P_p/P_o] \quad (9)$$

$$S_o = S_R \cdot P_o/P_A \quad (10)$$

$$S_p = -(C_R \cdot S_R) \cdot (P_o/P_A) \cdot \text{Log}(P_p/P_o) \quad (11)$$

Equation 11 with $C_R = 0.54$ and $S_R = 6.82$ is a reasonably accurate description of McDowell's family of swelling curves and can be used for identifying a particular swelling curve for any known point on the swelling curve S_p, P_p, using the computational routine shown in Figure 4.

COMPUTING HEAVE

The prediction of heave for a pavement, or a building foundation on an expansive clay subgrade, re-

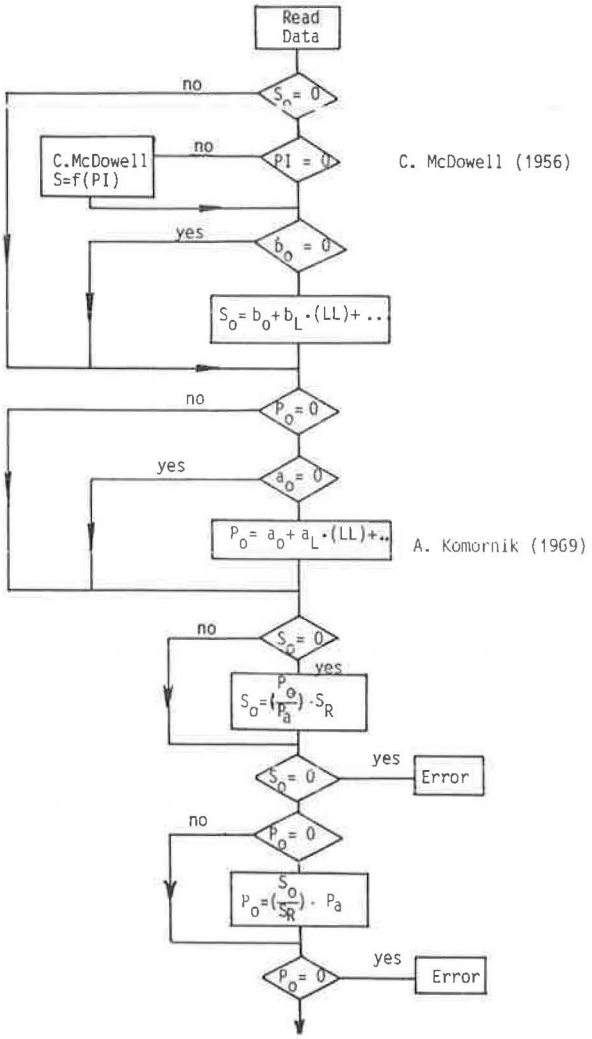

FIGURE 4 Compute S_o, P_o; for known S_p, P_p.

quires a knowledge of the percent expansion expected for each depth when allowed access to water (while suitably surcharged) under a controlled suction equal to that expected at equilibrium conditions. The heave is then calculated by integrating the percent expansion over the affected depth. The equilibrium suction varies with climatic conditions, the depth of the water table, the imperviousness of the surface, and the efficiency of the surface and subsurface drainage. The authors have found that these suction values can range from as low as zero, for conditions of very poor drainage, to as high as 1.0 kb/cm² or more for impervious surfacing and very good drainage and a very deep water table (7,14). Equilibrium suction values are sometimes assumed to be equal to the distance above the water table.

The reader interested in a treatment of the problem in all its complexity is referred to the work of Fredlund (15,16). Laboratory testing is usually done in consolidometers and should be performed on good-quality undisturbed samples, taken at a time such that their in situ moisture and density represent conditions expected to exist at the time of construction. To simplify the laboratory testing procedure, the effect of expected equilibrium suction can be accounted for by increasing the applied vertical pressure above the overburden or foundation pressure. The laboratory test can then be conducted by inundating the sample.

The basic requirement is, therefore, laboratory swelling tests on undisturbed samples under various vertical pressures. These test results can then be used to estimate final heave and also to quantify the beneficial effects of undercutting and replacement with nonswelling material. Presented next is a computational routine the authors have used to compute heave (7,14). Since time, site, and budget limitations frequently do not allow for complete laboratory testing, the procedure described can be used if only the index properties (liquid limit, in situ dry density, and moisture) are known.

The program presented is for a single homogeneous layer with or without foundation loadings. This program can be easily modified, however, so that it can be used for a layered soil profile.

Figure 5 shows the routine for computing P_o and S_o from index tests if these values are not known. Shown in Figure 6 are (a) the definition of stress conditions that can be specified for the top and bottom of the layer being computed and (b) a description of the method for computing the thickness (z_o) of the critical layer undergoing swelling.

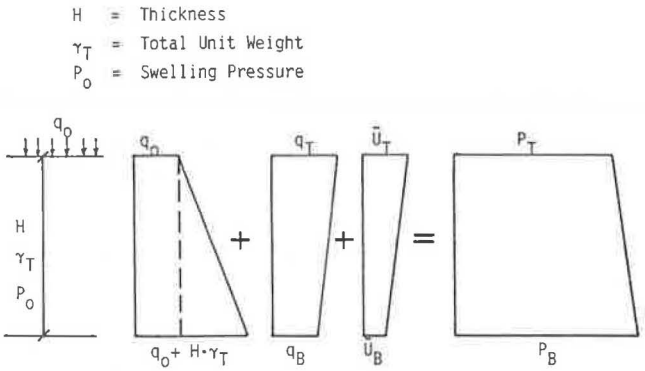

q_o = Uniform surcharge stress
q_T, q_B = Applied foundation stresses (top & bottom)
$\bar{U}_T, \bar{U}_B$ = Equivalent suction stresses (top & bottom) [opposite in sign & = or < actual estimated suction]

$$P_T = q_o + q_T + \bar{U}_T \quad : \quad P_B = q_o + H \cdot \gamma_T + q_B + \bar{U}_B$$

COMPUTE THICKNESS OF CRITICAL LAYER (z_o)

Case I $P_T = P_B$	if $P_T \geq P_o$	z_o = zero
	if $P_T < P_o$	$z_o = H$
Case II $P_B > P_T$	if $P_T \geq P_o$	z_o = zero
	if $P_B \leq P_o$	$z_o = H$
	if $P_T < P_o < P_B$	$z_o = \frac{P_o - P_T}{P_B - P_T} \cdot H$; $P_B = P_o$
Case III $P_T > P_B$	if $P_B \geq P_o$	z_o = zero
	if $P_T \leq P_o$	$z_o = H$
	if $P_B < P_o < P_T$	$z_o = \frac{P_o - P_B}{P_T - P_B} \cdot H$; $P_T = P_o$

FIGURE 5 Compute S_o, P_o; from index tests.

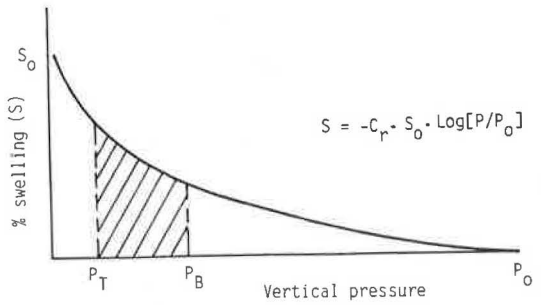

$$S_{avg} = \frac{-.4343 \cdot C_r \cdot S_o}{(P_B - P_T)/P_o} \int_{P_T}^{P_B} \text{Ln}(P/P_o)\, d(P/P_o)$$

$$= \frac{-.4343 \cdot C_R \cdot S_o}{(P_B - P_T)/P_o} \cdot [P/P_o \cdot (\text{Ln}(P/P_o) - 1)]_{P_T/P_o}^{P_B/P_o}$$

$$= \frac{-.4343 \cdot C_R \cdot S_o}{(P_B - P_T)/P_o} \cdot \left(\frac{P_B}{P_o}\left[\text{Ln}\left(\frac{P_B}{P_o}\right) - 1\right] - \frac{P_T}{P_o}\left[\text{Ln}\left(\frac{P_T}{P_o}\right) - 1\right]\right)$$

$$\text{HEAVE of LAYER} = f \cdot \frac{S_{avg}}{100} \cdot z_o$$

Note:

1) C. McDowell assumed Restraint Factor f = 1/3

   The authors assume f = 1.0 when the % swell data is for rigid ring consolidometers.

2) P_T min = 1.0 psi

   Maximum values for P_T and $P_B = P_o$.

FIGURE 6 Layer stresses (P_T, P_B) and thickness (z_o).

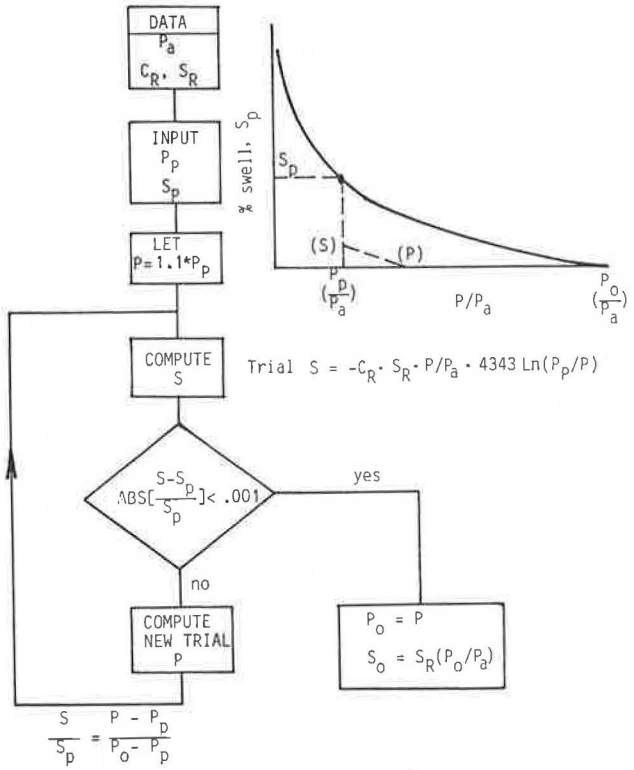

FIGURE 7 Compute heave of layer.

Figure 7 shows the equations used for computing the average percent swell and, hence, for the total heave of the layer. Figure 8 shows a data sheet for the program shown in Figure 9.

POST-CONSTRUCTION OBSERVATIONS

The performance of structures on expansive clay subgrades can be adversely affected by an unusually dry season or by a sequence of unusually dry seasons (or wet seasons) such as might occur once in 25 yr and therefore possibly outside the time span of reported experience for a particular area. Man-made environment, trees, sewer lines, leaky faucets, and flower beds in the vicinity of structures have all been experienced as sources of changes in subgrade moisture content and associated movements or pressures (17).

It is a reasonable assumption that sometime within the lifespan of every structure founded on expansive clays movements will occur that will be detrimental to the structure. It is surprising how difficult it sometimes is to know whether such movements are heave or settlement. If repairs have to be initiated or, as is becoming increasingly common,

DATA

UNITS			
L$		METERS	LENGTH
F$		TONS	FORCE
GW	γ_w	1.0	WATER
PA	Pa	10.0	ATM. PRESS

		LAYER 1	2	3	
Qφ	q_o	1.0			SURCHARGE TOP OF LAYER
H	H	100			LAYER THICKNESS
F	f	1.0			RESTRAINT FACTOR ⅓ TO 1.0
DT	γ_T/γ_w	2.00			RELATIVE TOTAL UNIT WEIGHT
QT	q_T	0			FOUNDATION STRESS TOP AND BOTTOM
QB	q_B	0			
UT	$\bar{U}_T$	10.0			EQUIVALENT SUCTION STRESS, TOP AND BOTTOM
UB	$\bar{U}_B$	10.0			
PI	PI	0			C. McDOWELL (1956) PLASTICITY INDEX
CM$		"A"			CODE - INITIAL MOISTURE "O" OPT: "A" AVG: "W" WORST
LL	LL	85			LIQUID LIMIT (%)
DD	γ_d/γ_w	1.50			RELATIVE DRY DENSITY
Wφ	w_o	22			INITIAL MOISTURE CONTENT (%)
Sφ	S_o	0			% SWELL - ZERO LOAD
Pφ	P_o	0			SWELLING PRESSURE
SR	SR	6.8	$(\frac{S_o}{P_o}) \times P_a$		S_R = 6.8 C. McDOWELL (1956); S_R = 3.0 REBOUND, KOMORNIK (1969)
CR	CR	0.54	$\frac{S}{S_o} = -C_R \cdot \text{LOG}(\frac{P}{P_o})$		C_R = 0.54 C. McDOWELL-DATA; C_R = 0.45 McKEEN - DATA

Aφ	a_o	-2.00	$P_o = a_o$	Bφ	b_o	0	$S_o = b_o$
AL	a_L	0.02	$+ a_L \cdot (LL)$	BL	b_L	0	$+ b_L \cdot (LL)$
AD	a_d	1.00	$+ a_d \cdot (\text{LOG}(\gamma_d/\gamma_w))$	BD	b_d	0	$+ b_d \cdot (\text{LOG}(\gamma_d/\gamma_w))$
AW	a_w	-0.04	$+ a_w \cdot (\text{LOG}(w_o))$	BW	b_w	0	$+ b_w \cdot (\text{LOG}(w_o))$

RESULTS

Zφ	z_o	4.95	(m)	
S1	AVG. % SWELL	0.96	(%)	
Pφ	P_o	20.9	(TON/m²)	
DH	HEAVE	.047	(m)	

FIGURE 8 Data sheet.

```
]LIST

100  REM  HEAVE CALCULATIONS
105  REM  SINGLE LAYER
110  REM   G.WISEMAN  14/AUG/1984

120  REM ANY CONSISTENT UNITS
130  REM  UNIT WEIGHT RELATIVE TO
      WATER
500  GOSUB 5000: REM  DATA
1000  REM   COMPUTE % SWELL (S0)

1001  REM  COMP SWELL PRESS (P0)
1005  IF S0 < > 0 THEN  GOTO 108
     0
1010  IF PI = 0 THEN  GOTO 1060
1020  IF CM$ = "O" THEN  LET S0 =
     .227 * (PI - 15)
1030  IF CM$ = "A" THEN  LET S0 =
     .289 * (PI - 11)
1040  IF CM$ = "W" THEN  LET S0 =
     .335 * (PI - 4)
1045 S0 = 1.25 * S0
1060  IF B0 = 0 THEN  GOTO 1090
1070 S0 = B0 + BL * LL + BD * DD +
     BW * W0
1075 S0 = 10 ^ S0
1080  IF P0 < > 0 THEN  GOTO 111
     0
1090  IF A0 = 0 THEN  GOTO 1110
1100 P0 = (A0 + AL * LL + AD * DD
      + AW * W0)
1105 P0 = PA * 10 ^ P0
1110  IF S0 = 0 THEN  LET S0 = P0
      / PA * SR
1120  IF S0 = 0 THEN  PRINT "DATA
      ERROR": STOP
1200  IF P0 = 0 THEN  LET P0 = S0
      / SR * PA
1210  IF P0 = 0 THEN  PRINT "DATA
      ERROR": STOP
1220  IF S0 < 0 THEN S0 = 0
1230  IF P0 < 0 THEN P0 = 0
5100  REM "O"OPT,"A"AVG,"W"WORST
5110  DATA   0,"A"
5120  READ LL,DD,W0
5130  DATA 85,1.50,22
5140  READ S0,P0
5150  DATA   0 ,0
5160  READ SR,CR
5170  DATA   6.8,0.54
5180  READ A0,AL,AD,AW
5190  DATA -2.00,0.02,1.00,-0.04
5200  READ B0,BL,BD,BW
5210  DATA  0,0,0,0
5300  RETURN
]RUN
UNITS =METERS,TONS
LAYER THICK.  =100 METERS
ACTIVE THICK. =4.946
SWELLING PRESS=20.893
% SWELL (S0)  =14.207
AVG % SWELL   =.955
HEAVE=  .047 METERS
1500  REM  COMPUTE CRITICAL DEPTH
      (Z0)
1510 PT = Q0 + QT + UT
1520 PB = Q0 + QB + UB + H * DT *
     GW
1530  IF PT < > PB THEN  GOTO 15
     60
1540  IF PT > = P0 THEN Z0 = 0
1550  IF PT < P0 THEN Z0 = H
1555  GOTO 2000
1560  IF PT > PB THEN  GOTO 1610
1570  IF PT > = P0 THEN Z0 = 0
1580  IF PB < = P0 THEN Z0 = H
1590  IF PT < P0 AND P0 < PB THEN
      Z0 = (P0 - PT) / (PB - PT) *
      H:PB = P0
1600  GOTO 2000
1610  IF PB > = P0 THEN Z0 = 0
1620  IF PT < = P0 THEN Z0 = H
1630  IF PB < P0 AND P0 < PT THEN
      Z0 = (P0 - PB) / (PT - PB) *
      H:PT = P0
2000  REM  COMPUTE HEAVE
2003  IF  ABS ((PB - PT) / PB) <
     0.001 THEN S1 =  - 0.4343 *
     CR * S0 *  LOG (PT / P0): GOTO
     2030
2005  IF PT < (PA / 14.2) THEN  LET
     PT = PA / 14.2
2010 S1 = PB / P0 * ( LOG (PB / P
     0) - 1) - PT / P0 * ( LOG (P
     T / P0) - 1)
2020 S1 =  - .4343 * CR * S0 / (P
     B - PT) * P0 * S1
2030 DH = F * S1 / 100 * Z0
2035  IF Z0 < H THEN  LET DH = F *
     S1 / 100 * Z0
3000  REM  PRINT RESULTS
3010  DEF  FN A(X) =  INT (1000 *
     X + .5) / 1000
3100  PRINT "UNITS =";L$;",";F$
3110  PRINT "LAYER THICK.  =";H;"
      ";L$
3120  PRINT "ACTIVE THICK. ="; FN
     A(Z0)
3130  PRINT "SWELLING PRESS="; FN
     A(P0)
3140  PRINT "% SWELL (S0)  ="; FN
     A(S0)
3150  PRINT "AVG % SWELL   ="; FN
     A(S1)
3160  PRINT "HEAVE=  "; FN A(DH);
      " ";L$
4900  END

5000  REM  DATA
5010  READ L$,F$
5020  DATA  "METERS","TONS"
5030  READ GW,PA,Q0
5040  DATA  1.0,10.0,1.0
5050  READ H,F,DT
5060  DATA   100,1.0,2.00
5070  READ QT,QB,UT,UB
5080  DATA  0,0,10.0,10.0
5090  READ PI,CM$: REM  MCDOWELL
```

FIGURE 9 Program listing.

blame has to be assigned, the first step that has to be taken is to establish reference points on the structure and to monitor their elevation with time with respect to a reliable bench mark. It is preferable for such fixed points and an associated initial survey to be established at the time of construction. It is the experience of the authors that the discussion of the foregoing item with the owners is one of the best ways of drawing attention to the limitations of available knowledge and to what reasonably might be expected to happen within the life-span of the structure.

In recent years, there has been increasing awareness of the role of differential heave of expansive clay subgrades in the development of pavement roughness (18,19). The authors' experience has been that pavement roughness on expansive clay subgrades sometimes starts to become troublesome as early as 4 to 5 years after pavement construction. When deciding on a pavement overlay it is important to know if pavement roughness has developed as a result of factors associated with traffic loadings or as a result of differential subgrade heaving. A slightly thicker pavement overlay can be very effective in increasing the time between pavement overlays in the case of traffic-induced roughness. Extra overlay thickness is only of limited usefulness in reducing the length of time before pavement roughness due to differential subgrade heaving becomes a problem.

Proper identification of the subgrade soils is of the utmost importance. It is also important to recognize that despite all the measures the engineer may take to design and construct the subgrade, pavement, shoulders, and drainage in order to minimize differential horizontal and vertical subgrade movements, pavement distress may occur due to moisture changes before it occurs due to traffic loading. The monitoring of pavement elevations should therefore be included in the follow-up procedures of every pavement constructed on a swelling clay subgrade.

CONCLUDING REMARKS

The methods the authors have used with a fair measure of success for identifying and quantifying the problems associated with roads and buildings on expansive clays have been described. These methods are based on the results of laboratory swelling tests or on swelling parameters as predicted from simple index tests after calibration, if possible. The computed results for heave are strongly influenced by the assumed effect of in situ cracking and lateral restraint on the relation between volume change and vertical heave and by the assumed final equivalent suction values. At the present time guidance can be found only by a study of case histories. To further complicate matters, satisfactory performance of a highway or building in terms of acceptable distortions or cracking is not judged only by the engineer; the final judgment is in the hands of the public and the courts.

REFERENCES

1. R. Wyles. The Legal Aspects of the Influence of Vegetation on the Swelling and Shrinking of Clays. Geotechnique, Vol. 23, 1983, pp. 85-163.
2. F.H. Chen. Legal Aspects of Expansive Soils.

Proc., 4th International Conference on Expansive Soils, Denver, Colo., (D. Snethen, ed.), Vol. 1, ASCE, New York, 1980, p. 639.
3. H.C. Porter. Observations of the Texas State Highway Department on the Subsequent Effects of the Uniformity and the Non-uniformity of Foundation Soil--Types on Pavements and The Effects of Uniformity of Moisture Content Fluctuations in Soil Foundations of High Volumetric Change. Proc., 1st International Conference on Soil Mechanics and Foundation Engineering, Cambridge, Mass., Vol. 2, 1936, p. 256.
4. D. Wooltorton. A Preliminary Investigation into the Subject of Foundations in the "Black Cotton" and Kyatti Soils of Mandalay District, Burma. Proc., 1st International Conference on Soil Mechanics and Foundation Engineering, Cambridge, Mass., Vol. 3, 1936, p. 242.
5. W.G. Holtz and H.J. Gibbs. Engineering Properties of Expansive Clays. Transactions ASCE, Vol. 121, 1954, pp. 641-663.
6. C. McDowell. Interrelationship of Load Volume Change and Layer Thickness of Soils to the Behaviour of Engineering Structures. Proc., 35th Annual Meeting Highway Research Board, 1956, p. 754.
7. A. Komornik, G. Wiseman, and Y. Ben-Yaacob. Studies of In-Situ Moisture and Swelling Potential Profiles. Proc., 2nd International Conference on Expansive Soils, Texas A&M University, College Station, 1969, p. 348.
8. D. David and A. Komornik. Stable Embedment Depth of Piles in Swelling Clays. Proc., 4th International Conference on Expansive Soils, Denver, Colo., Vol. 2, ASCE, New York, 1980, p. 798.
9. D. Johnson and D.R. Snethen. Prediction of Potential Heave of Swelling Soils. Geotechnical Testing Journal, Vol. 1, ASTM, Philadelphia, Pa., 1978, p. 117.
10. A.A.B. Williams and G.W. Donaldson. Buildings on Expansive Soils in South Africa: 1973-1980. Proc., 4th International Conference on Expansive Soils, Denver, Colo., (D. Snethen, ed.), Vol. 2, ASCE, New York, 1980, p. 834.
11. A. Komornik and D. David. Prediction of Swelling Pressure of Clays. Journal of Soil Mechanics and Foundations Division, Vol. 95, No. SM1, ASCE, New York, Jan. 1969, p. 209.
12. V.N. Vijayvergiya and O.I. Ghazzaly. Prediction of Swelling Potential for Natural Clays. Proc., 3rd International Conference on Expansive Soils, Haifa, Israel, Vol. 1, 1973, p. 227.
13. R.G. McKeen and D.J. Hamberg. Characterization of Expansive Soils. Transportation Research Record 790, TRB, National Research Council, Washington, D.C., 1981, pp. 73-78.
14. G. Wiseman, M. Livneh, and J. Uzan. Performance of Full Depth Asphalt Pavement on an Expansive Clay Subgrade. Proc., 3rd Conference of Road Engineering Association of Asia and Australia, 1981, p. 747.
15. D.G. Fredlund. Appropriate Concepts and Technology for Unsaturated Soils. Canadian Geotechnical Journal, Vol. 16, No. 1, Feb. 1979, p. 121.
16. R.T. Yoshida, D.G. Fredlund, and J.J. Hamilton. The Prediction of Total Heave of a Slab-On-Grade Floor on Regina Clay. Canadian Geotechnical Journal, Vol. 20, No. 1, Feb. 1983, p. 69.
17. J.G. Zeitlen and A. Komornik. A Foundation Code for Expansive Soil Conditions. Proc., 4th International Conference on Expansive Soils, Denver, Colo., Vol. 1, ASCE, New York, 1980, p. 609.
18. G.R. McKeen and R.L. Lytton. Expansive Soil Pavement Design Using Base Studies. International Conference on Case Histories in Geotechnical Engineering, Rolla, Mo., Vol. 3, May 1984, p. 1421.
19. J. Uzan, S. Frydman, and G. Wiseman. Roughness of Air Field Pavement on Expansive Clay. Proc., 5th International Conference on Expansive Soils, Adelaide, South Australia, May 1984.

Publication of this paper sponsored by Committee on Environmental Factors Except Frost.

The Effect of Vegetation Transpiration on the Deformation of High Void Ratio Expansive Soil Foundation

CHEN LIN and TIAN KAIMING

ABSTRACT

Vegetation transpiration may significantly decrease the moisture content of active soils causing soil shrinkage and deformation. Severe damage to engineering structures may result. This phenomenon has been identified in reports from South Africa, Australia, and China as a cause of structural damage. This paper contains analyses of data collected in Mengzi County and other regions in China. The relationship between vegetative transpiration rates and deformation of high void ratio expansive soils is examined, and a formula for calculating estimated maximum contraction is presented. Also, current practices for dealing with active soils are discussed.

DAMAGE TO ENGINEERING

Plants that cover the earth surface are termed vegetation. Water and nutrients are assimilated by the plant root system and delivered to the leaf surface, stems, and other plant parts via capillary tubes. Only 1 percent of the absorbed water is consumed for the growth of the plants; the balance is dispersed into the atmosphere in the form of vapor by stomata on the leaf surface.

This process of water evaporation through the plant organ is called transpiration. It is shown by the measured data that different types of trees have different transpiration rates (Table 1). Among the more common trees, the jarrahs have the greatest transpiration.

Used as one of the measures to lower the groundwater table in Australia, the jarrahs are often compared to pumps. In some regions, because of the large loss of water from the foundation soil, which was caused by the transpiration of jarrahs, irregular shrinkage deformation of the foundation occurred. This caused serious engineering failures to take place.

Investigation indicated that in the expansive soil regions of Yunnan and Guangxi Province, China, building damage phenomena due to the vegetation effect are rather common (Table 2).

In these regions, building damage rates in places with growing trees are higher than in places without trees, which obviously shows the close relationship between building damage and vegetation. In Mengzi, for example, most buildings on expansive soil foundations not surrounded by trees remained in good condition. Only slight damage caused by uneven expanding and shrinking deformation of the foundation soil occurred. The deformation amplitude is not more than 15 mm and the width of wall crack is less than 10 mm. However, 90 percent of the buildings close to jarrahs and grevillea were seriously damaged. The maximum deformation amplitude of foundations of buildings near trees is up to 187.2 mm, and the

TABLE 1 Transpiration of Common Species of Trees

	Jarrah	African Eucalyptus	Grevillea	Glossy Privet	Chinese Parasol	Barren Land
Transpiration kg/day						
South Africa	1,090	454	342		61.2	0.54
Mengzi		432		68		

TABLE 2 Investigative Data of Houses Destroyed by Vegetation Influence

				Tree-Growing Site			Non-Tree Site		
Region	No. Houses Investigated	No. Houses Destroyed	Rate Destroyed (%)	No. Houses Completed	No. Houses Destroyed	Rate Destroyed (%)	No. Houses Completed	No. Houses Destroyed	Rate Destroyed (%)
Mengzi	145	109	75.1	9	100	91.7	27	9	25.0
Jianshui	56	44	78.5	4	17	80.9	8	27	77.1
Ningming	53	35	66.0	3	30	90.9	15	5	25.0
Nanning	46	25	54.3	13	21	61.7	8	4	33.3
Gui County	79	39	49.3	30	28	48.2	9	12	57.1
Yanshan	42	25	59.5	3	12	80.4	14	13	48.1
Kunming	34	20	58.8	2	12	85.7	12	8	40.0

maximum width of wall crack is 240 mm. Partial wall inclination reaches 18.9 percent (Table 3). In this area the greater the afforestation the more serious the damage. In the vicinity of the trees, structural walls nearest the trees exhibit cracks, deformation, or foundation damage.

A 36-m long, single-story building with a jarrah near one end of the front wall and no other trees nearby experienced partial shrinkage of the foundation soil near the tree. The brick work was twisted, the side line and foundation beam of the back wall was bent in the form of an arc with the tree as a circle center and the brick side line of the front wall squeezed in undulation form (Figure 1). Figures 2-6 show the damage to houses under the influence of trees. These figures also show the corridor brick pillar of some houses displaced 10 cm horizontally toward the trees. Figure 7 shows the depth of the tree roots near the houses. In some houses, reinforced concrete foundation beams with 40 x 40 cm^2

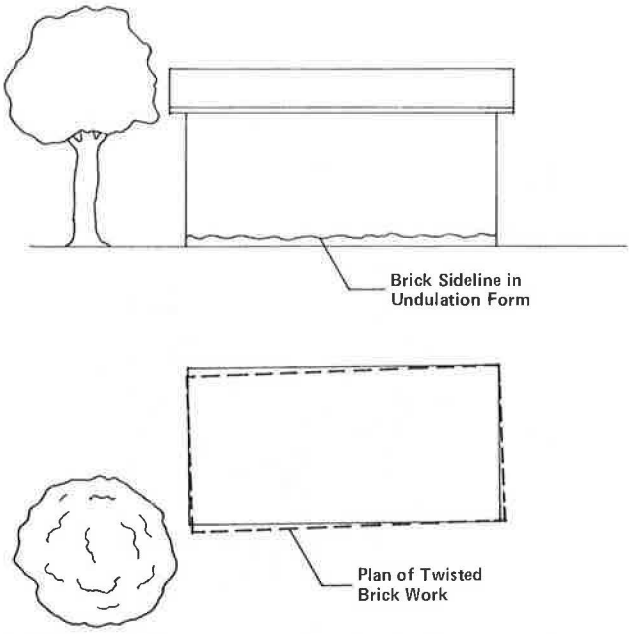

FIGURE 1 Orthogonal projection of twisted house near jarrah.

FIGURE 2 Horizontal displacement of corridor brick pillar.

FIGURE 3 Crack on gable of building near jarrah.

FIGURE 4 Inclination of external wall.

FIGURE 5 Collapse of roof.

TABLE 3 Statistical Data of the Relationship Between Building Deformation and Vegetation

Building No.	Foundation Type	Embedded Foundation Depth (m)	Construction Type
I-5	Strip footing on sand cushion	1.50	Brick and wood, one-story
I-7	Pier foundation	1.20	Brick and wood, one-story
II-1	Pier foundation	3.95	Brick and concrete, three-stories
II-3	Pier foundation	3.95	Brick and concrete, three-stories
II-5	Pier foundation	3.95	Brick and concrete, three-stories
II-2	Pier foundation	3.95	Brick and concrete, three-stories
II-20	Strip footing	0.80	Brick and concrete, one-story
II-16	Pedestal pile	3.00	Brick and concrete, two-stories
IV-6	Strip footing	0.80	Brick and concrete, two-stories
Jiang-shuidi Hotel	Strip footing	0.80	Brick and concrete, one-story
I-Auditorium	Strip footing	0.80	Brick and wood
III-24	Strip footing	0.80	Brick and wood, two-stories

[a]Due to the high solid rigidity of building no crack occurred.

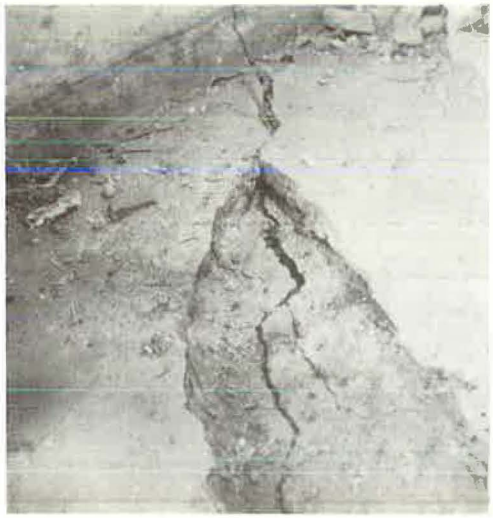

FIGURE 6 Breakage of foundation and foundation beam caused by crack through soil under foundation.

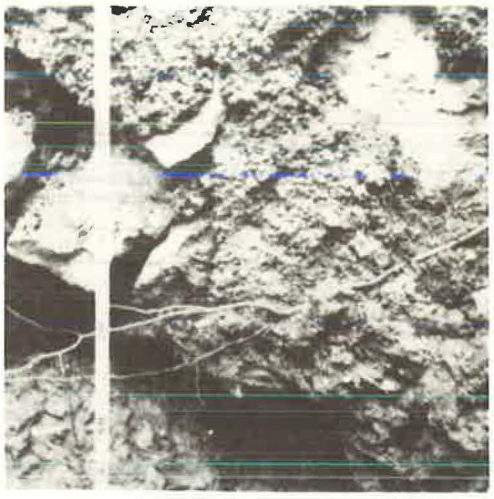

FIGURE 7 Extended depth of tree roots, which is equal to the height of the tree and observed from the excavated cross section.

cross sections were broken by stretching. Some roofs caved in, exposing the rooms to the sky, and some external walls collapsed. Many houses collapsed without demolition. The remaining houses were no longer usable. They had suffered damage as severe as that caused by an earthquake.

FOUNDATION DEFORMATION

Vegetation transpiration causes water loss of foundation soils and forms a limited shrunken section--the main reason that adjacent buildings suffer differential settlement of foundation elements. The data observed in the Mengzi region indicated that the lower limit of water content variation of foundation soil is low in an area influenced by jarrahs, and the water content variation is wide. The amplitude between expansive and deformation is substantial. At a shringage depth of 3 m, amplitude of water content variation of foundation soil in forest zones is 2 to 3 times that in barren land, and the deformation amplitude is 8 to 20 times as great (Table 4). It is evident that the effect of vegetation transpiration on foundation soil is greater than the effect of weather evaporation.

In vegetated areas, foundation deformation is related to seasonal weather variations. Measuring mark deformation curves show regular variation as they move upward in the rainy season and downward in the dry season (Figure 8). The measuring mark of those that drop greatly also rise significantly. Those that drop slightly rise only slightly. This indicates that the foundation soil experiences reversible expansive and shrinking deformation, which alternate endlessly as humidity and soil moisture increase and decrease. Because the observed contraction of foundation soil was greater than the expanding deformation in a period of 1 1/2 yr, the curve of relationship between measuring mark and time inclines downward continuously, and the maximum sinking value at 1 m depth is up to 128 mm. Elimination of the tree roots causes the curve to rise continuously. In 8 months the rising amplitude

Effect

Vegetation Condition	Distance to Tree (m)	Maximum Deformation Amplitude Near Tree (mm)	Maximum Deformation Amplitude (mm)	Building Condition
Non-tree			7.6	Good
Non-tree				Good
Non-tree				Good
Non-tree			11.4	Good
Rows of jarrahs	5-8	35.0		2.94 percent inclined to direction of tree[a]
Rows of jarrahs	8-10	69.2		6.6 percent inclined to direction of tree[a]
Rows of jarrahs	3-10	83.1		Medium damage, wall crack width 3-5 cm
Rows of jarrahs	3-5	46.8		Slight damage, wall crack width 2-5 cm
Independent jarrah	3-6	187.2		Serious damage, wall crack width 8-20 cm
Rows of jarrahs	3-5	66.8		Medium damage, wall crack width 2-3 cm
Rows of jarrahs	3-2			Serious damage, gable and roof truss collapse
Rows of jarrahs	3-5			Serious damage, gable and roof truss collapse

TABLE 4 Jarrah Deformation Amplitude—Forest Area and Barren Land

	Depth (m)									
	Barren Land, 1.0	Forest Area, 1.0	Barren Land, 1.5	Forest Area, 1.5	Barren Land, 2.0	Forest Area, 2.0	Barren Land, 2.5	Forest Area, 2.5	Barren Land, 3.0	Forest Area, 3.0
Water content										
Rainy season	36	38	36	38	37	36	41	41	39	37
Dry season	32	26	30	26	31	26	35	30	35	29
Amplitude of variation	4	12	6	12	6	10	6	11	4	8
Deformation amplitude of measuring mark, mm	12.6	105.1	11.9	99.1	7.7	96.2	3.8	74.5	3.2	42.8

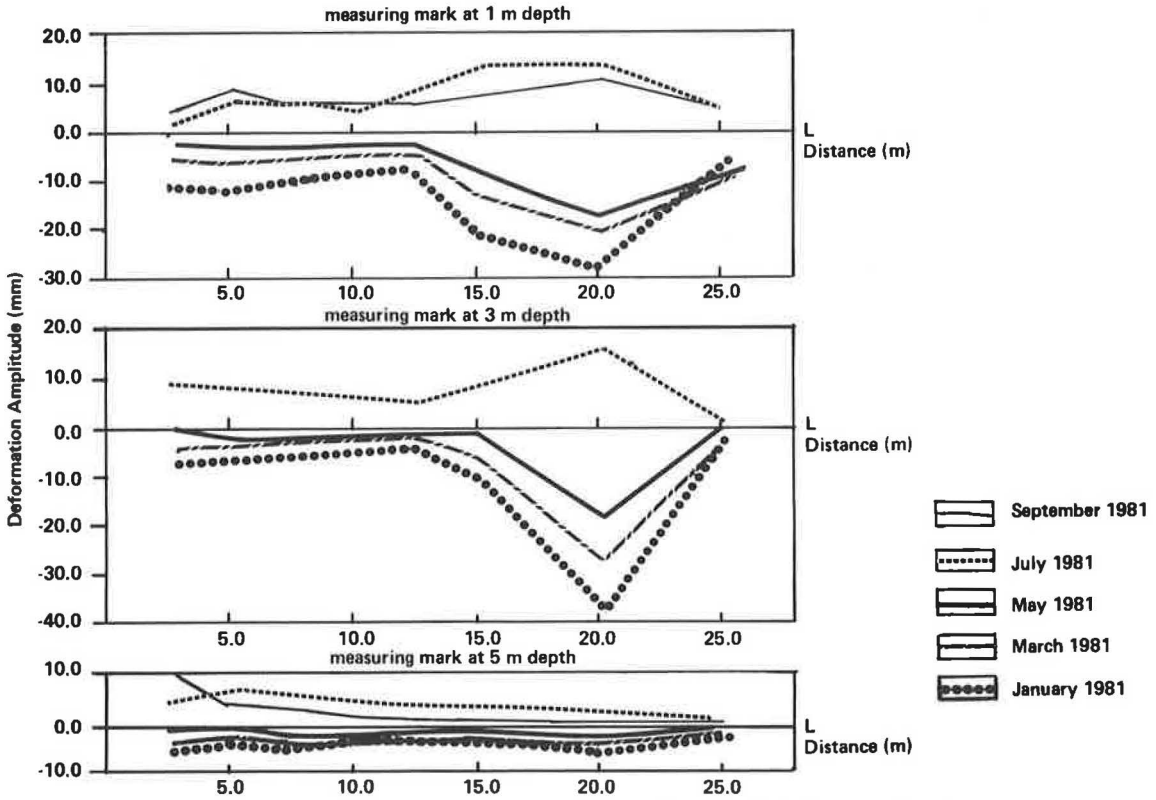

FIGURE 8 Deformation curves of measuring marks at different depths under the influence of jarrahs.

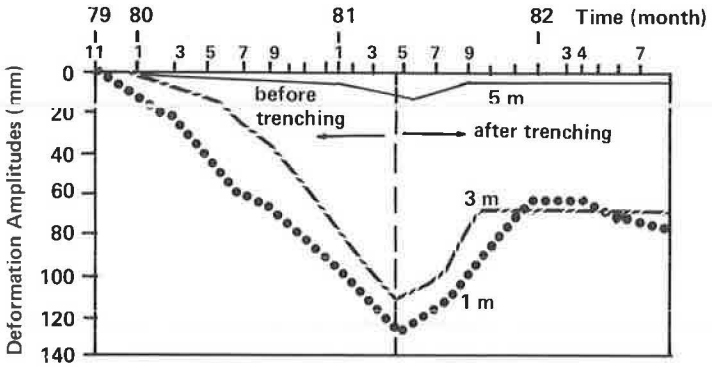

FIGURE 9 Curve of relationship between measuring mark and time.

reached 66 mm (Figure 9). The reversible deformation character of the expansive foundation soil and the formation of partial "dry shrunk area" of the foundation soil caused by vegetation transpiration were obviously indicated by the previously mentioned effect of return rising.

Vegetation transpiration unbalanced the water condition in the soil, thus causing the formation of a new humidity field as well as humidity variation within the foundation soil in the dry shrunk area (Figure 10). Therefore the water suction ability of the foundation soil matrix also varied. Because of

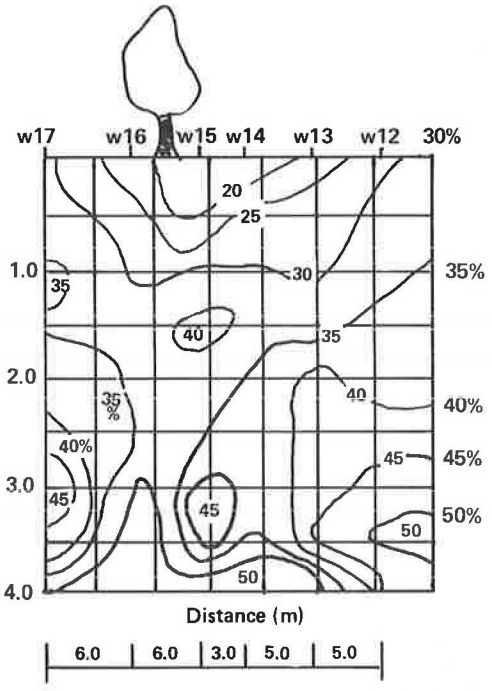

FIGURE 10 Humidity isogram of jarrah influence area.

this difference, the water in the soil transfers continuously to the tree roots. After cutting a lime trench between the house and tree in the jarrah-affected area, both the C and D measuring mark groups at the side of the house had 2 yr rising deformation, whereas sinking deformation occurred on the A and B measuring mark groups (Table 5 and Figure 11). On the house side, transfer of the soil water to the tree had been stopped after separation of the foundation soil from the influence of the tree roots. Before trenching, the water content of the foundation soil inside the house was 31 percent, after trenching it increased to 41 percent. Thus, the C and D measuring mark groups rose rapidly, and the D group, which was inside the house, had the largest rising amplitude--the maximum rising rate reached 40 mm/month. On the tree side, due to the decrease of dry shrunk area, water consumption from the foundation soil for vegetation transpiration increased, and the foundation soil showed substantial deformation.

In the foundation soil affected by the tree, the sphere to be bounded within the deformation-influenced radius horizontally and depth vertically is called dry shrunk area. Its scope depends on the species, age, trunk diameter, and root growing condition of the trees. In the Mengzi region, a growing jarrah 10 yr old with a 20- to 40-cm diameter trunk caused the ground surface to be deformed with 15 to 37 mm amplitude, and it has an influence sphere of about 8 m radius (Figure 12). A deformation curve of 72 measuring marks in different depths near a fully grown jarrah 17 m high with a trunk diameter of about 50 cm shows that deformation differential of measuring marks in different parts of the dry shrunk area is great (Figure 13). It was discovered after excavation that the humidity of the part of the foundation soil where the tree hair reaches varies greatly as well as the deformation amplitude (Figure 7). The deformation amplitude of the measuring mark with distance to tree beyond 25 m was obviously reduced and nearly equal to the deformation amplitude of measuring mark in the area free of trees. This indicates that the deformation-influenced radius under the jarrah is 25 m, which approximately equals 1.4 times the tree height. As a rule the deformation amplitude of measuring mark in the dry shrunk area decreases progressively with the increase in depth (Figures 8 and 13). Assuming the depth of measuring marks with deformation amplitude $\leq$ 10 mm to be the tree-influence depth, the influence depth of jarrahs in the dry shrunk area is 3.5 to 8 m. The farther the spot from the tree, the smaller the influence depth will be (broken line in Figure 14). The influence depth measured from the mark with 25 m distance from the tree is 3.5 m. This is similar to the weather influence depth in space without trees.

INFLUENCE FACTORS

As mentioned previously, the main factor that affects the foundation soil deformation in vegetation areas is vegetation transpiration and the expanding and shrinking character of the soil. Beyond the species of tree, the amount of transpiration is

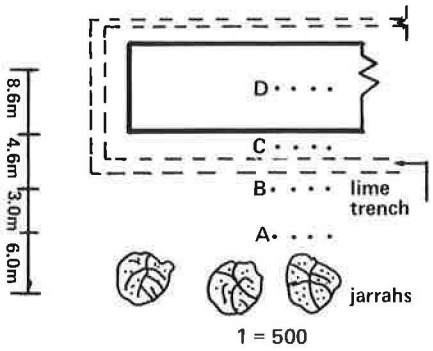

FIGURE 11 Location of measuring marks at different depths on both sides of lime trench.

related to the local weather in addition to the restrictions of the hydrogeology and engineering geology condition of the site. Rothenberg believes that the relative humidity of the environment can restrain vegetation transpiration (1). The higher the relative humidity, the lower the vegetation transpiration.

Thus, the effects of vegetation transpiration on deformation of foundation soil in humid climates are smaller than in dry climates. The effects of vegetation transpiration on water content variation and deformation of foundation soil are small on the site that has a thick earth cover or a high groundwater table. But on the site that has a thin earth cover and a low groundwater table, because of the transpiration influence caused by water suction of the tree root, the water loss of the foundation soil is

TABLE 5 Deformation Amplitude of Measuring Marks at Both Sides of Lime Trench

Measuring Mark Deformation (mm), Depth (m)	Group A			Group B			Group C			Group D		
	Rising	Sinking	Amplitude	Rising	Sinking	Amplitude	Rising	Sinking	Amplitude	Rising	Sinking	Amplitude
1.0	0.0	-21.2	21.2	0.0	-22.6	22.6	9.3	0.0	9.3	43.2	0.0	43.2
2.0	0.0	-21.1	21.1	0.0	-17.5	17.5	9.0	0.0	9.0	23.4	0.0	23.4
2.5	0.0	-13.0	13.0	0.0	-10.8	10.8	6.8	0.0	6.8	10.4	0.0	10.4
3.0	0.0	-8.8	8.8	0.0	-5.3	5.3	4.2	-1.1	5.3	8.4	0.0	8.4

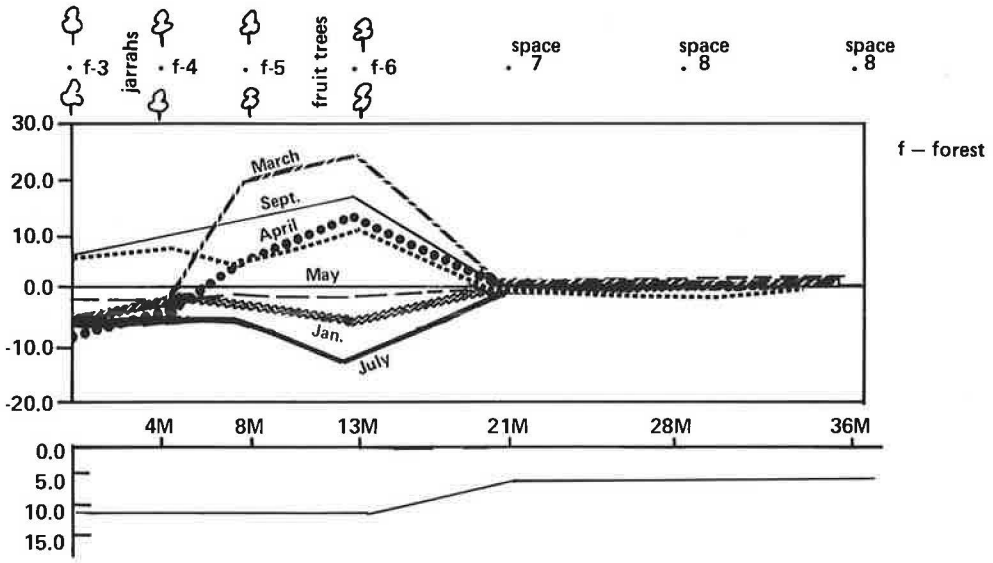

FIGURE 12 Observed cross section of surface deformation near jarrahs in Mengzi region.

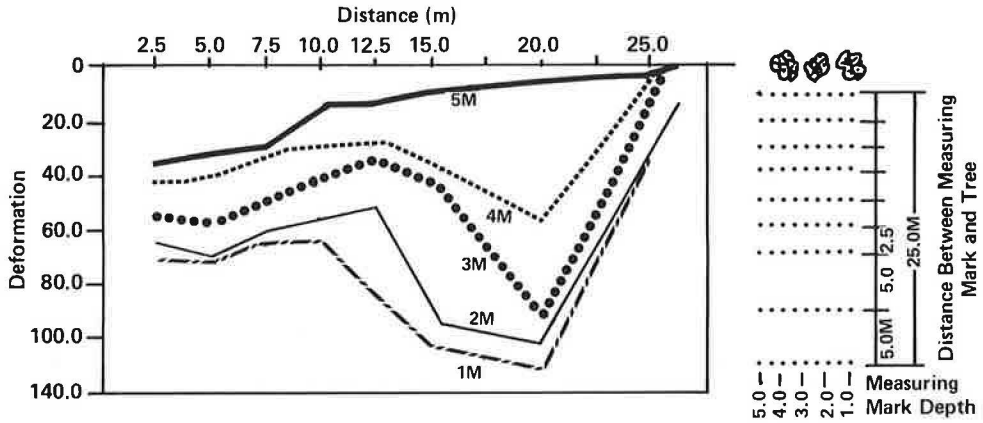

FIGURE 13 Relationship between deformation amplitude of measuring mark and distance to tree.

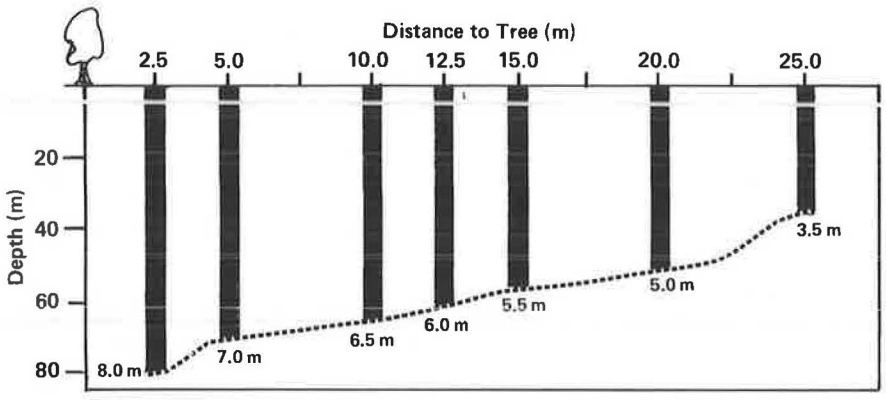

FIGURE 14 Influence depth of measuring marks at different distances to tree.

high; therefore, substantial shrinking deformation can easily occur.

It should be pointed out that vegetation transpiration is an external factor that causes the humidity variation of the foundation soil. Only the expanding and shrinking character of the soil is the essential factor of deformation of foundation soil. Under the influence of vegetation transpiration, the foundation soil with high void ratio and strong expanding character will have a low lower limit of water content variation and remarkable shrinking deformation. For example, in the Mengzi region, the humidity coefficient of foundation soil is Km = 0.6, free expansion ratio is e_{FS} = 81 percent, and the natural void ratio is e_o = 1.15. Because of the small humidity coefficient of foundation soil, dry weather, high vegetation transpiration, as well as high void ratio and strong expanding character, the effect of vegetation on deformation of foundation soil in the Mengzi region is rather great (Tables 3 and 4).

The deformation amplitude of measuring marks adjacent to the tree is up to 105.1 mm, that of parts of the house close to the tree reaches 187.2 mm. In this same area, however, the nonexpansive foundation soil is e_{FS} = 30 percent and e_o = 1.41, and the deformation amplitude of measuring marks near the jarrah at a 1-m depth is only 30 mm.

Hefei has a subhumid climate (Km = 0.8, e_{FS} = 64 percent, and e_o = 0.65); deformation amplitude of parts of the house near the tree is 7.82 to 11.3 mm. In the Chengdu area (Km = 0.9, e_{FS} = 61 percent, and e_o = 0.64), deformation amplitude of parts of the house close to the tree is 18 mm. This value is approximately equal to the deformation amplitude of an area without trees; therefore it is evident that the deformation of foundation soil is not affected by the tree. It is evident from the preceding examples that the deformation of foundation soil is related to Km in inverse ratio and to e_o in direct ratio. Therefore the effect of vegetation on buildings with high void ratio expansive foundation soil is remarkable in dry and sub-dry regions in China.

The possible shrinkage rate (S_1) of the foundation soil under the influence of weather and soil character may be calculated from the formula given below when the following conditions are satisfied:

1. Foundation soil is beyond the influence of groundwater and $e_{FS} \geq 40$ percent; and
2. Deformation of foundation soil refers to the shrinkage that is caused by the decrease of water content, and the void ratio variation of soil is in direct proportion to the variation of water content.

$$S_1 = e_o - e_m / 1 + e_o \times 100\%$$

where

S_1 = possible shrinking deformation rate at 1-m depth of foundation soil because in measuring on-site the greatest deformation is obtained at 1-m depth in the vegetation area; therefore, only the deformation amplitude of foundation soil at 1-m depth is calculated, and the average rate of deformation within the 1-m depth of foundation soil is taken for calculating rate;
e_o = natural void ratio of soil;
e_m = void ratio of soil in which water content is minimum W_m, $e_m \approx 0.028\ W_m + 0.041$ may be taken in lack of measuring data, and
W_m = minimum water content that depends on character of soil, weather, and humidity of foundation (2).

Possible shrinkage rates of foundation soil in 40 places in regions with high vegetation transpiration have been calculated according to the preceding formula. The results are compared with the actual destroyed condition of the corresponding houses. The following conclusions can be drawn: in areas in which S_1 is inversely proportional to Km and directly proportional to e_o, Km $\geq$ 0.9, $e_o \leq$ 0.7, or S_1 < 10 percent, damage is not a result of vegetation; in areas in which Km < 0.9, e_o > 70.7, or $S_1 \geq$ 10 percent, damage to the houses is related to the vegetation, and the greater the S_1, the greater the vegetation's influence (Table 6 and Figures 15, 16). Thus the conclusion may be drawn that S_1 may be used as a quantitative index in predicting and estimating the effect of vegetation on foundation soil deformation. In the area in which $S_1 \geq$ 10 percent, the possible engineering damage caused by the influence of trees with high transpiration should be taken into account, whereas in the area in which S_1 < 10 percent the influence of trees can be discounted.

TREATMENT

The vegetation influence presenting measurements and afforestation experience in Mengzi and other regions can be summarized as follows:

1. When building houses in areas expected to be influenced by vegetation, the general layout should be planned rationally with the buildings laid out beyond the tree influence radius, and light transpiration trees should be selected for afforestation (see Table 3).
2. A lime trench may be dug between the house site and the tree before construction to create a

TABLE 6 The Calculated Foundation Soil Shrinkage Rate of Different Regions

Index	Region													
	Mengzi	Panxi	Kunming	Qujing	Wenshan	Ningming	Yun County	Linyi	Gui County	Hefei	Jingmen	Chengdu	Nanjing	Nanning
e_{FS} (%)	81	64	62	80	52	68	53	61	50	64	64	61	57	56
I_p	34	25	32	28	27	29	22	29	35	23	24	21	21	29
K_m	0.60	0.60	0.70	0.70	0.70	0.74	0.74	0.76	0.80	0.80	0.80	0.90	0.90	0.87
e_o	1.15	1.04	1.16	1.13	1.21	0.79	0.63	0.83	0.92	0.65	0.60	0.64	0.65	0.89
e_m	0.70	0.63	0.67	0.59	0.71	0.58	0.56	0.59	0.76	0.54	0.51	0.57	0.55	0.70
S_l	21.0	20.0	22.7	25.0	22.6	11.7	4.3	13.1	8.3	6.7	5.6	4.3	6.1	10.0
	*	*	*	*	*	*	+	+	*	+	+	+	+	*

Note: Mark "*" means damage to houses is related to tree influence. Mark "+" means damage is not a result of tree influence.

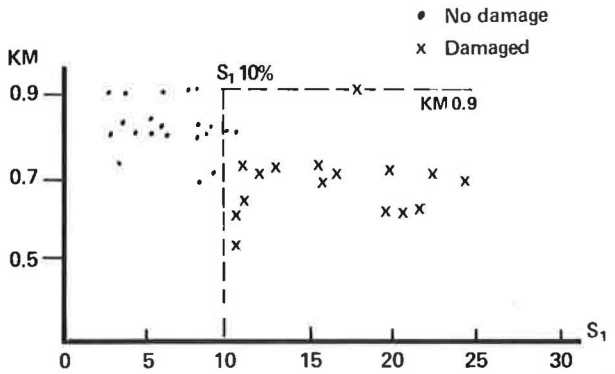

FIGURE 15 Relationship between Km and S_1.

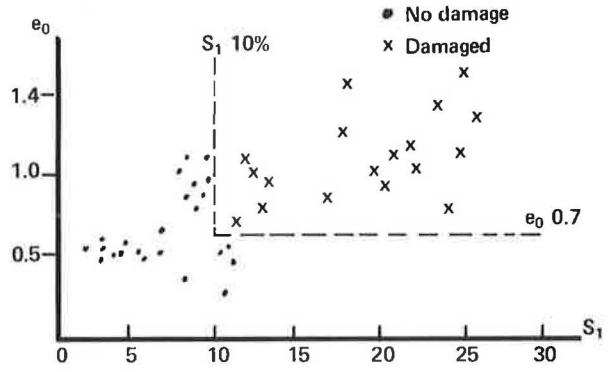

FIGURE 16 Relationship between e_o and S_1.

moisture transfer barrier. The depth of the trench should be 2 m and the length should be equal to the tree influence radius. One side of the trench should be filled with lime to the ground surface; the thickness of the lime fillings should be 10 to 20 cm. The other side of the trench, after having been filled with earth, should be rammed and sealed with cement (Figure 17). Whether using this method or cutting down the tree to build the house, the land should not be used for construction for 0.5 to 1 yr. The house cannot be built until the humidity variation of the foundation soil is balanced and becomes stable.

The following trees are suitable for afforestation:

Evergreen Trees
Pine, Cypress
Deciduous Trees
Arbor: Chinaberry, Dawn redwood, Gingko
Bush: Chinese scholartree, Rose
Shrub: Cottonrose, Crape Myrtle

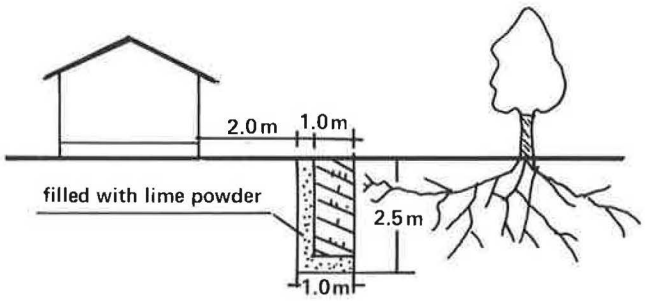

FIGURE 17 Schematic of lime trench separation method.

CONCLUSIONS

The following conclusions can be drawn:

1. Transpiration by water suction of tree roots causes partial shrinking deformation of foundation soil, which causes substantial differential settlements of engineering structures and resulting damage. This is the result of the effect of vegetation on foundation soil.
2. The radius and depth of the sphere in which the vegetation transpiration affects foundation soil is dependent on the species, age, and the growing condition of the roots of the tree. The influence radius of a grown-up tree is 1.4 times the tree height, and its influence depth is 3.5 to 8 m. The degree of deformation will become greater closer to the tree.
3. The effects of vegetation transpiration on dry high void ratio expansive foundation soil mainly occurs in dry and sub-dry climate areas. In the area in which $Km > 0.9$, $e_o < 0.7$, or $S_l < 10$ percent, the vegetation effects are not significant.

REFERENCES

1. N.J. Rothenberg and B.L. Blace. Microclimate--Biological Environment. John Wiley and Sons, New York, 1983.
2. Hexinfang and C. Lin. Moisture Coefficient of Expansive Soil and Its Application in Engineering Practice. Fifth National Session of Expansive Soil, 1984.

Publication of this paper sponsored by Committee on Environmental Factors Except Frost.